T I T L E

AN INVESTIGATION INTO THE DEVELOPMENT OF A PORTABLE, ULTRASONIC, DENSITY MEASURING INSTRUMENT

A U T H O R

NIGEL DOUGLAS HULSE N.H.Dip.(Natal)

DISSERTATION SUBMITTED IN COMPLIANCE WITH THE REQUIREMENTS FOR THE NATIONAL MASTER'S DIPLOMA IN TECHNOLOGY: ELECTRICAL ENGINEERING (LIGHT CURRENT) IN THE DEPARTMENT OF ELECTRONIC ENGINEERING AT THE TECHNIKON, NATAL.

SUPERVISOR: Dr A.B. Stewart Ph.D.(Elec.Eng.)(Wits.)Pr.Eng.

DATE OF SUBMISSION: 3rd NOVEMBER, 1987

EXCEPT WHERE OTHERWISE INDICATED BY REFERENCE, THIS DISSERTATION REPRESENTS THE AUTHOR'S OWN WORK IN CONCEPTION AND EXECUTION

AN INVESTIGATION INTO THE DEVELOPMENT OF A PORTABLE ULTRASONIC, DENSITY MEASURING INSTRUMENT

by

N.D. HULSE

S Y N O P S I S

In the gold mining industry, one of the significant physical properties of the mineral slurry is its density and it is important to be able to measure this parameter in most processes.

There are many techniques for determining the density of fluids, but because of the hostile, abrasive nature of mineral slurry, very few of these are suitable.

This dissertation describes the development, construction and testing of a portable, ultrasonic, density measuring instrument. The instrument uses an ultrasonic transducer as the primary measuring element, and system operation is based on the fact that the driving impedance of the transducer varies with changes in the physical properties, and hence the characteristic impedance, of the surrounding medium into which the ultrasonic energy is being transferred.

The technique may also be used to measure the relative concentrations of two liquids in a mixture or emulsion, provided that the characteristic impedances of the liquids are sufficiently dissimilar. The electronic circuitry is fairly straightforward, consisting essentially of an oscillator, driving circuit for the transducer and a voltage monitor to provide a d.c. voltage proportional to the impedance of the transducer, and hence to the density of the surrounding medium. Most of the research has been concentrated on the probe design, as the type of transducer, the type and thickness of facing material and the method of construction all contribute to the sensitivity of the instrument. A design of probe assembly has been developed that may be used for both slurry density measurement and the measurement of the ratio of aqueous to organic liquids in emulsion.

Results from laboratory and plant experiments have proven the technique to be suitable for use in the mineral processing environment and although the object of the investigation was to develop a portable instrument, the system may also be used on-line for continuous measurement or control. Such an instrument has been successfully tested at the solvent extraction (sx) plant of a uranium mine. In this application, the ratio of organic to aqueous liquids is monitored continuously, the outputs from the instrument being connected through to the central process computer where the solvent content is calculated.

A second, on-line instrument is presently being tested and calibrated for installation at a carbon-in-pulp, gold-recovery plant. It is to be used in conjunction with a carbon concentration meter and will provide a signal that will be used to compensate for changes in the density of the slurry.

S A M E V A T T I N G

In die goudmynbedryf is een van die belangrike fisiese eienskappe van die mineraalflodder sy digtheid en dit is in die meeste prosesse belangrik om hierdie parameter te kan meet.

Daar is baie tegnieke vir die bepaling van die digtheid van vloeistowwe, maar baie min daarvan is vir die bogenoemde doel geskik vanweë die vyandige, skurende aard van mineraalflodder.

Hierdie skripsie handel oor die ontwikkeling, konstruksie en toetsing van 'n draagbare, ultrasoniese instrument om digtheid mee te meet. Die instrument gebruik 'n ultrasoniese oordraer as die primêre meetelement en die werking van die stelsel is gebaseer op die feit dat die oordraer se aandryfimpedansie wissel ooreenkomstig met veranderinge in die fisiese eienskappe, en gevolglik die kenmerkende impedansie van die omringende medium waarin die ultrasoniese energie oorgedra word.

Die tegniek kan ook gebruik word om die relatiewe konsentrasie van twee vloeistowwe in 'n mengsel of emulsie te meet, mits die kenmerkende impedansies van die vloeistowwe genoeg verskil. Die elektroniese kringwerk is redelik eenvoudig en bestaan in hoofsaak uit 'n ossillator, 'n aandryfkring vir die oordraer en 'n spanningsmonitor om 'n gs - spanning eweredig met die impedansie van die oordraer, en dus die digtheid van die omringende medium aan te gee. Die grootste deel van die navorsing was toegespits op die ontwerp van die sonde aangesien die soort oordraer, die soort en dikte van die voorwerkmateriaal en die konstruksiemetode almal tot die sensitiwiteit van die instrument bydra. Daar is 'n ontwerp van 'n sondesamestel ontwikkel wat gebruik kan word om die digtheid van flodders en die verhouding van waterige tot organiese vloeistowwe in 'n emulsie te meet.

Die resultate van laboratorium - en aanlegeksperimente het bewys dat die tegniek geskik is vir gebruik in die mineraalverwerkingsomgewing en hoewel die oogmerk van die ondersoek was om 'n draagbare instrument te ontwikkel, kan die stelsel ook gekoppel vir deurlopende meting of beheer gebruik word. So 'n instrument is suksesvol getoets by die oplosserekstraksieaanleg (sx) van 'n uraanmyn. In hierdie toepassing word die verhouding van organiese tot waterige vloeistowwe deurlopende gemoniteer en die afvoer van die instrument is verbind aan die sentrale prosesrekenaar waar die oplosserinhoud bereken word.

'n Tweede gekoppelde instrument word op die oomblik getoets en gekalibreer vir installering by 'n goudherwinningsaanleg wat van die koolstof-in-pulp proses gebruik maak. Dit gaan saam met 'n koolstofkonsentrasiemeter gebruik word en sal 'n sein gee wat gebruik sal word om te kompenseer vir veranderinge in die digtheid van die flodder.

ACKNOWLEDGEMENTS

Support for the project by the Council for Mineral Technology is gratefully acknowledged.

Special thanks are due to:

Mr G. Sommer : Director of the Measurement and Control Division, for allowing the results of the DENCAR project to be submitted for consideration.

Prof. A.B. Stewart: Assistant Director of the Measurement and Control Division, for making my candidacy for the Diploma possible.

Prof. J.F.W. Bell : Department of Electrical Engineering, M & C Research Group, University of Cape Town for his continued guidance and encouragement.

Technikon Natal : For accepting the project for consideration.

Dr D. Coertze : For assisting in the final preparation of this dissertation

And to the members of Measurement and Control, in particular the Ultrasonics Group, for their support.

LIST OF ABBREVIATIONS

CIP	:	Carbon-in-pulp
D:t	:	Diameter-to-thickness (ratio)
Δz	:	Change in impedance
Δv	:	Change in voltage
fp	:	Parallel resonance
fs	:	Series resonance
PZT	:	Lead-Zirconate-Titanate
ρC	:	Characteristic impedance
PVC	:	Polyvinylchloride
Rr	:	Radiation resistance
Rm	:	Frictional losses
R_T	:	Rm + Rr
r	:	Correlation coefficient
t_c	:	Transmission coefficient
vco	:	Voltage controlled oscillator
V_0	:	Instrument output voltage proportional to the impedance of the transducer (PZT)
V_T	:	Instrument output voltage proportional to the temperature of the PZT

C O N T E N T S

1. INTRODUCTION

One of the significant physical properties of a material is its density. This is supported by the extensive literature available on the subject, as well as the many techniques for measuring it. Some of these methods are the magnetic densimeter/viscometer (Hodgins 1971), use of a tuning fork (Stemme 1983), and the hydrostatic weighing method, use of a picnometer, flotation method, hydrometer, balanced column and elastic helix method (Hidnert, 1950). However these instruments are generally used for laboratory determinations of density, and are not suitable for use in the plant environment of the mineral processing industry.

In this dissertation, the medium of interest is a mineral slurry. In the processing of minerals for the extraction of the valuable components, the rock is invariably crushed into very fine form to expose the valuable components and the comminuted material is then combined with water to form a slurry. The various physical, chemical and mineralogical properties of a slurry have a strong effect on its response to further processing, so it is important to be able to measure them, preferably continuously and on line. The density of a slurry, is of particular importance and needs to be determined in most processes. Three gold mining processes that require slurry density measurement and control are the thickeners, the leaching and the carbon-in-pulp (CIP) operations (Adamson, 1972). Examples of these plants are shown in Plate I.

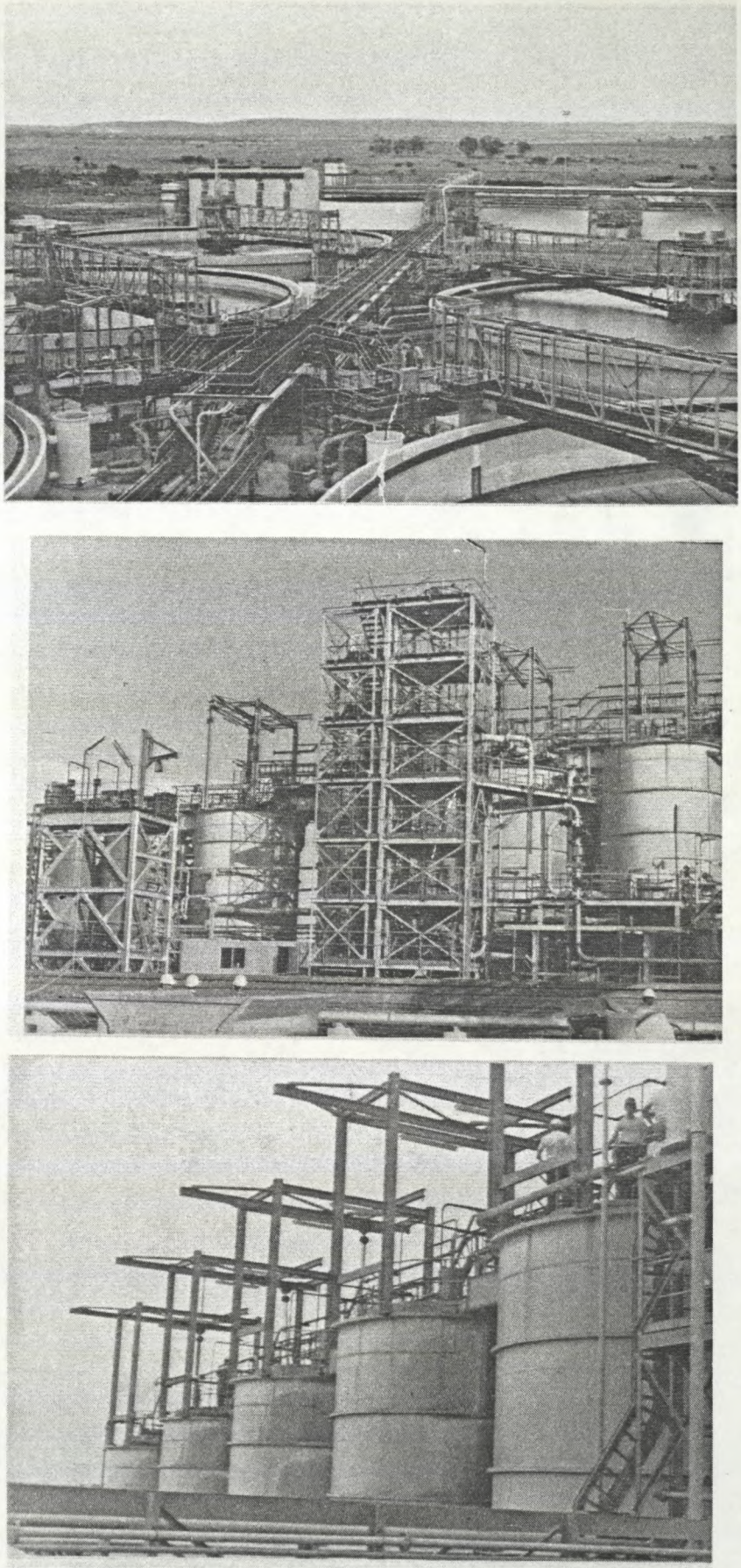

PLATE I : Example of open slurry vessels on a gold plant, showing thickeners (top), leach (centre) and CIP

1.1 The Thickeners

As the name implies, the thickeners are used to thicken slurry. This is done to ensure the correct operation of subsequent processes. An output density of 1,46 is normal for gold plants and this is obtained with a liquid/solid ratio of 1:1 by mass. Under these conditions, viscosity and suspension are good and the amount of solution is suitable. If the density is too low, then the slurry is recirculated until the density is correct (Rubin, 1987).

1.2 The Importance of the Correct Density in the Leach and CIP Processes

The viscosity of the pulp is a function of the system density (Marsden, 1962). Moreover in the region above a density of 1,5, the viscosity of the pulp increases dramatically (Marsden, 1962). In the gold leaching system it is necessary to transfer material (gold) between the solid particles and the surrounding liquid phase which contains the reagents. In the CIP process the reverse is true: material is transferred from the liquid phase to carbon particles (solid phase). Clearly, the more effective the transfer of material, the faster will be the rate of gold dissolution (leach) or adsorption (CIP) (Adamson, 1972).

When quantifying the transfer of material between a solid particle suspended in a liquid, in an agitated vessel, a correlation developed by Frössling (Sherwood, 1975) is used to describe the mass transfer coefficient for such a system. Obviously, the transfer of material between solid and liquid is proportional to this mass transfer coefficient, Kc (Sherwood, 1975). The Frössling equation takes the form:

$$Kc = \frac{D}{dp}\left(2 + 0{,}6\ Re^{\frac{1}{2}} Sc^{\frac{1}{2}}\right) \quad \ldots\ldots\ldots\ldots\ldots\ldots\ldots\ldots (1)$$

Where D = Diffusion coefficient

dp = Diameter of particle

R_E = Reynolds number

Sc = Schmidt number (Sherwood, 1975)

From this equation, it is apparent that:

$$Kc = A + \frac{B}{\mu^{\frac{1}{2}}} \quad \ldots\ldots\ldots\ldots\ldots\ldots\ldots\ldots\ldots\ldots\ldots\ldots (2)$$

Where

$$A = \frac{2D}{dp} \quad \text{and} \quad B = \frac{0{,}6D}{dp}\,(dp\ v\rho)^{\frac{1}{2}}(\rho D)^{\frac{1}{2}}$$

v = Characteristic velocity

μ = Viscosity

It is clear from equation (2) that an increase in viscosity will cause the mass transfer coefficient to decrease, which implies inefficient dissolution in the leach process and inefficient adsorption in the CIP system if density is too high.

In addition to the loss of revenue because of either inefficient dissolution or adsorption, power is wasted in stirring a high-density slurry. The power used in mixing is directly proportional to density; as is shown in the following expression (Hicks, 1976).

$$Hp = (D/394)^5 SgN^3 \quad \ldots\ldots\ldots\ldots\ldots\ldots\ldots\ldots\ldots\ldots\ldots\ldots\ldots\ldots (3)$$

Where

Dt = Turbine diameter

Sg = Density

N = Turbine speed (rpm)

If the slurry density falls too low in the CIP vessels, the carbon particles and heavier particles of the slurry itself may settle out, causing a poor distribution of carbon and hence poor adsorption of gold.

If the density of the slurry in the leaching process falls too low, then as in the CIP, the heavier fractions of the slurry may settle out. Apart from that, a greater volume of pulp has to be treated and the chemicals become diluted, due to excessive liquid. Again this causes poor dissolution due

to a reduced pulp residence time, (Vetter, 1988) and an accompanying loss of revenue.

The importance of knowing the density of slurry has been shown and the problem of measuring this property has to be addressed.

As a slurry is a suspension of crushed rock, continuous agitation is necessary to prevent the solids from settling. Because of this, the medium is extremely abrasive in nature and provides a hostile environment for a measuring instrument. It is therefore generally beneficial for the instrument to be non-intrusive. (Carlson, 1977; Snowden, 1969).

1.3 Methods of On-Line Slurry Density Measurement

There are very few density measuring instruments that are suitable for, and robust enough to withstand, this sort of environment. The only well established method involves the use of a nuclear technique based on the measurement of the loss,or attenuation, of a signal, between a radioactive source and a detector, as the radiant energy (gamma) passes through the slurry (Fribance, 1962). However, because of the hazard involved in the use of nuclear energy, this technique is only viable for closed systems in which the slurry is transported in pipes, or where the probe is immersed to a reasonable depth in a reaction vessel (Howarth, 1973), thus allowing safe working conditions to be maintained.

Another means of on-line slurry density measurement is the ultrasonic attenuation method as used in particle-size analysis (Herbst, 1985). This operates on the same principle as the nuclear density guage, that is it measures density as a function of attenuation of a signal between a transmitter and receiver. The analyser sensor assembly uses a number of different frequencies - one of which is used for the measurement of density. To provide a correction factor for fluctuations in density.

Other techniques are the buoyancy method, where the depth of immersion of a float is monitored while suspended in the slurry, its degree of buoyancy being proportional to the density of the slurry and the differential pressure technique where the difference in back pressure between two air-fed pipes, at different depths, is proportional to density (Considine, 1974).

1.4 Advantages and Disadvantages

All of these methods have their advantages and disadvantages. The gamma density gauge is robust, accurate and needs very little maintenance. However because of its use of a radio-active isotope, its application is limited mainly to the measurement of slurry density in pipes. Unfortunately, the density in the pipe is not necessarily representative of that in the receiving vessel, as settling out of solids can occur in the vessel.

The buoyancy type, as used in open reaction vessels is robust, but calibration can change due to build-up of pulp on the suspending wire and the float itself. Regular removal of this build up is therefore necessary.

The main disadvantage with the differential pressure method is the eventual blocking of the measuring pipes. Again, regular service is necessary to keep the pipes open.

Apart from these disadvantages, these instruments have one common failing; they are all fixtures and therefore measure the density of the slurry in one place only. Unfortunately, these measurements need not reflect the homogeneity of the slurry and cannot indicate any silting up that may be in progress.

1.5 The Need for a Portable Density Measuring Instrument

The foregoing observations suggest that there is an area of measurement that is not being addressed and that is the measurement of slurry density at various positions and depths in open containers, such as thickeners, leach and C.I.P. vessels. Obviously, some form of portable measuring instrument would be necessary to address this problem. The most common method by which density is measured at various positions in reaction vessels is the spring-balance method. A 1ℓ sample is suspended from a balance, and density is indicated directly by means of a pointer and scale. Because this is a manual technique, these measurements are confined to the surface of the slurry and, once again there is an

area of measurement that is not being accommodated, namely, anywhere in a given vessel at depths greater than about 300 mm. The density of the slurry therefore is not known below this level.

To address this problem a portable measuring system using a dip-in probe is needed. Such a system would be based either on a nuclear technique or on the use of ultrasound. An instrument using a radioactive isotope may be feasible, but its use might cause a health hazard in the event of damage to the probe assembly. It was decided to use an ultrasonic technique to develop the proposed portable instrument.

1.6 Ultra-Sound as a Basis for the Portable Instrument

As the use of ultra-sound is well established in the measurement of the flow-rate (Miller, 1974) and particle-size (Hind, 1975; Herbst, 1985) of mineral slurries, it was decided to use an ultrasonic technique as the basis for the proposed density measuring instrument. There would be no health hazard involved in its use and the system would be relatively simple to construct and possibly less expensive than the instruments mentioned previously.

1.7 The Choice of Technique

There are two possible approaches to the measuring technique. One method would be the ultrasonic analogue of the gamma gauge, that is, the measurement of slurry density by the degree of attenuation of a signal between a

transmitter and receiver (Dann, 1986). However, this implies the use of two transducers which suggests additional cost and a more complex design of probe and electronic circuitry.

The other alternative would be to attempt to monitor changes in density by the measurement of the change in driving impedance of a single transducer. It was this approach that was chosen.

1.8 The Purpose of the Investigation

The purpose of this investigation, therefore, was to design and construct a portable, single-element, ultrasonic, density measuring instrument for use with mineral slurries and to evaluate its performance in the laboratory and on site.

1.9 The Investigation

There are two sub-problems to be addressed during the investigation.

1.9.1 Sub-problem one

The first sub-problem will be to determine whether it is possible to design and construct a relatively simple, single-device, density measuring instrument.

It is hypothesized that the change in the driving impedance of an ultrasonic transducer is directly related to the acoustic impedance, ρc, of the surrounding medium (Appendix I) and therefore it would be possible to measure the relative concentration of two liquids in a mixture, or

emulsion, based on the assumption that the acoustic impedances of the liquids are sufficiently dissimilar.

1.9.2 Sub-problem two

The second sub-problem would be to evaluate the instrument in the laboratory and on site.

It is hypothesized that the operation of the instrument will compare favourably with that of the commonly-used spring balance density gauge.

2. THE ULTRASONIC TRANSDUCER

2.1 Introduction

The transducer most commonly used in ultrasound application at Mintek is the PZT (lead-zirconate-titanate) piezoelectric ceramic disc. The device uses the piezoelectric effect to transform electrical energy into ultrasonic vibrations and vice versa.

The measurement of impedance and admittance is a valuable tool for the analysis and design of ultrasonic transducers and is used to determine the series and parallel resonance frequencies of a transducer, as well as acoustic matching, efficiency and equivalent circuit component values.

2.2 The Transducer Analysis System (T.A.S.)

The determination of series and parallel resonance frequencies the generation of impedance and admittance curves and circle diagrams, and the calculation of the component values of the equivalent circuit of the PZT, are complex procedures and so a software package was developed to simplify and computerize these measurements and present all relevant information derived from the data in a usable form. (Smith, 1985).

For this purpose, an HP 4193A Vector Impedance Analyser, controlled by an HP 9816 computer, is used to measure the impedance of a transducer over a specified frequency range. The magnitude and phase of the impedance or the admittance may then be plotted as a function of frequency. The series and parallel resonance frequencies can be determined from these graphs. There are options for plotting the impedance and admittance circle diagrams as well as for calculating the equivalent circuit component values. The data from each analysis is automatically stored on disc. Plate II shows the equipment for accomplishing these analyses and measurements.

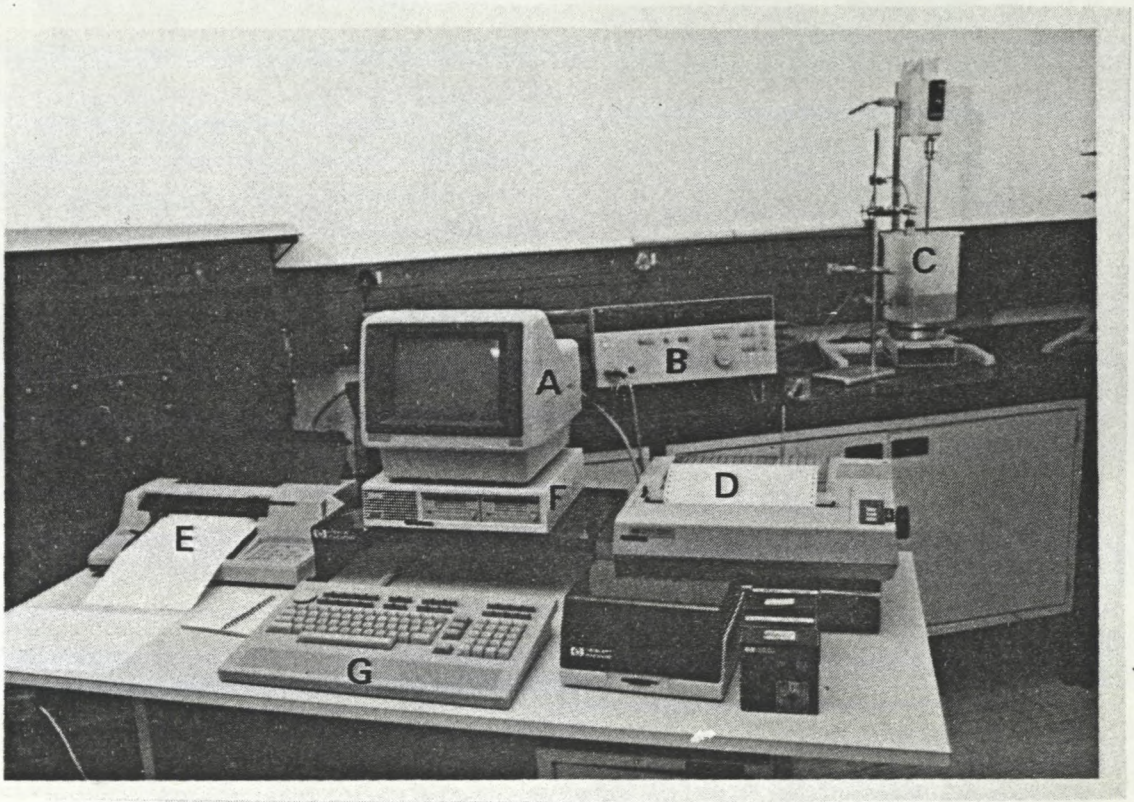

PLATE II : The computerised system used in the analysis of ultrasonic transducers

Where

A = Computer/Monitor

B = Vector impedance analyser

C = Vessel for mixing slurry

D = Printer

E = Plotter

F = Disc drive

G = Keyboard

2.3 Equivalent Circuit of a Transducer

A piezoelectric transducer can be characterized by the simple equivalent circuit shown in Figure 1. (Cady, 1946).

The components in the series arm represent the motional piezoelectric properties of the ceramic. The component L represents the resonating mass of the ceramic and C represents the elastic compliance. The component R_T is a combination of the resistance representing the frictional losses during vibration, Rm, and the load resistance representing radiated energy, Rr. Co is the capacitance between the electrodes on the surface of the ceramic, and Ro is a resistance representing the dielectric losses of the transducer.

If the moduli of the electrical admittance |Y| or the electrical impedance |Z| are plotted against the frequency, curves are obtained as shown in Figure 2 and Figure 3.

The impedance of the series arm is at a minimum at the series resonant frequency, and the transducer can be characterized by the equivalent circuit shown in Figure 4.

The series resonance (fs) is determined by L and C (Fig. 1). The following standard equation is used:

$$fs = \frac{1}{2*\pi\sqrt{LC}} \qquad \ldots\ldots\ldots\ldots\ldots\ldots \quad (1)$$

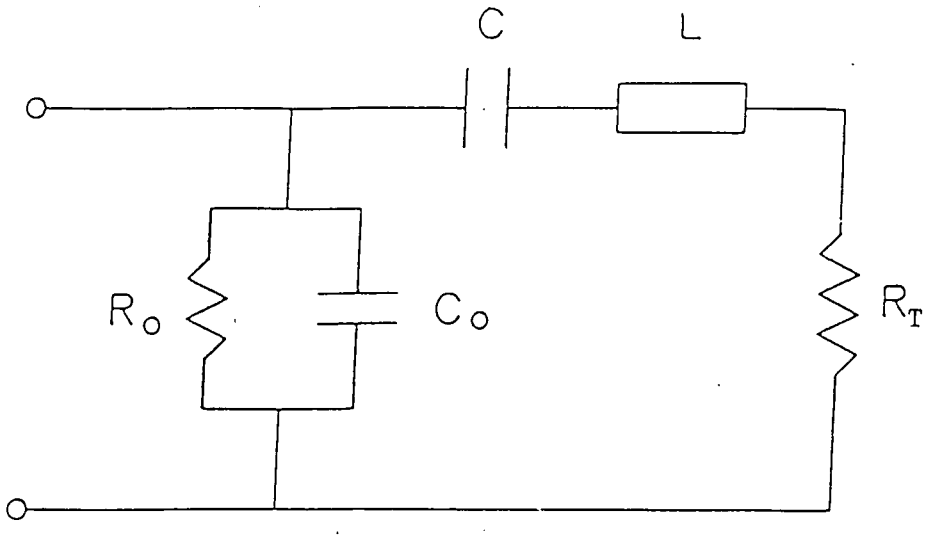

FIGURE 1 : EQUIVALENT CIRCUIT OF A TRANSDUCER

Where R_o = Dielectric losses
C_o = Capacitance between surfaces
C = Elastic compliance
L = Resonating mass
R_T = Load resistance plus mechanical losses

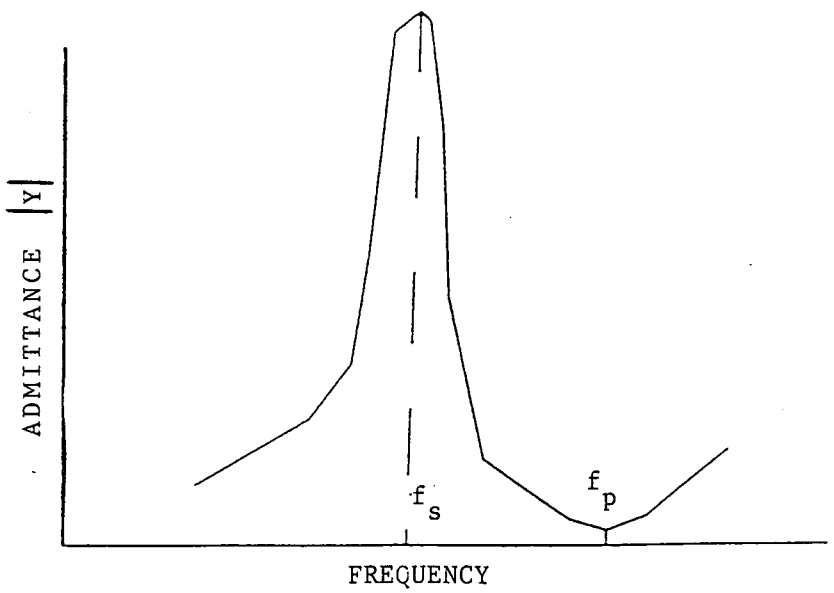

FIGURE 2 : ADMITTANCE AS A FUNCTION OF FREQUENCY

Where f_s = Series resonant frequency
f_p = Parallel resonant frequency
$|Y|$ = Absolute value of admittance

The parallel resonant frequency (fp) is the frequency at which the impedance of the equivalent circuit is at a maximum. The frequency fp is determined by Co in parallel with the series combination of C and L (Figure 1).

The following equation is used:

$$fp = \frac{1}{2*\pi} \sqrt{\frac{C+Co}{C*L*Co}} \qquad \ldots\ldots\ldots (2)$$

The difference between the two resonant frequencies is given by the following equation:

$$fp-fs = \frac{fs}{2} . \sqrt{\frac{C}{Co}} \qquad \ldots\ldots\ldots\ldots\ldots\ldots\ldots\ldots\ldots (3)$$

These two resonant frequencies are clearly indicated in Figure 2 and Figure 3.

The admittance circle diagram, which is a plot of the susceptance against the conductance at different frequencies, is shown in Figure 5. At low frequencies the curve begins near the coordinates (1/Ro,0). As the frequency increases, the curve develops a clockwise loop and then goes to (1/Ro, ∞) as f$\rightarrow \infty$.

The diameter of the circle is 1/R and the centre point lies at (1/Ro+$\frac{1}{2}$ R,ωCo).

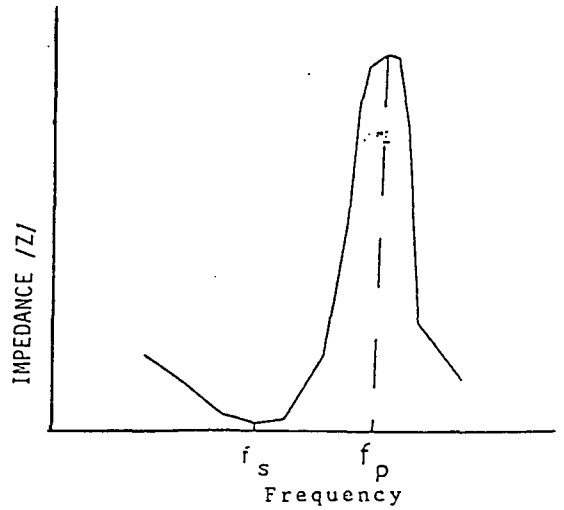

FIGURE 3 : IMPEDANCE AS A FUNCTION OF FREQUENCY

Where f_s = Series resonance f_p = Parallel resonance

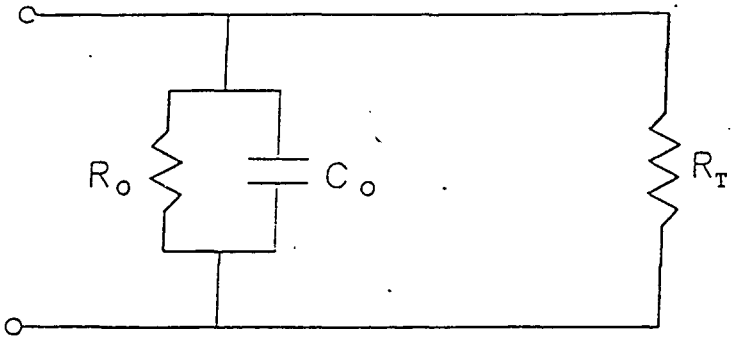

FIGURE 4 : EQUIVALENT CIRCUIT AT SERIES RESONANCE

Where R_o = Dielectric losses

C_o = Capacitance between surfaces

R_T = Load resistance and mechanical losses

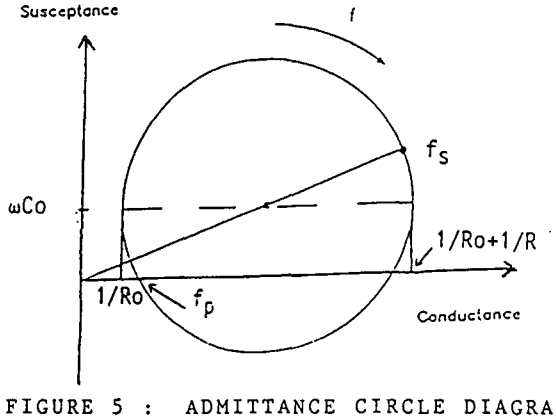

FIGURE 5 : ADMITTANCE CIRCLE DIAGRAM

Where $\frac{1}{R_o} + \frac{1}{R}$, ωC_o = Coordinates of centre

f_s = Series resounance

f_p = Parallel resonance

By using the equivalent circuit in Figure 1 as an electrical model of a transducer, more insight may be gained into what is actually changing when the impedance response changes.

2.4 Equivalent Circuit Calculation

In order to calculate the component values of the equivalent circuit, it is necessary to use formulae (1), (2) and (3) given in section 2.3 for the series and parallel resonant frequencies and their difference. These formulae alone, however, are not enough to solve for C,Co and L (Figure 1). Further information, which is supplied by the admittance circle diagram, must first be obtained.

Because the centre point of the admittance circle diagram lies at $(1/Ro+\frac{1}{2}R, \omega Co)$, Co can be obtained once the centre point is known. Because the circle diagram is not always a perfect circle, it is necessary to do a best fit using the least squares method to obtain the best circle through the points. A subprogramme is called to handle this function.

It was found that using the equation of a circle as a model and trying to minimize the square of the difference between the actual data point and the one predicted by the model, was too difficult.

Instead of this, a different approach was taken. The radius R of a circle is given by:

$$R = \sqrt{(X-B1)^2 + (Y-B2)^2} \quad \ldots\ldots\ldots\ldots\ldots\ldots\ldots\ldots\ldots\ldots (4)$$

where are X and Y are the points on the circle and B1 and B2 are centre point co-ordinates. The following model was chosen:

$$Y = f(X,Y,B1,B2,R) \quad \ldots\ldots\ldots\ldots\ldots\ldots\ldots\ldots (5)$$

where X and Y are the independent variables and B1, B2, and R are the parameters to be estimated. The functional form of f is:

$$Z = \sqrt{(X-B1)^2 + (Y-B2)^2} \; -R \quad \ldots\ldots\ldots\ldots\ldots\ldots (6)$$

where X and Y are the X and Y co-ordinates of the data points of the admittance circle diagram, B1 and B2 are estimates of the centre point co-ordinates and R is an estimate of the circle radius. Z is taken as zero for all cases.

The programme thus requires the user to enter initial estimates for the circle radius and centre point and then adjusts these parameters to minimize the following:

$$Q = \sum_{i=1}^{n} \{o- (\sqrt{(xi - B1)^2 + (Yi - B2)^2} -R)\} \ldots\ldots\ldots\ldots (7)$$

When the final three values have been calculated, the programme then calculates Co and R from these values. Co is substituted into the above mentioned formulae and the other component values are calculated.

Figure 6a is a typical print-out of an admittance curve and figure 6b illustrates the corresponding circle diagram using the T.A.S. package. The transducer under test was a 500kHz, 50mm diameter device, faced with a thin disc of polyester. The curve is particularly clean, having only one very small satellite response, (indicated by the arrow) and the circle is therefore well defined.

Figure 7 compares the circle fitted by the computer with the actual result. The print-out of the centre co-ordinates, radius and equivalent circuit components are shown below the plot. Table 1 shows the variation in equivalent circuit component values when a PZT is immersed in various liquids.

TABLE 1 : Variation in equivalent circuit values when a PZT is immersed in various liquids

	ETHYL ALCOHOL	ACETONE	BENZINE	CHLOROFORM
Co(nF)	3,39	3,51	3,46	3,65
R_T (Ω)	23,17	23,35	27,40	31,23
L (μH)	171,67	155,11	147,79	127,22
C (nF)	0,57	0,64	0,68	0,80

For purposes of this investigation, only the value of 'R_T' is of interest, as this is the combination of mounting losses, Rm and the radiation resistance, Rr. The radiation resistance is a measure of the ultrasonic energy being transmitted to the surrounding medium.

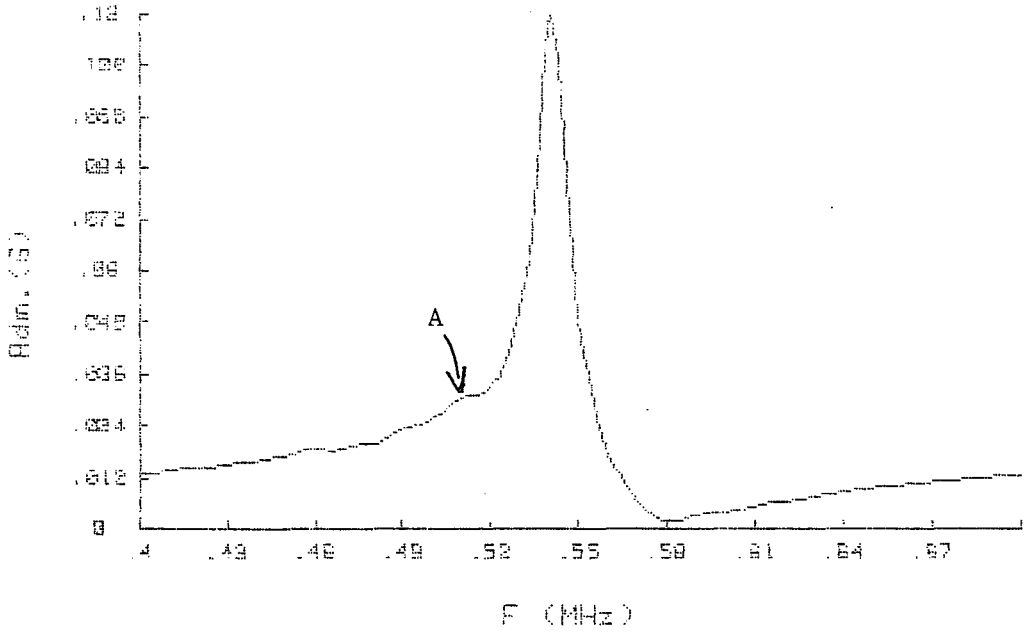

FIGURE 6a : DEVICE FACED WITH POLYESTER

Where A = Satellite response

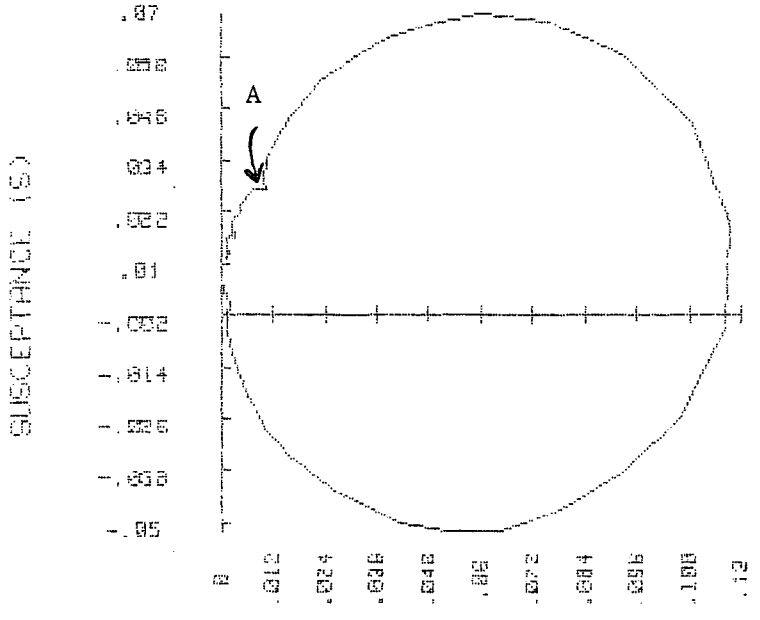

FIGURE 6b : ADMITTANCE CIRCLE DIAGRAM

Where A = Satellite response

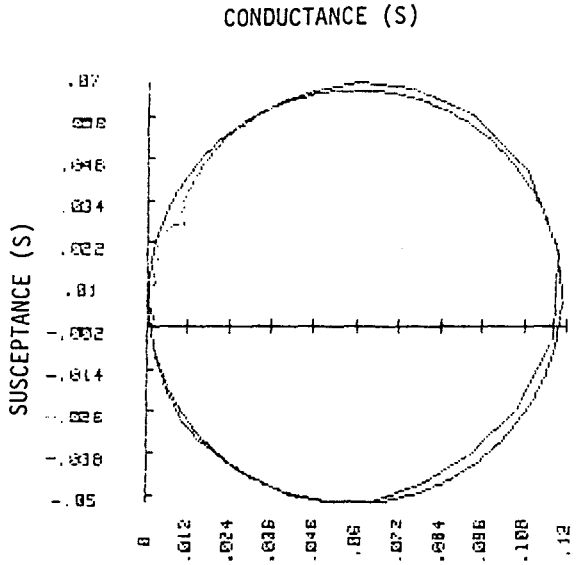


```
          PARA-                                          8773458E-03)
          PARAMETER  3=          .0589684 ( 5.8968424896E-02)
Do you want the heading underlined ? (DEFAULT=YES)
GRAPHICS WILL NOW BE DISPLAYED************************************************

ENTER Y-axis label :AL VALUE OF SUM OF SQUARED RESIDUALS = .00597627657664
          AFTER 3 ITERA                                  UALS= 9.1167747575E-5
Press <cont> to continue
CHOOSE OPTIONo label the curves on your graph ?(DEFAULT=YES)
THE CENTER POINT IS  .0595818402288  .00860084016024
THE RADIUS IS  .0589685143683
Co= 2.53025180452E-9
Ro= 1630.45464787
R= 8.47910118402
L= .000223061013832
C= 3.87991365982E-10
```

FIGURE 7 : COMPUTER PRINTOUT SHOWING BEST FIT ON ACTUAL CIRCLE

Of more relevance are the circle diagrams and corresponding equivalent circuit values for a transducer immersed in water (Figure 8) and a slurry of density 1,6 (Figure 9). Figure 10 shows a comparison of the two impedance circles, the smaller diameter corresponding to immersion in the slurry, which causes greater loading. As will be seen, the difference in resistance between the liquids is relatively small, as is also the case with different densities of slurry. However there is still sufficient resolution for the changes in resistance, due to variations in the density of a fluid or slurry, to be monitored.

3. THE DEVELOPMENT OF THE INSTRUMENT

In its simplest form, the measurement device consists of an oscillator set to the appropriate driving frequency for the PZT transducer, an output stage, and a monitoring circuit which measures the voltage developed across the PZT disc. The voltage is proportional to the impedance of the device, which is related to changes in Rr.

The development of this instrument comprised two phases. Initially, a PZT disc that gave acceptable performance was selected and constructed into a probe. An appropriate electronic circuit was then developed, and the instrument was subjected to a range of laboratory and plant tests to establish basic performance criteria. Once the viability of the technique had been established, the second phase of the investigation was devoted to optimization of the characteristics of the PZT disc and the development of packaging - interfacing methods.

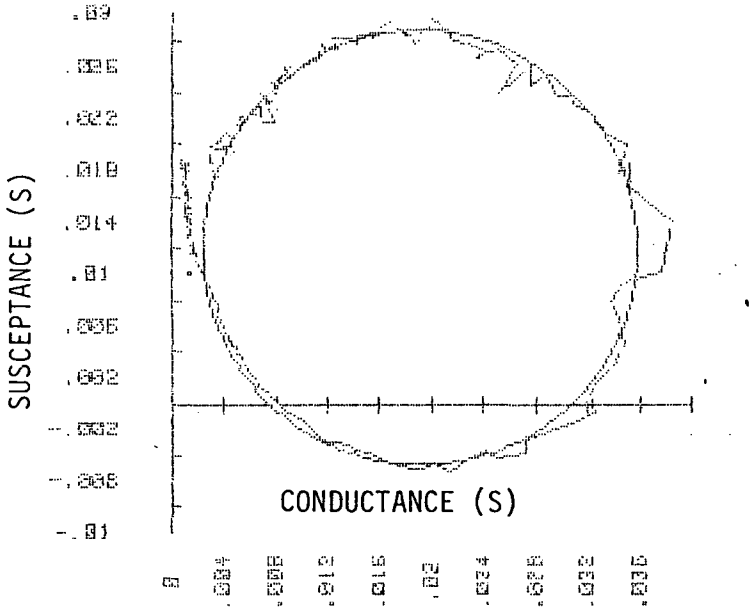

THE ESTIMATED PARAMETER VALUES AFTER 2 ITERATIONS ARE :

PARAMETER 1= .0191576 (1.9157613626E-02)
PARAMETER 2= .0120034 (1.2003413638E-02)
PARAMETER 3= .0167165 (1.6716498170E-02)

****

THE INITIAL VALUE OF SUM OF SQUARED RESIDUALS = .00209888453849
AFTER 2 ITERATIONS THE SUM OF SQUARED RESIDUALS= 7.2255615515E-5
APPROXIMATE STANDARD ERROR FROM SQUARED RESIDUALS= .00069872284801?

THE CENTER POINT IS .0191579475967 .0120026319061
THE RADIUS IS .0167165808145
Co= 3.58401162845E-9
Ro= 409.606621711
R= 29.9104228041
L= .00013616824278
C= 6.45323693696E-10

FIGURE 8 : PERFORMANCE OF TRANSDUCER IN WATER SHOWING DEVIATIONS CAUSED BY STANDING WAVES

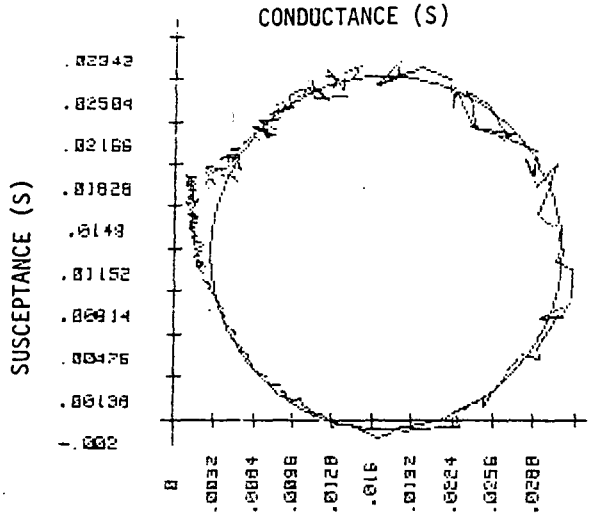

THE ESTIMATED PARAMETER VALUES AFTER 2 ITERATIONS ARE :

PARAMETER	1=	.0168908	(1.6890755267E-02)
PARAMETER	2=	.0132643	(1.3264324907E-02)
PARAMETER	3=	.0140180	(1.4018024198E-02)

****

THE INITIAL VALUE OF SUM OF SQUARED RESIDUALS = .00124980176752
AFTER 2 ITERATIONS THE SUM OF SQUARED RESIDUALS= 5.20953778936E-5
APPROXIMATE STANDARD ERROR FROM SQUARED RESIDUALS= .000560203157499

THE CENTER POINT IS .0168903205756 .013264644098

THE RADIUS IS .0140178390022
Co= 4.02888106213E-9
Ro= 348.131040853
R= 35.6688359684
L= .000101694792907
C= 9.07149724613E-10

FIGURE 9 : PERFORMANCE OF TRANSDUCER IN SLURRY

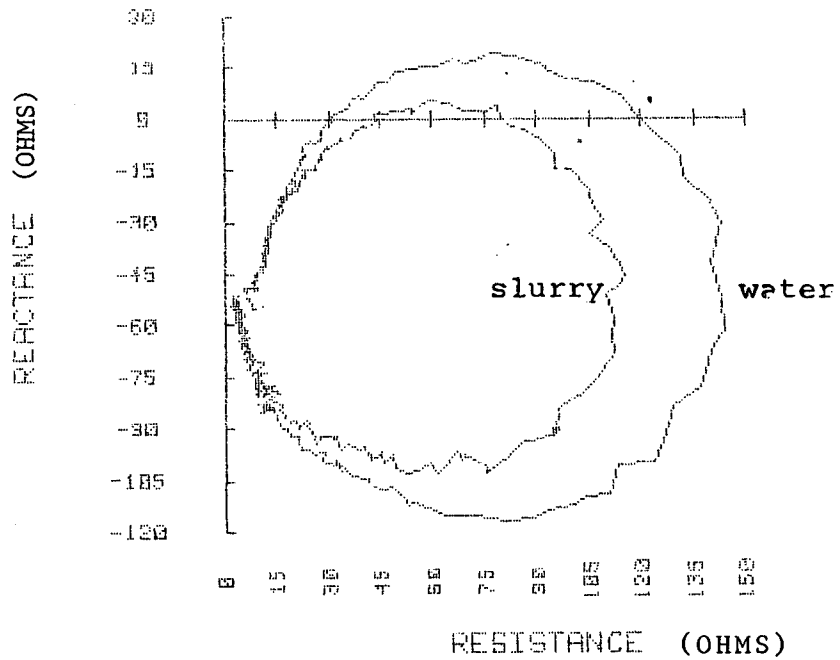

FIGURE 10 : COMPARISON OF IMPEDANCE CIRCLES FOR WATER AND SLURRY SHOWING THE DIFFERENCE IN LOADING ON THE PZT WITH INCREASE IN DENSITY OF MEDIUM

3.1 The Initial Phase

A 20mm, type 5A, 500 kHz disc was used in the initial stages of the investigation. The disc was encapsulated in Araldite 'M' resin to isolate it from the medium. The transducer was driven with a signal of constant current and frequency, and the voltage drop across the PZT was rectified so that the d.c. voltage produced would be proportional to changes in the driving impedance and hence to changes in the density of the medium.

The frequency at which the transducer is driven is the frequency at which there is the greatest change in impedance for a given change in slurry density. Figure 11 shows how this frequency was determined. The probe was immersed in a slurry of low density and the impedance was measured over the frequency range 0,4 to 0,7 MHz. This procedure was repeated using a high density slurry. The resulting curves of frequency against impedance for the two slurry densities were generated. The frequency at which the difference in impedance was greatest was selected as the operating, or driving frequency.

3.2 Evaluation of the Prototype Instrument

The oscillator - driver circuit is shown in Figure 12. A voltage controlled oscillator (vco) drives an amplifier. The tank circuit of the amplifier was tuned to 500kHz. The PZT transducer was connected across the secondary of the transformer, and the voltage developed across it was rectified and displayed on the voltmeter. The instrument was then evaluated using CIP slurry at various temperatures and stirring speeds.

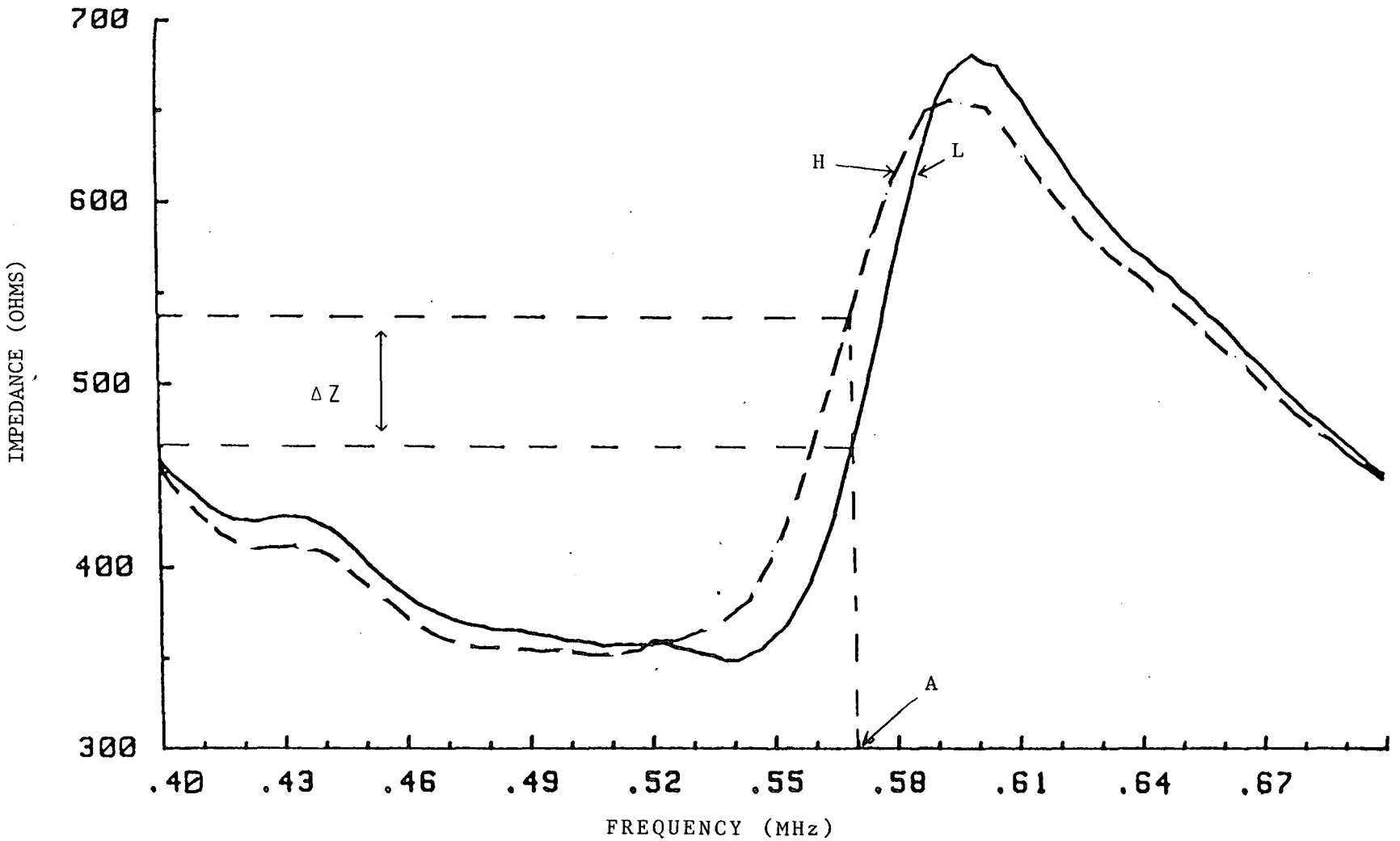

FIGURE 11 : THE COMPARISON OF TWO GRAPHS WHICH ARE USED TO DETERMINE THE OPERATING FREQUENCY OF THE TRANSDUCER

Where A = Operating frequency, Δz = Change in impedance
Curve H = High density Curve L = Low density

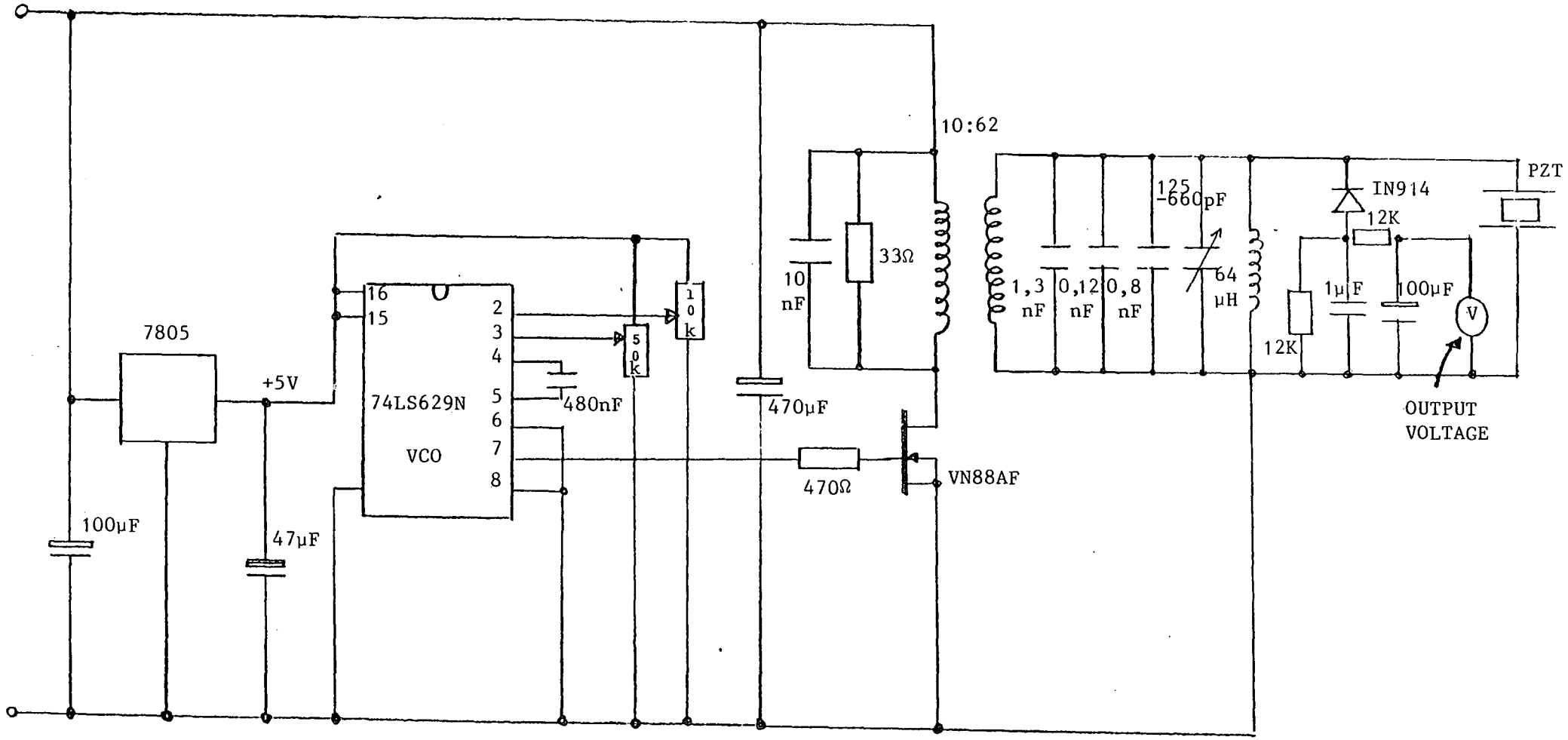

FIGURE 12 : TRANSDUCER DRIVER CIRCUIT

3.2.1 Performance of instrument with CIP slurry

The instrument was tested in a range of slurries, prepared from a bulk sample of CIP slurry. The densities were first measured using a spring balance. The range was 1,247 to 1,506 and the temperature was 25^{0}C. The probe was then immersed in the various slurries. Figure 13 shows a graph of output voltage against density and a table of the results appears below. The correlation co-efficient is 0,998.

TABLE 2 : Output voltage as a function of density

DENSITY	OUTPUT VOLTAGE (V)
1,247	10,44
1,316	10,60
1,344	10,68
1,400	10,82
1,42	10,84
1,465	11,00
1,506	11,10

3.2.2 The effect of temperature changes in slurry

For this experiment, the impeller speed was held constant at 136 rpm.

To determine the effect on the PZT of changes in the temperature of the medium, the probe was immersed in a slurry of density 1,2, at a temperature of 38^{0}C. The output voltage was monitored as the slurry cooled. The first reading was taken at 35,5^{0}C, thus allowing the system to stabilize. The results appear below in Table 3.

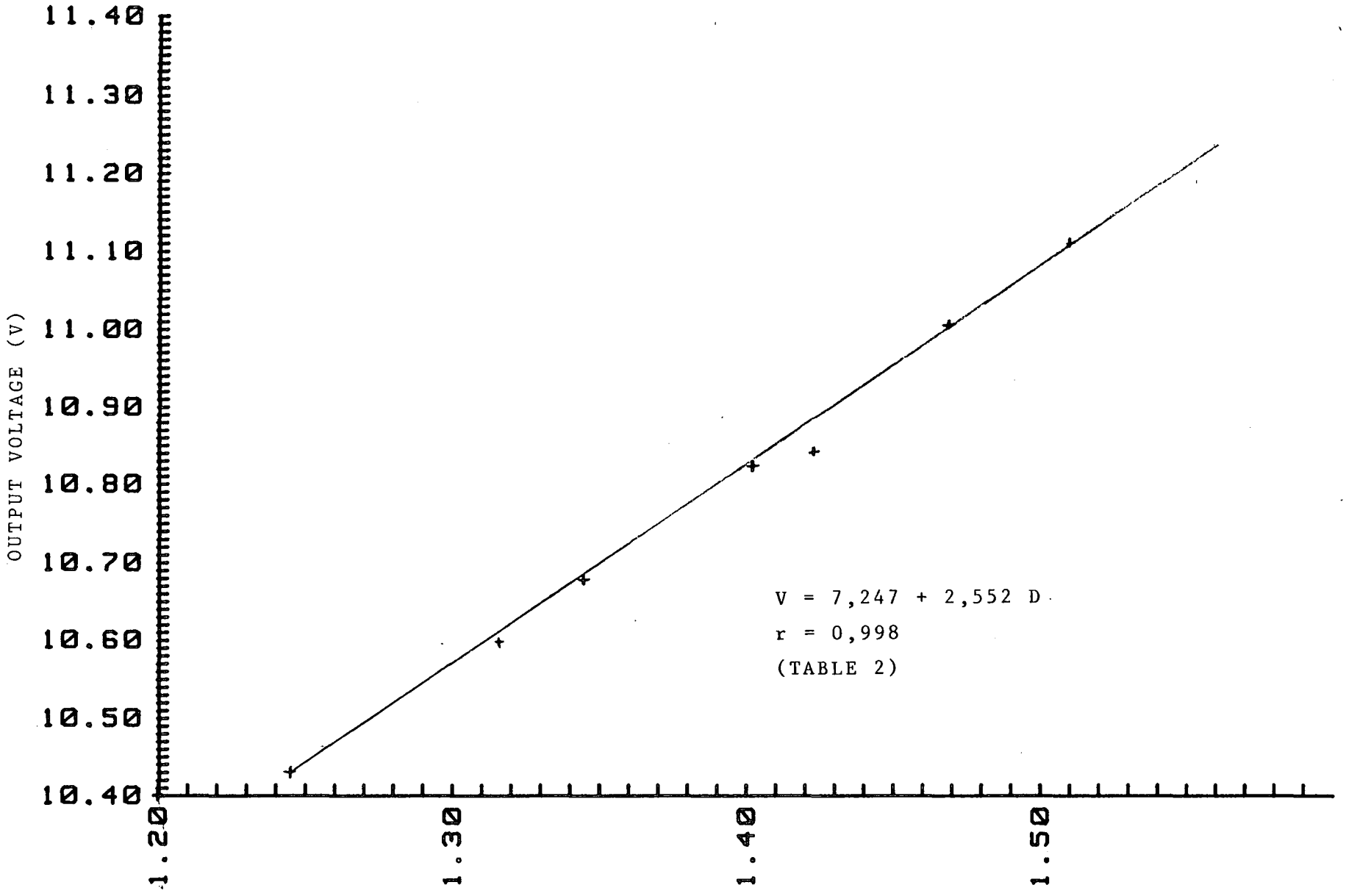

FIGURE 13 : GRAPH SHOWING THE RESPONSE OF THE INSTRUMENT TO CHANGES IN SLURRY DENSITY

TABLE 3 : Output voltage as a function of temperature

TEMPERATURE (^{0}C)	OUTPUT VOLTAGE (V)
35,5	10,68
34,2	10,60
33,75	10,57
31,10	10,55
31,50	10,47

The results show a decrease in V_0 of 210 mV for a 4°C decrease in temperature: in terms of voltage, this is only a 1,97 % change. However in terms of density, it represents an APPARENT change of 16,4% or 1,345 to 1,263, bearing in mind that the range of the instrument is only 0,5 (1,1 to 1,6). The values of apparent density change were obtained by substituting the upper and lower values of voltage (Table 3) into the equation of the graph in Figure 13. It was obvious, from these results, that temperature compensation was necessary.

A second similar test was conducted, this time raising the temperature of the slurry from 24°C to 40°C. V_0 increased from 10,77 to 11,19 - a change of 420 mV for a change in temperature of 16°. In terms of voltage this is a 3,9 % increase for a 67 % change in temperature. In terms of density it represents an increase of 33%, or 1,38 to 1,545.

These results not only confirmed the findings of the first test, but showed that the effect of temperature change was non-linear.

3.2.3 The effect of stirring speed

It was anticipated that turbulence in a small volume of slurry would effect the performance of the instrument. A test was conducted to determine this effect.

Using 3ℓ of slurry of density 1,3, the output voltage was monitored while the impeller speed was increased from 136 to 210 rpm. V_0 increased from 11,08 to 11,13. Referring to Figure 13, this is an apparent increase in density of 0,022 (1,5 to 1,521) a negligible amount of 4% over the range. In fact, this small increase could have been a genuine increase in density, as the heavier fraction of a slurry will settle out if there is insufficient agitation, that is at lower impeller speeds. This test was conducted at room temperature.

3.2.4 Summary of the initial results

Because of the effect of temperature on the PZT transducer, compensation is necessary and a sensor has to be included in the probe assembly to measure the temperature of the medium and hence of the PZT itself. (Table 3). Furthermore, the change in the impedance of the PZT is non-linear with temperature, which means that a simple method of compensation is not possible. (3.2.2).

In addition to their properties varying with temperature, different PZTs may have different operating frequencies. For example in a batch of five 500kHz devices, the parallel resonance can be anywhere in the range 500 kHz to 580 kHz. A more flexible oscillator was therefore necessary.

The output voltage was found to vary with variations in ambient temperature, this meant that the oscillator was temperature dependent, and this suggested a need for a crystal - controlled oscillator to replace the vco and its associated timing components.

4. THE PROTOTYPE PORTABLE UNIT

The initial trials of the 'Table Model' in the laboratory have demonstrated that the concept of the direct measurement of slurry density, using this technique, is possible.

The next stage of the development would be to manufacture a portable version of the original design. This would entail the construction of a new probe and its associated electronic circuitry.

4.1 The Probe

Figure 14 shows how the second probe assembly was constructed. The temperature sensor, encapsulated with the PZT, is a type TSP102 semiconductor device and provides a voltage output proportional to the temperature of the slurry. The circuit diagram is shown in Figure 1, Appendix II. The PZT disc is a 50 kHz, 5A, 20mm device with a range of operating frequencies from 491 to 532 kHz.

A photograph of the probe is shown in Plate III. The encapsulation material is Araldite 'M' resin, the thickness of which is approximately 1mm on either side of the PZT. 'M' resin was chosen because of its clarity and because it is easy to use and machine.

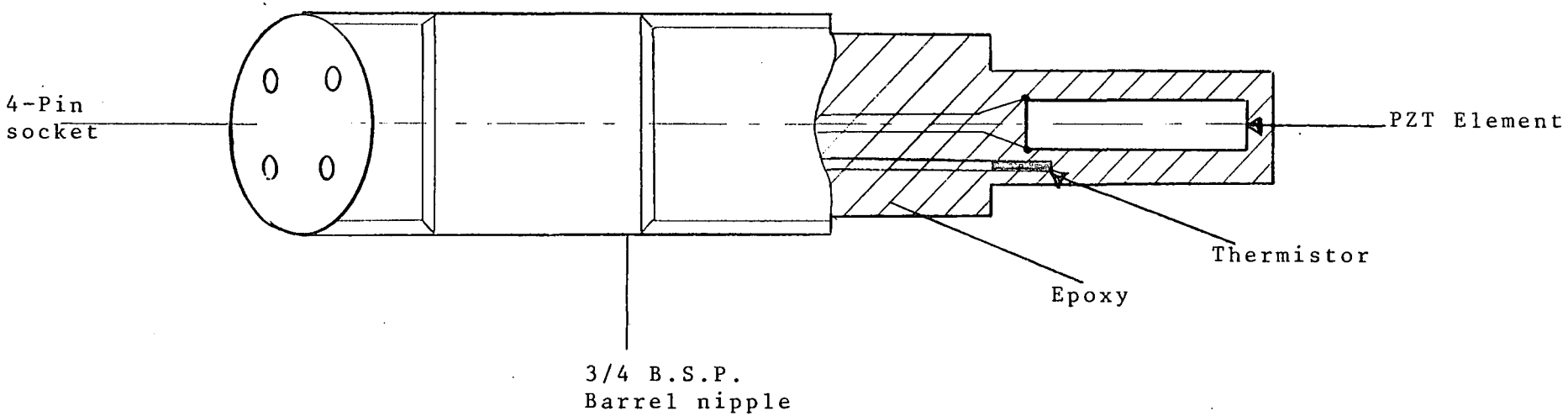

FIBURE 14 : DIAGRAM SHOWING CONSTRUCTION OF PROBE ASSEMBLY

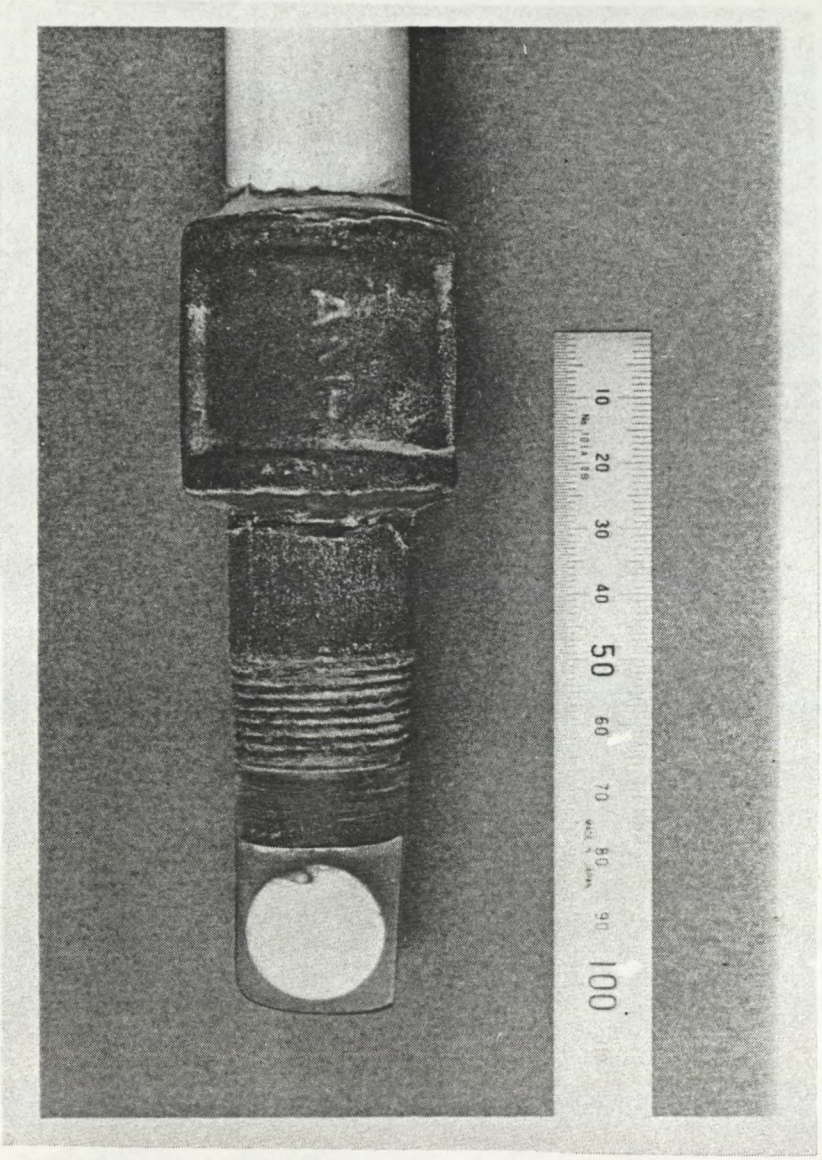

PLATE III : The Probe Assembly

4.2 Construction of the Driving Circuit

The range of operating frequencies was determined as described in Section 3.1, and was found to be 491 - 532 kHz. A crystal controlled transducer driver was constructed (Figure 15), and the frequency of the oscillator was 4,19355MHz. This frequency was divided by 8 to provide the two drivers of T1 with a signal of frequency 534, 194 kHz. This therefore was the driving frequency applied, via T1 to the transducer, and fell within the established operating range. It has already been shown in Section 3.2.1 that the output voltage, V_0, is directly proportional to the impedance of the transducer, and hence to the density of the slurry.

4.3 The Thermometer Circuit

The operation of the thermometer circuit and its calibration are described in Appendix II.

4.4 The Instrument

A digital panel meter was mounted in the lid of the instrument case to indicate the values of V_0 end V_T from the measurement and temperature circuits respectively. Either of these voltages could be applied via a toggle switch to the meter. Co-axial sockets were used to provide outputs for connection of the two voltages to a data logger. (Plate IV).

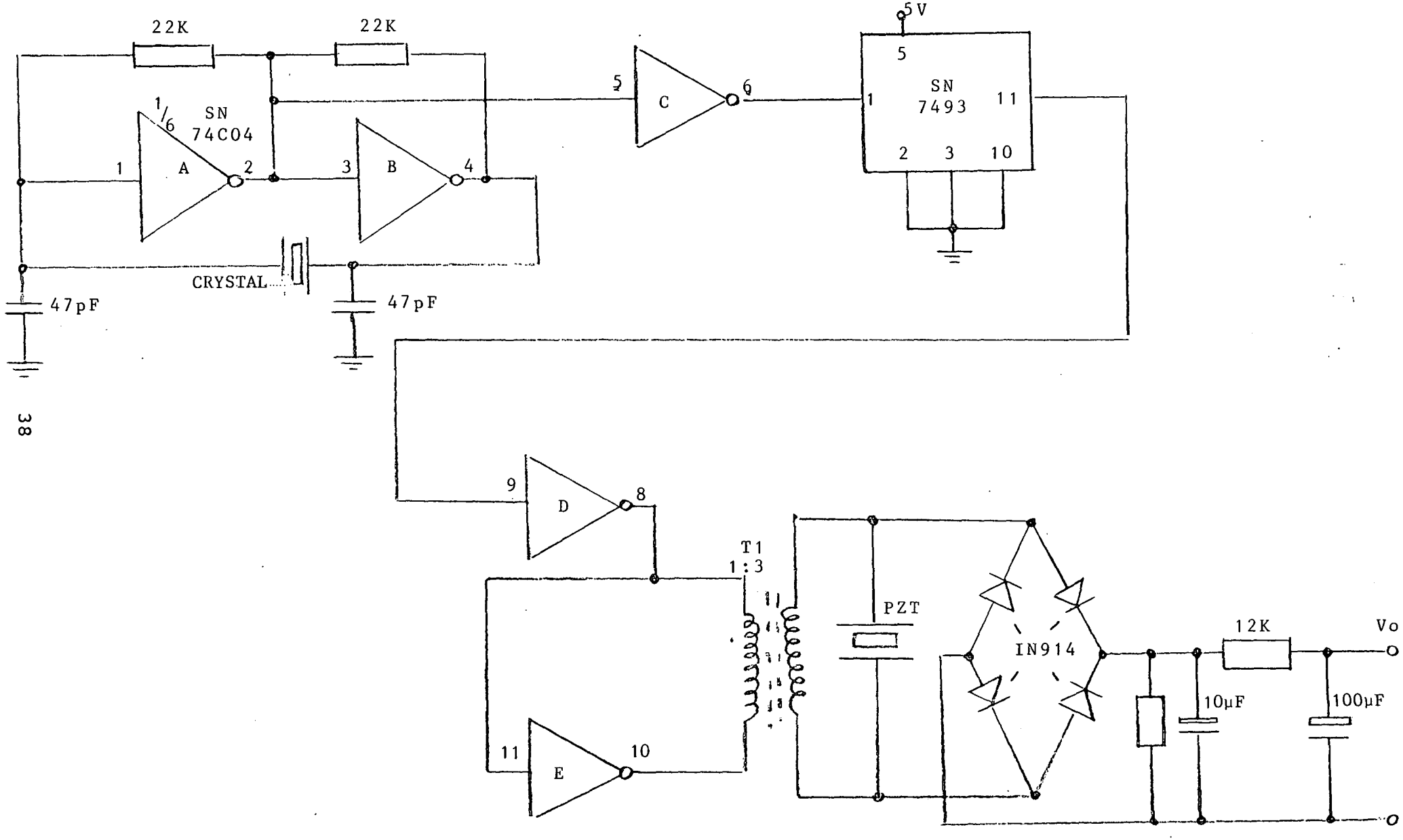

FIGURE 15 : CRYSTAL-CONTROLLED OSCILLATOR AND DRIVER

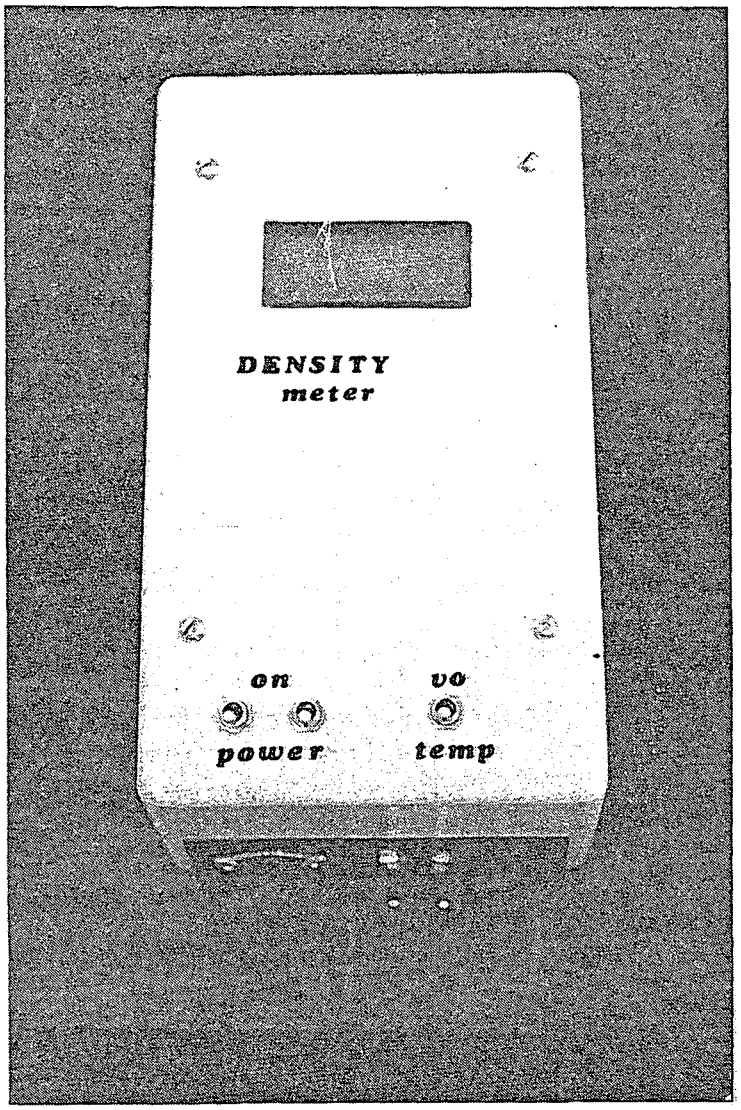

PLATE IV : THE PROTOTYPE PORTABLE INSTRUMENT

Power for the unit was provided by PM9 alkaline batteries, but provision was made for the use of an external power supply for laboratory use of the instrument. The probe assembly was connected to the instrument case via a 5-pin D.I.N. plug and socket. Co-axial cable was used for both the PZT driving signal and the d.c. supply to the temperature sensor.

4.5 Testing and Calibrating the Instrument

Before calibration, the instrument was tested in several slurries of different densities, and the result is shown in Figure 16. The correlation coefficient is 0,9899 and the slope: $y = 0,923x + 1,6356$. The temperature of all the slurries was 20^0C.

4.5.1 Calibrating the Instrument

Following this initial test, a series of temperature experiments was conducted to determine more accurately the effect of temperature changes on the PZT and hence the output voltage. Twelve slurries were used, covering the density range 1,1 to 1,69. In each case, the slurry was heated from 8^0C to 40^0C. During this procedure, the values of V_0 and V_T were recorded at regular intervals, and the results were plotted to obtain the curves shown in Figure 17 and 18. It will be noticed that the effect of temperature is more pronounced at lower densities, especially at the higher end of the temperature range. This is thought to be due to the effect of reflected waves in the lighter, or less absorbant slurries. (Kinsler, 1982).

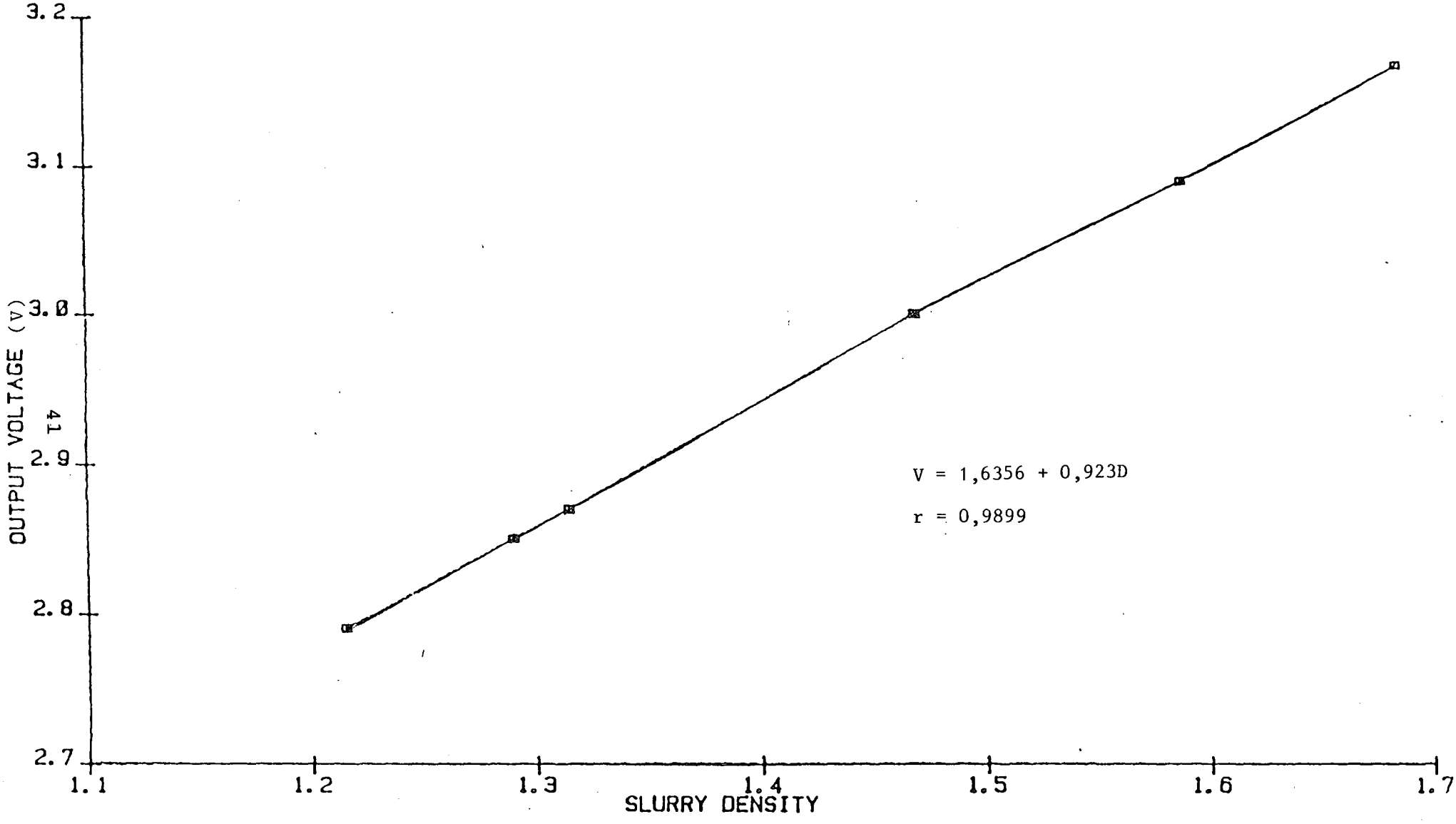

FIGURE 16 : RESPONSE OF INSTRUMENT TO CHANGES IN DENSITY

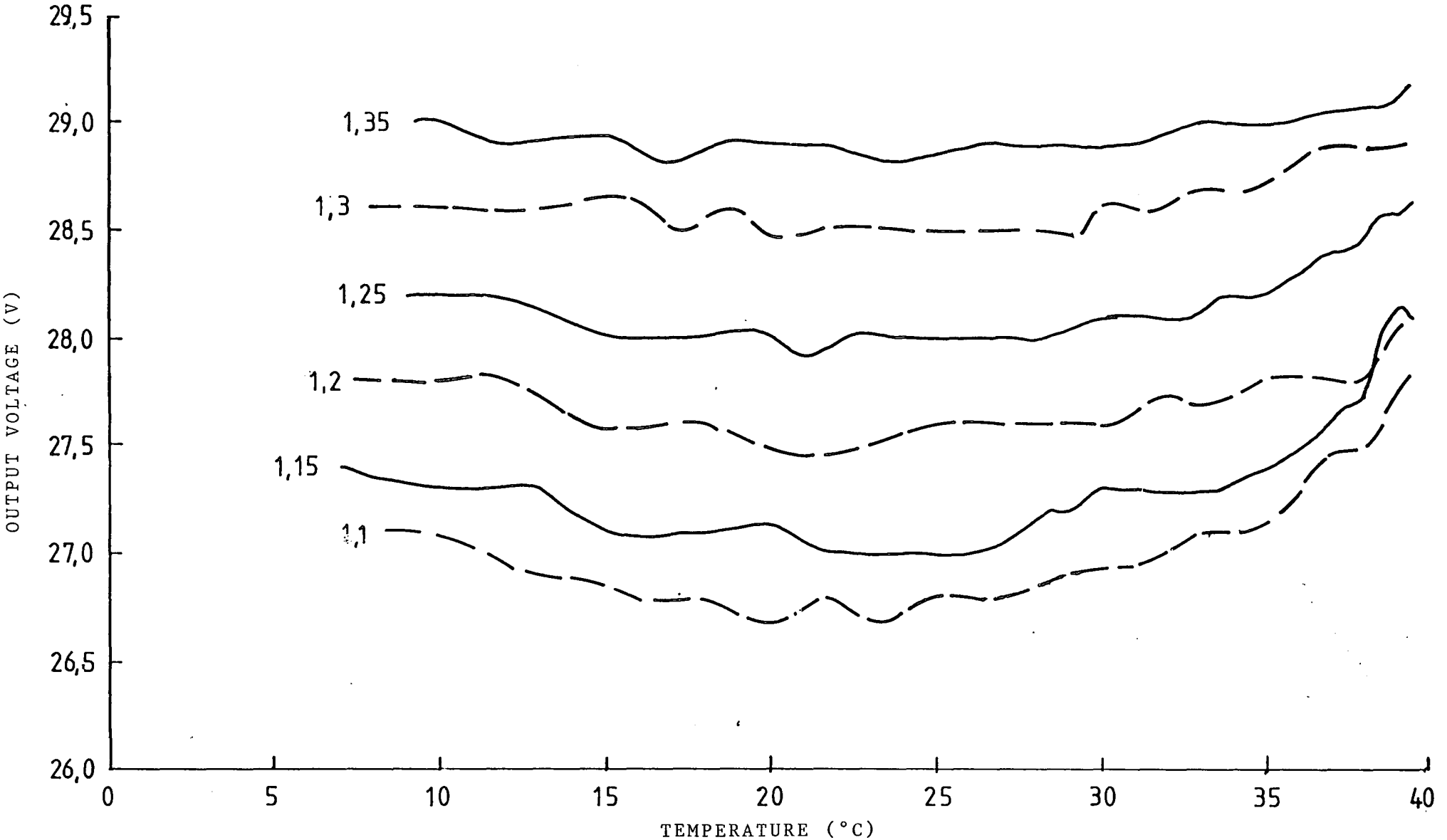

FIGURE 17 : OUTPUT VOLTAGE AS A FUNCTION OF TEMPERATURE AT DIFFERENT DENSITIES OF SLURRY FROM 1,1 to 1,35

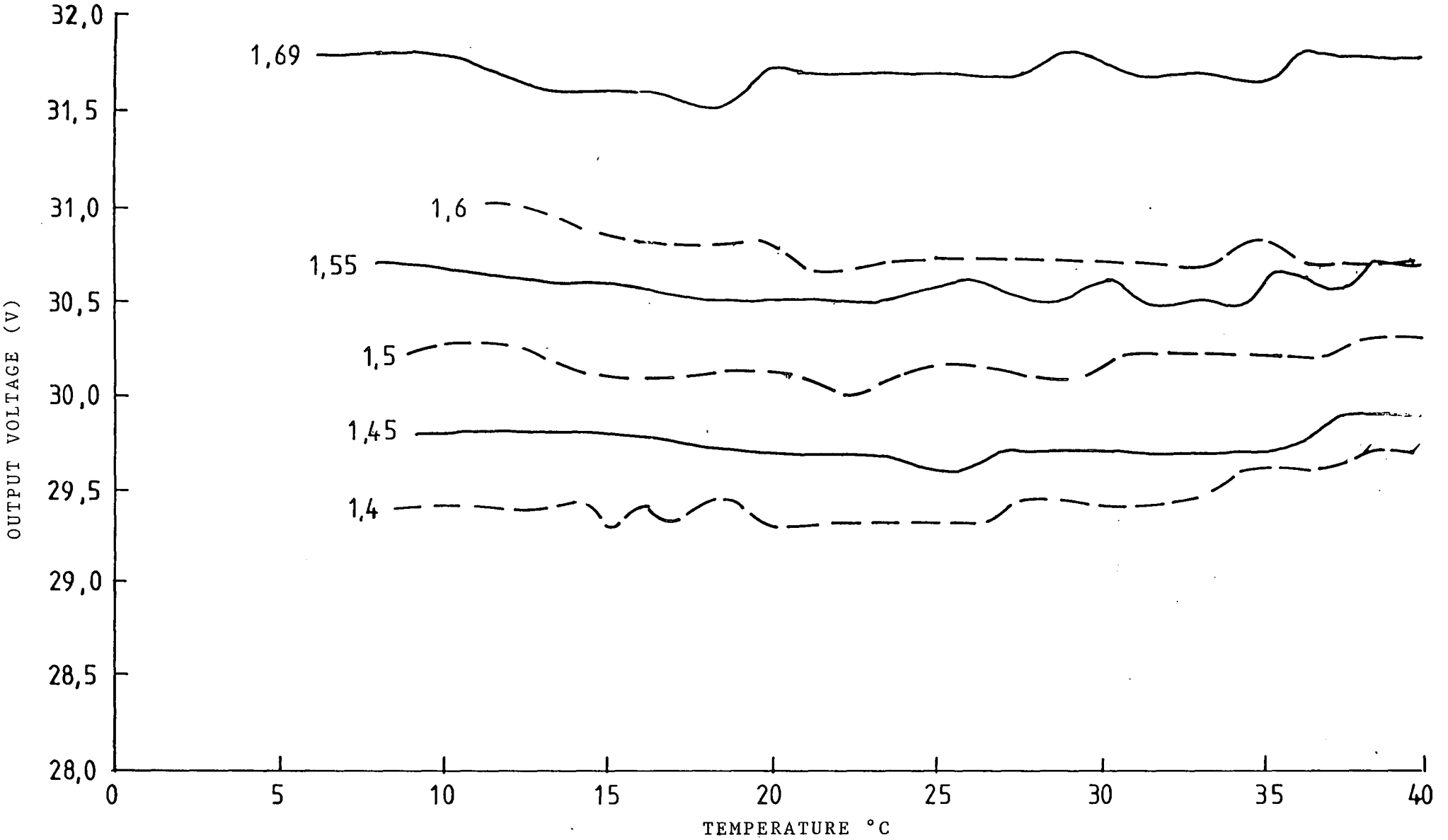

FIGURE 18 : OUTPUT VOLTAGE AS A FUNCTION OF TEMPERATURE AT DIFFERENT DENSITIES OF SLURRY FROM 1,4 to 1,69

Because of the nature of the temperature effect, simple temperature compensation was not possible and so a mathematical solution was sought.

Curve fitting was applied to the experimental data and the resultant curve fitted, takes the form:

$$\text{Density} = a_1 + a_2V_0 + a_3V_T + a_4V_0V_T + a_5V_T^2$$

where: a_i are fitted coefficients

v_0 is the output voltage

v_T is the temperature of the sensor

For this particular calibration:

$a_1 = -1,9417$

$a_2 = 0,1115$

$a_3 = 18,228 \times 10^{-3}$

$a_4 = 5,379 \times 10^{-4}$

$a_5 = -1,680 \times 10^{-4}$

Figure 19 shows a plot of actual values of density vs. fitted values of density.

4.5.2 Accuracy of the Expression

A calculator was programmed to provide a value for density, using the above expression, and six slurries of various densities were tested: a table of the results appears below in table 4. The correlation coefficient is 0,9945.

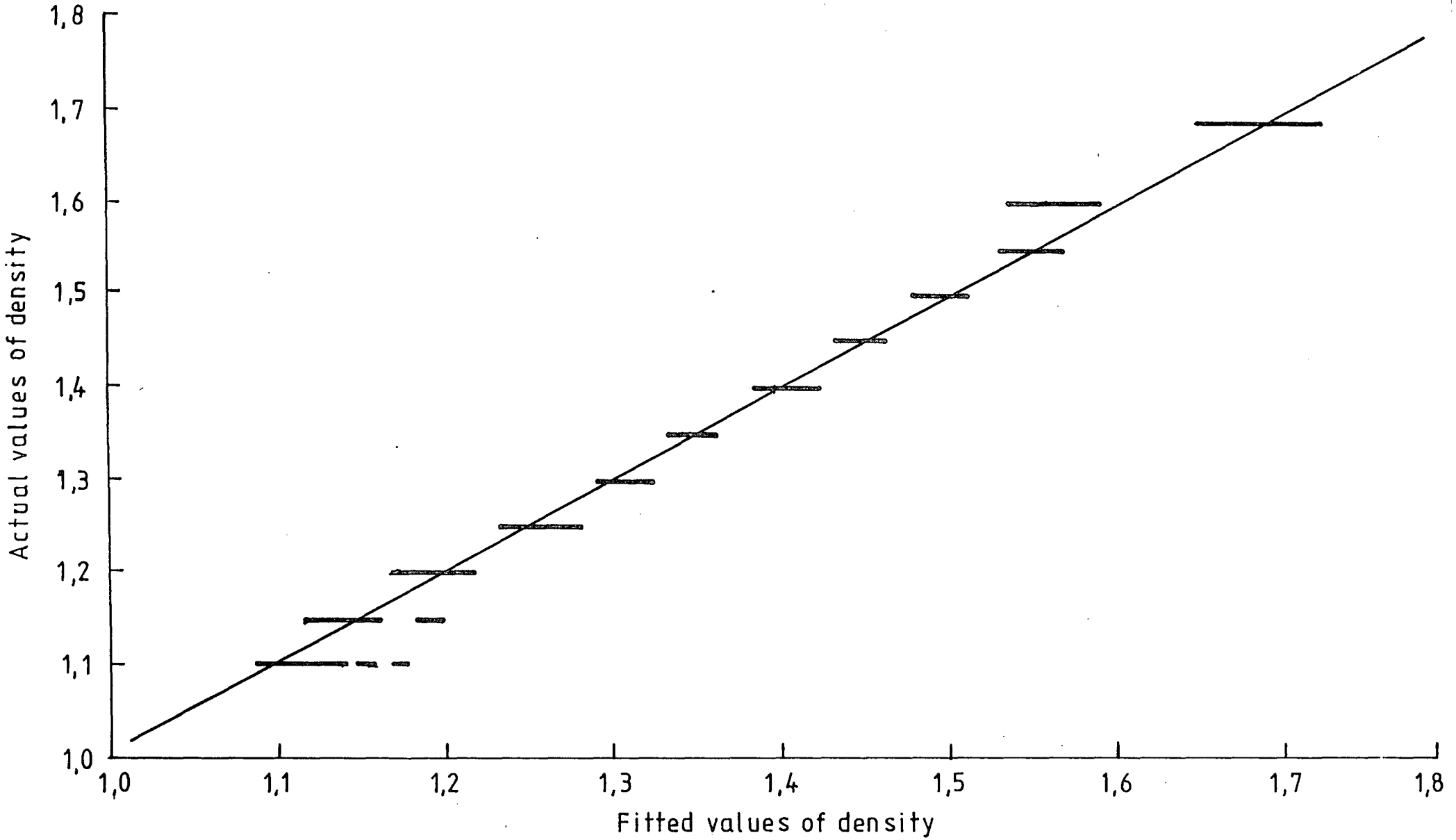

FIGURE 19 : ACTUAL DENSITY vs. FITTED VALUES OF DENSITY

TABLE 4 : A check on the calibration over a temperature range of 18,6^{0}C to 19,1^{0}C, and a density range of 1,27 to 1,58

ACTUAL DENSITY	TEMPERATURE	V_0	CALCULATED DENSITY
1,58	19,1	30,7	1,58
1,48	19,0	30,0	1,49
1,41	19,1	29,5	1,43
1,35	19,7	29,0	1,37
1,33	19,7	28,9	1,36
1,27	18,6	28,3	1,27

The experiment was repeated and the results appear in table 5. The correlation coefficient is 0,9968.

TABLE 5 : A check on the calibration over a temperature range of 28,6^{0}C to 36,9^{0}C and a density range of 1,3 to 1,58

1,58	28,6	30,5	1,56
1,49	28,7	29,8	1,47
1,41	29,0	29,4	1,42
1,35	34,3	29,0	1,35
1,32	35,4	28,8	1,32
1,30	36,9	28,7	1,30

Curves of both of these experiments appear in Figure 20 and a plot of accuracies in Figure 21. The results adequately demonstrate the accuracy of the expression.

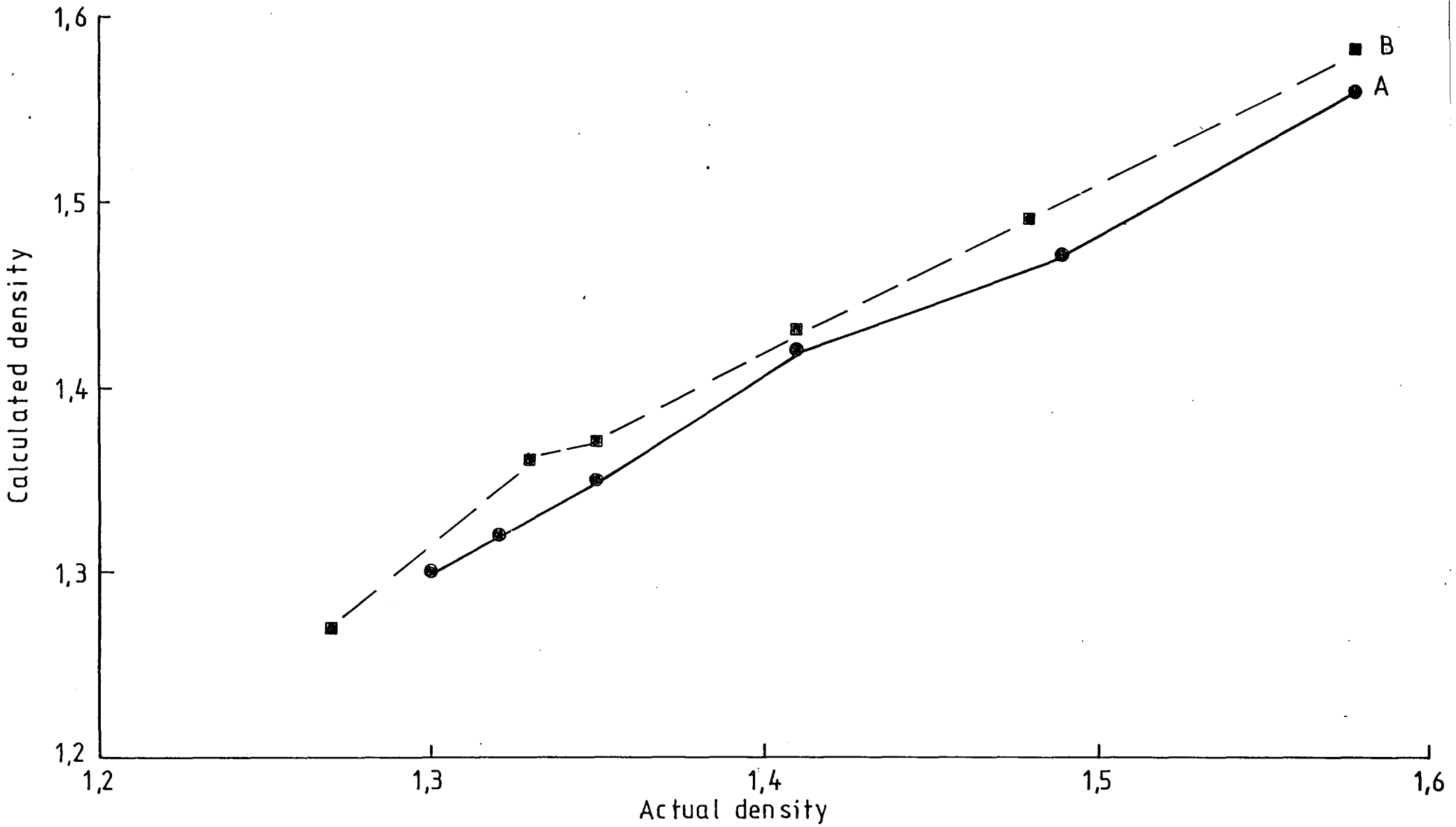

FIGURE 20 : ACTUAL DENSITY vs. CALCULATED DENSITY OVER TWO RANGES OF TEMPERATURE

A = Range of temperature from 28,6 to 36,9°C
B = Range of temperature from 18,6 to 19,7°C

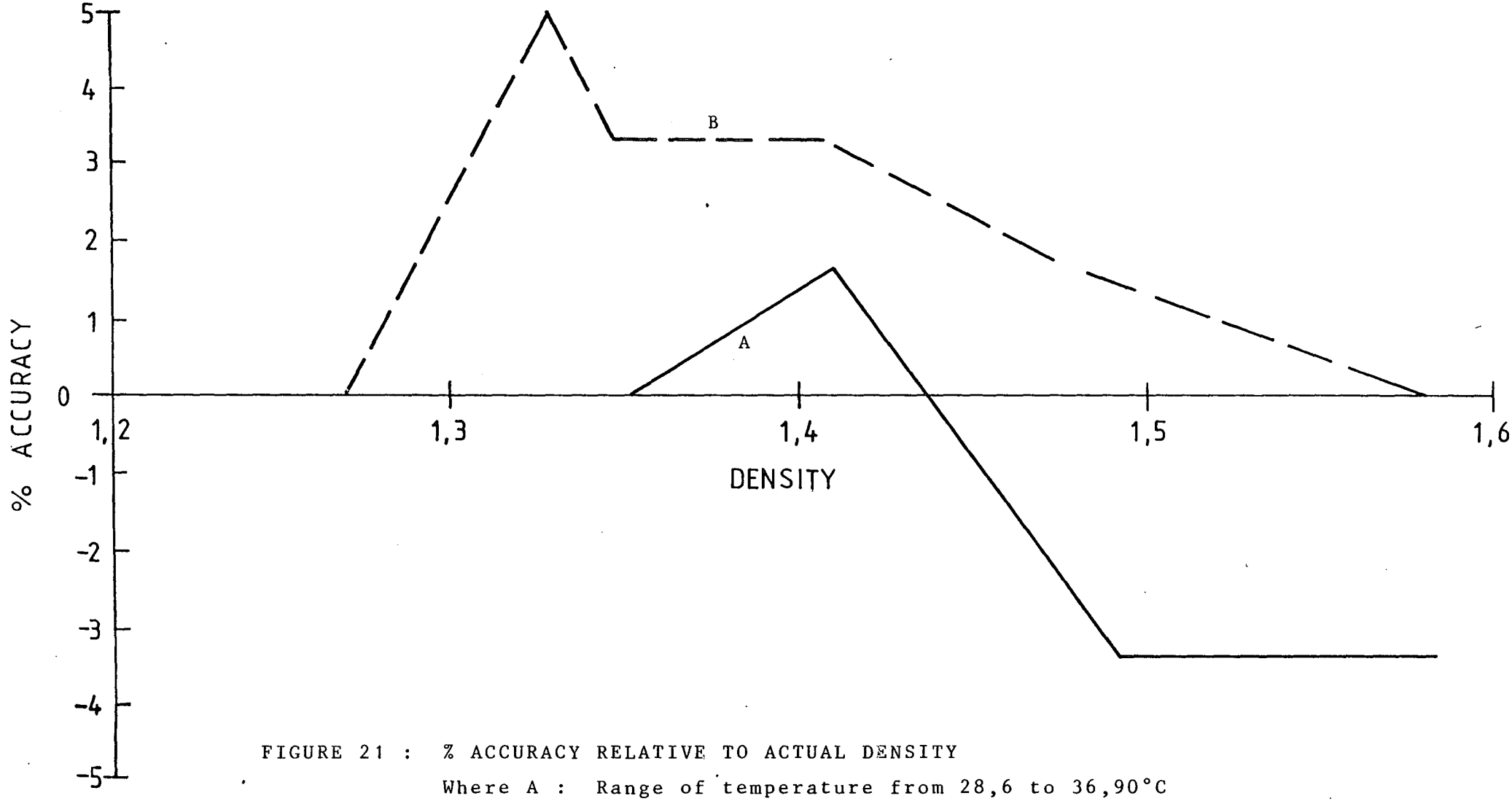

FIGURE 21 : % ACCURACY RELATIVE TO ACTUAL DENSITY

Where A : Range of temperature from 28,6 to 36,90°C
B : Range of temperature from 18,6 to 19,7°C

5. AN INSTRUMENT FOR PLANT USE

A portable laboratory instrument was constructed and tested, thereby demonstrating the feasibility of such a device. The next step in the development was to manufacture an instrument that would be suitable for use in the mineral processing environment.

The probe assembly was protected by a PVC cover with apertures parallel to the faces of the PZT (Plate V). There was no particular reason for choosing PVC apart from the fact that it was readily available and easy to machine.

The electronics was rebuilt and made use of an improved oscillator circuit that provided a range of synthesized frequencies to suit a wide range of 500kHz PZT transducers. A die-cast metal box was used as the electronics enclosure and instrument outputs are via co-axial sockets. Three of these are provided: one for temperature (V_T), one for the PZT (V_0) and one for output to a voltmeter: this is connected to either of the other two outputs via a single-pole, double throw toggle switch, so that either V_0 or V_T may be selected for display. A socket is provided to allow the connection of an external power supply and the probe is connected to the enclosure via a 5 pin, DIN plug and socket. The co-axial cable previously used between the probe and the enclosure has been replaced by a cable consisting of two separately shielded, twisted pairs: one for the PZT and one for the temperature sensor. Plate VI shows the instrument enclosure.

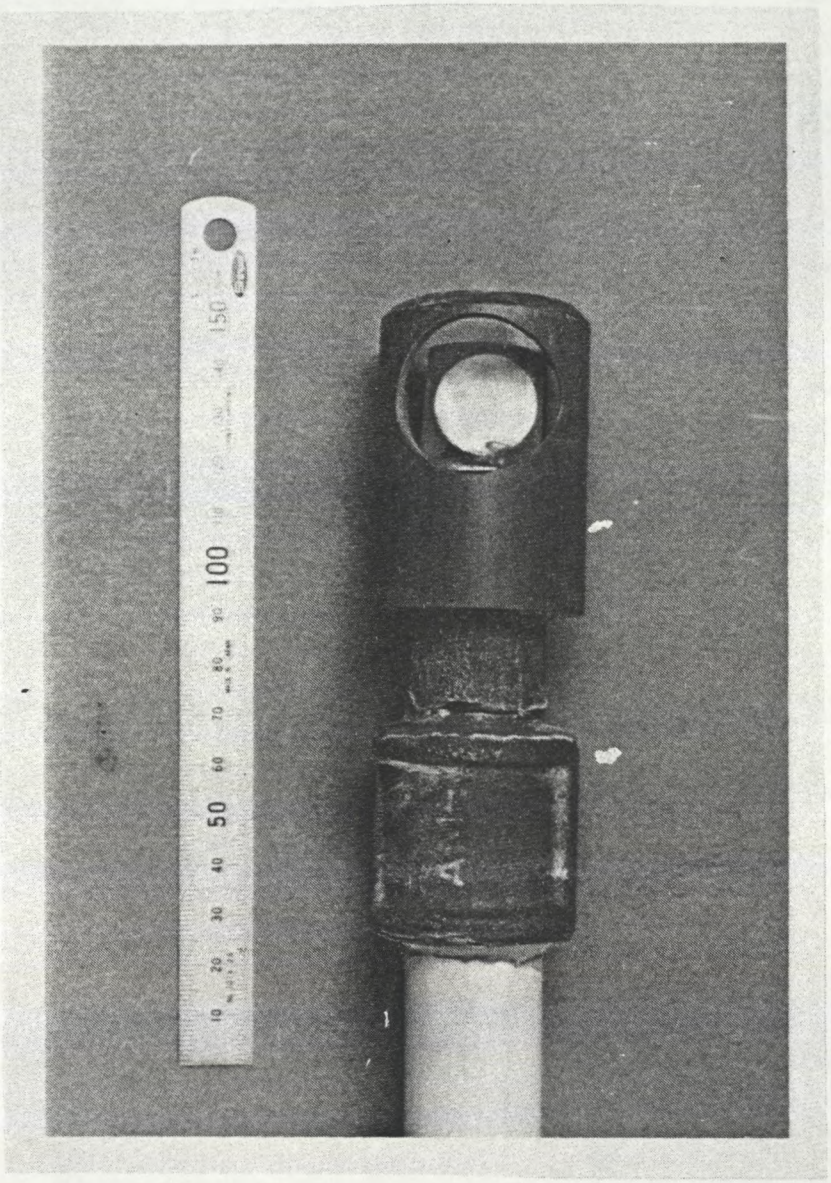

PLATE V : THE PROTECTIVE COVER

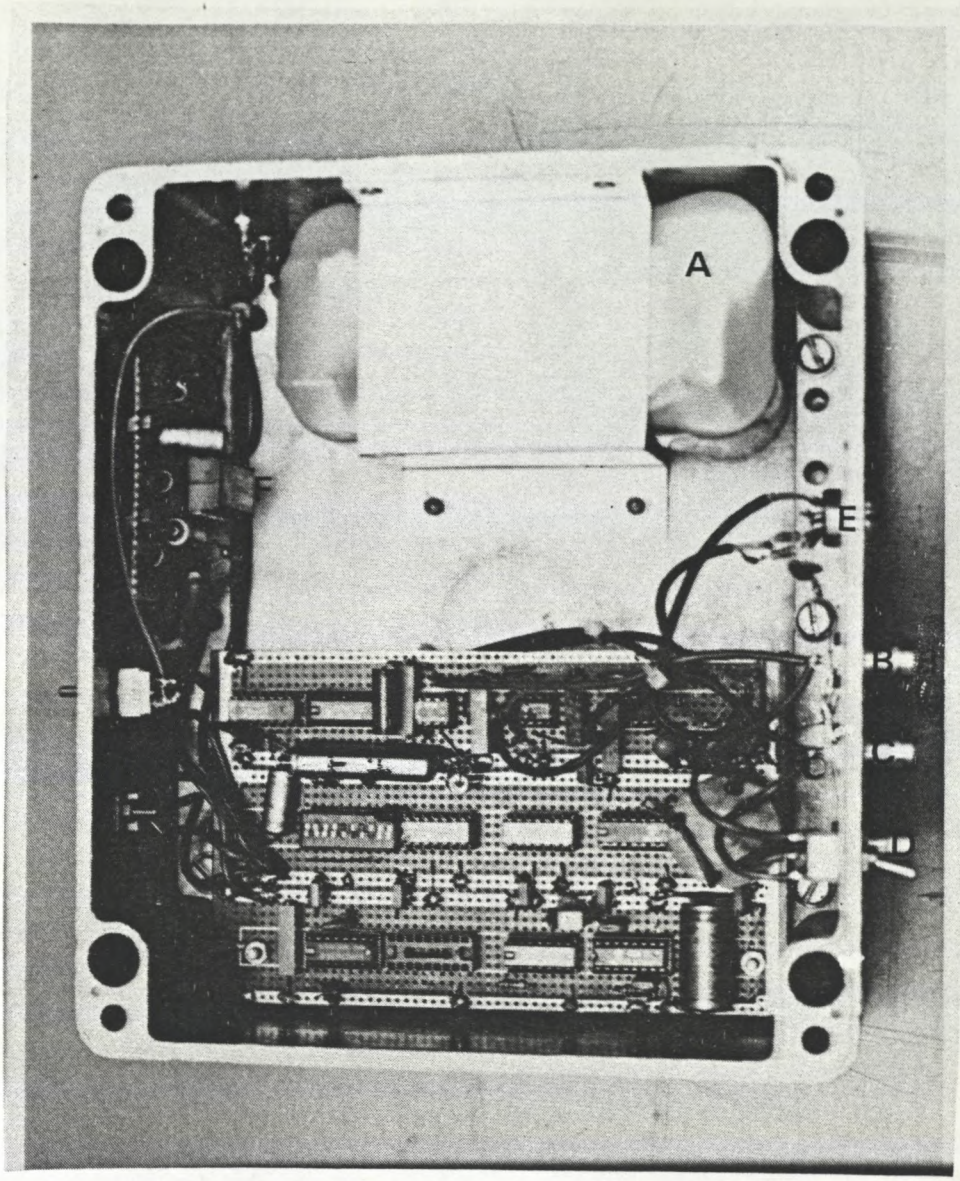

PLATE VI : THE INTERIOR OF THE ELECTRONICS ENCLOSURE

Where

A	=	Battery pack
B,C, and D	=	Outputs to computer and voltmeter
E	=	Probe output socket
F	=	dc to dc Converter

5.1 The Modified Instrument

5.1.1 The frequency synthesizer

The output frequency range of the circuit is 500 kHz to 600 kHz in increments of 10 kHz: the 100 kHz pulse train, f_1, is divided by 10, (M) and the resultant 10 kHz signal applied to the phase comparator. (Figure 22).

An example of an output frequency calculation is shown below.

Assuming a value for fo of 500 kHz and because $fo = \frac{f_1 N}{M}$,

where

f_1 = Oscillator frequency (100 KHz)

N = Dividing factor, and

M = Oscillator frequency dividing factor

The value of N will be:

$$\frac{Mf_0}{f_1}$$

$$= \frac{10 \times 500 \times 10^3}{100 \times 10^3} = 50$$

The output frequency of the divide-by-N circuit will therefore be 10 kHz and the circuit is locked at 500 kHz.

If it is desired to select another frequency, the circuit operates in the following manner.

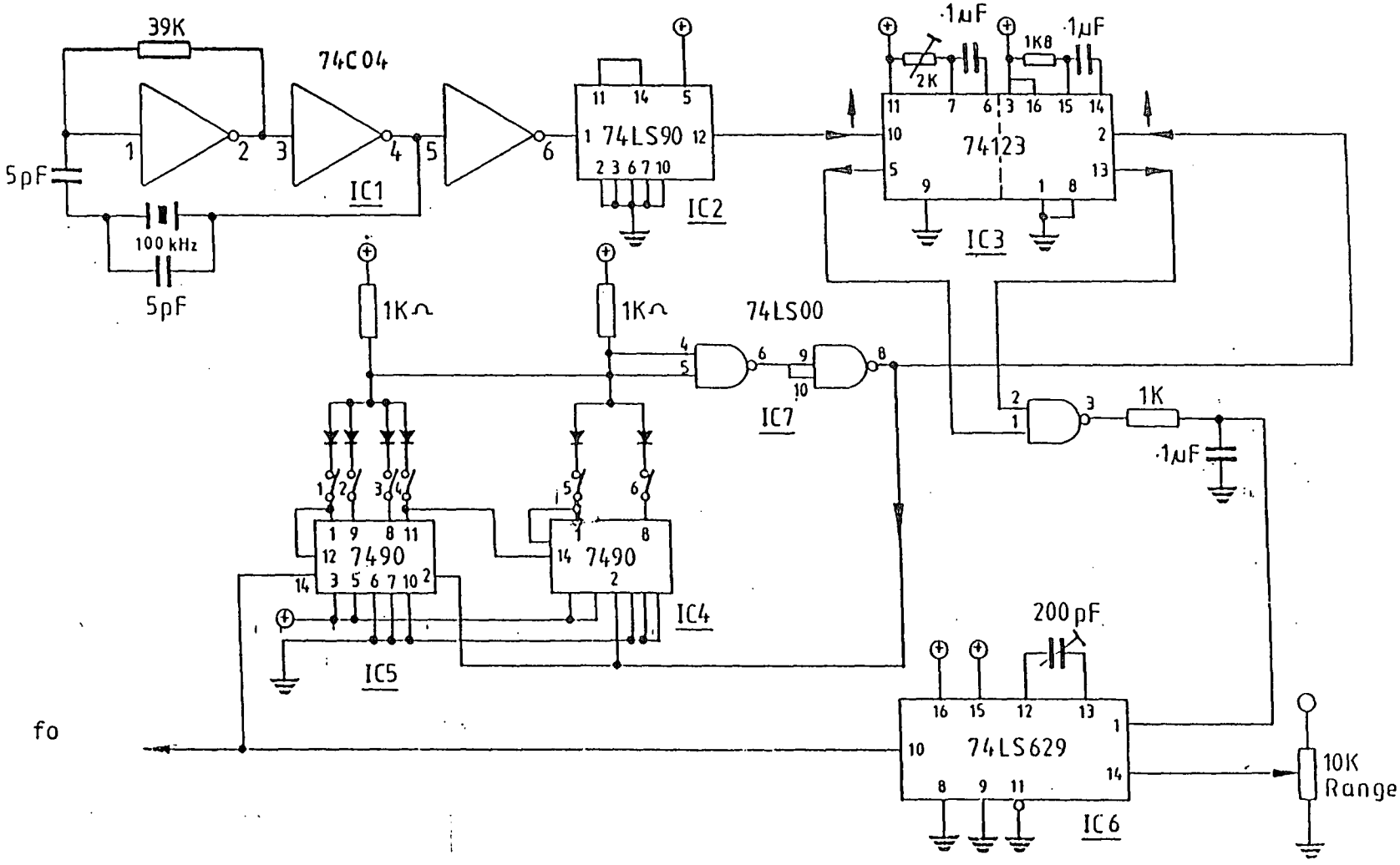

FIGURE 22 : CIRCUIT DIAGRAM OF THE FREQUENCY SYNTHESIZER

If a frequency of 550 kHz is required, the value of N is set at 55: the pulse width at the output of the phase comparator increases, with a corresponding increase in dc. voltage at the output of the low pass filter. This increase in control voltage causes the frequency of the voltage controlled oscillator to increase, until the output of the divide-by-N circuit is again 10 kHz, at which point the circuit locks on to the new frequency of:

$$f_0 = \frac{f_1 N}{M} = \frac{100 \times 55}{10} \quad \text{or 550 kHz.}$$

5.1.2 The power supply and driver circuits

Power for the instrument is derived from a re-chargeable Nickel-Cadmium battery pack: the pack consists of eight VR4D cells connected in series, and is charged via the protection diode and the 4,7Ω resistor. Operating time of the unit between charges is approximately ten hours and to charge the battery pack fully, takes about 14 hours, at a current of 0,4A.

Three voltages are needed for the circuitry: 5V for the synthesizer and +12V and -12V for the operational amplifiers: the 5V regulator supplies both the synthesizer and the type PM651 d c -d c converter, which in turn provides the ∓ 12V for the thermometer circuit, and also buffer, A1, at the output of the low pass filter in the driving circuitry. (Figure 23).

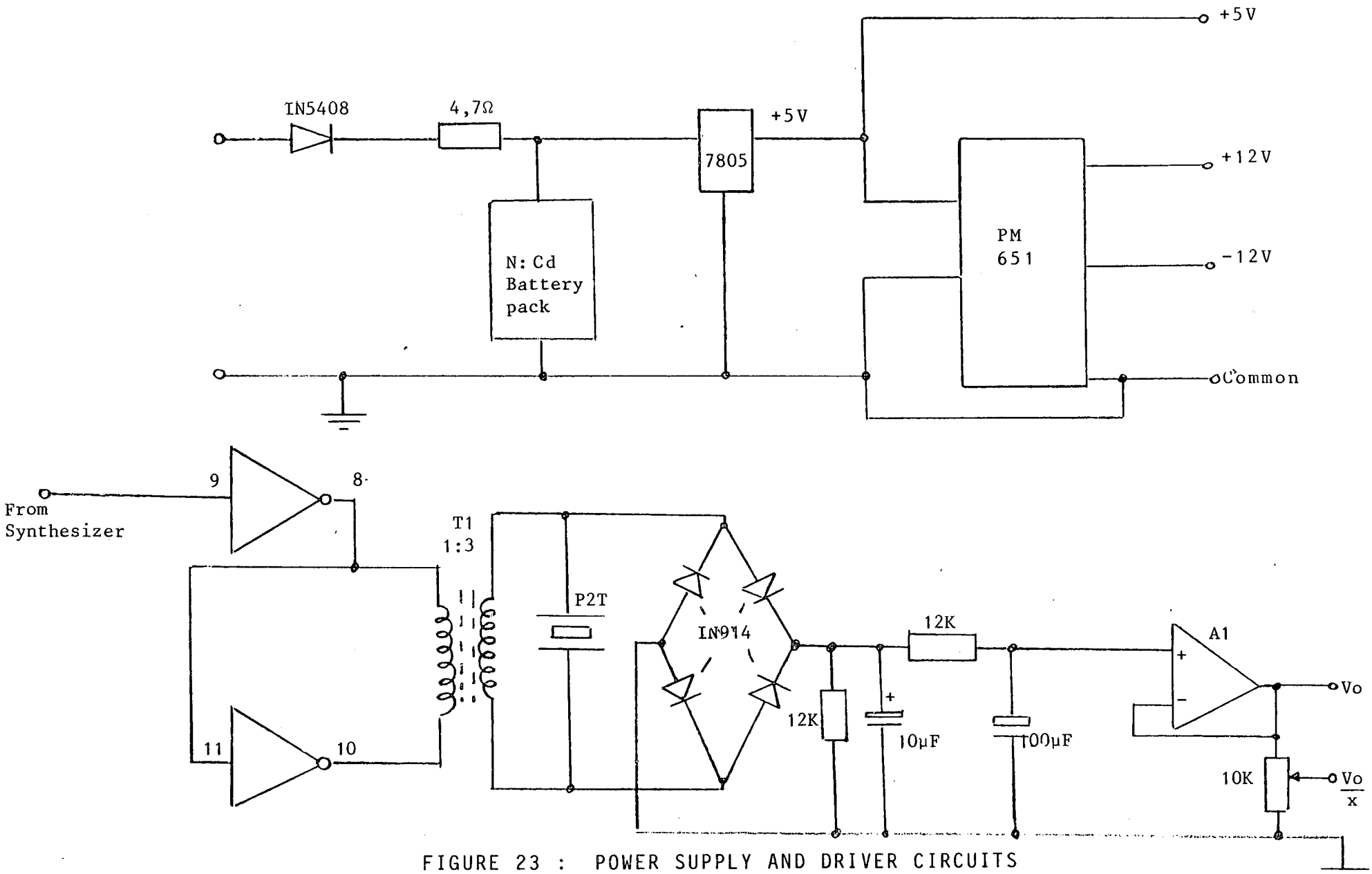

FIGURE 23 : POWER SUPPLY AND DRIVER CIRCUITS

The driving circuit has remained unaltered, (Figure 23) and the original probe assembly is being used. The operating frequency has been changed from 524,2 kHz to 520,6 kHz, as this is the nearest synthesised frequency.

5.2 Testing the Unit

Because of re-building and re-cabling the unit and also changing its operating frequency, a re-calibration was necessary, and the temperature experiments described in section 4.5 were repeated. However, prior to this, three experiments, not requiring calibration, were performed:

It was thought that wall proximity would have an effect on the performance of the instrument, due to transmitted waves striking the wall and reflecting back to the probe. (Blitz, 1971; Kinsler, 1982). An experiment was conducted to determine this effect.

There was a possibility that changes in hydrostatic pressure would effect the instrument: this was also investigated.

The third experiment was conducted to compare the performance of the instrument in non-particulate and particulate media.

5.2.1 Hydrostatic pressure experiment

The hydrostatic pressure experiment was brief and showed that V_0 did not change with changes in depth of immersion - the probe was immersed to a depth of 10m in water, a pressure of about 100KPa. The cable was lengthened for this test.

5.2.2 Performance in particulate and non-particulate media

For a particulate medium to 'appear' homogenous to a sound wave, the particles should be at least 30 times smaller than the wavelength of the transmitted wave, i.e. less than 115μm.

Assuming a velocity of 1800ms^{-1} for sound waves in slurry, the wavelength, λ, is calculated as follows:

$$\lambda = \frac{C}{f} = \frac{1800 \times 10^3}{520 \times 10^3} = 3,462 \text{ mm}$$

where: C = speed of sound in the medium, mm s^{-1}

f = frequency, Hz

A size analysis was conducted on the test slurry and showed that only 13 % of the particles were larger than 106μm, and the slurry was therefore considered to be homogeneous. A linear result of V_0 against density was obtained with this slurry.

A second test was conducted where a mixture of water and glycerine was used as the non-particulate medium. The medium was prepared as follows:

500mℓ of glycerine were added, in 50mℓ steps, to 1,5ℓ of slowly stirred water: the table of V_0 vs. solution density, appears below and the graphical results in Figure 24. It will be seen that the result is linear, the correlation coefficient is 0,9969.

TABLE 6a : The response of the instrument to changes in density of a non-particulate medium

DENSITY	V_0
1	0,259
1,0077	0,260
1,015	0,262
1,022	0,264
1,028	0,266
1,034	0,267
1,04	0,269
1,045	0,271
1,051	0,272
1,055	0,273
1,06	0,274

5.2.3 To determine the effect of wall proximity

The experiment was performed to determine the effect of the proximity of the vessel walls on the instrument performance. Two media were used - glycerine, with a density of 1,26 and slurry, as the particulate medium, with a density of 1,2.

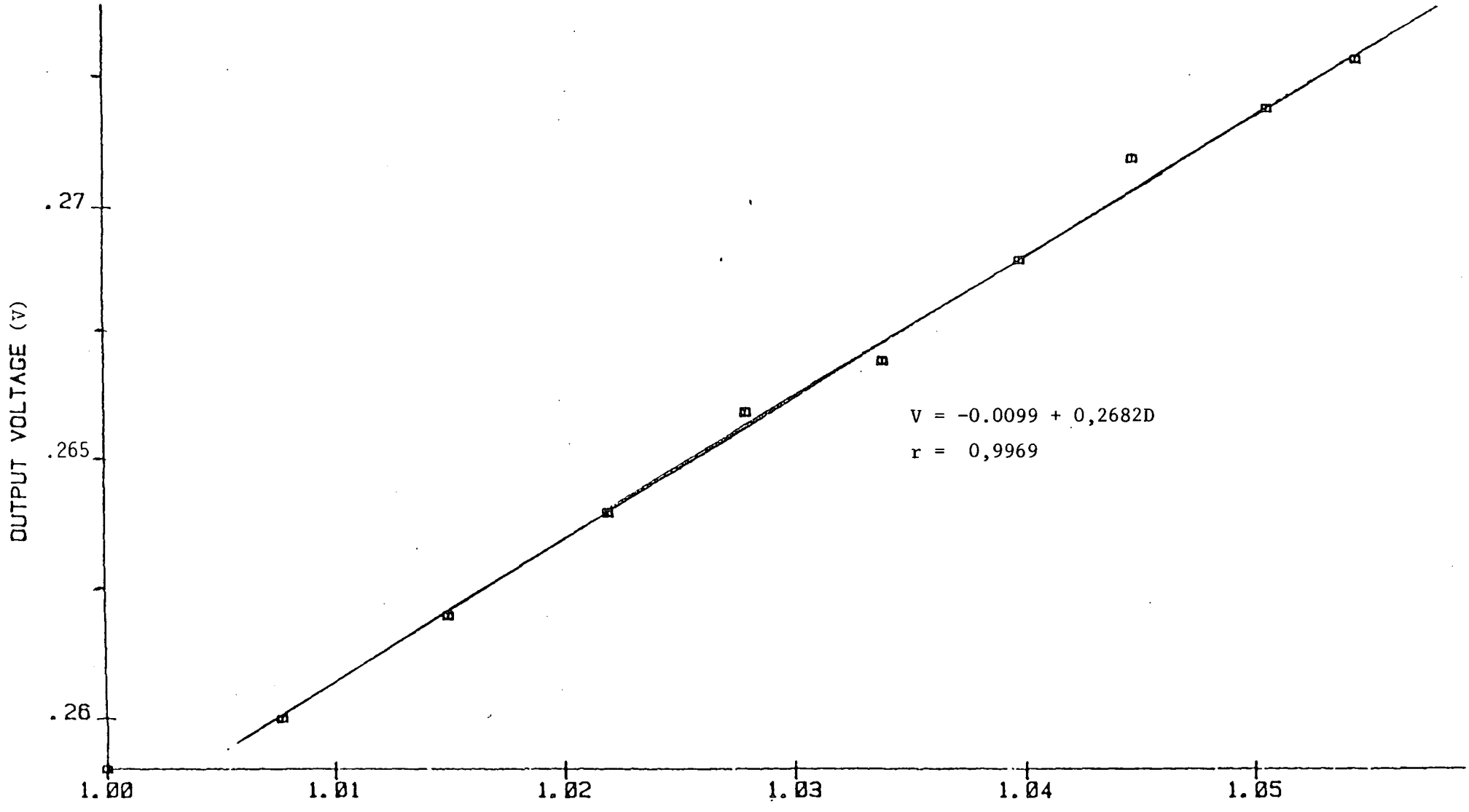

FIGURE 24 : RESPONSE OF INSTRUMENT USING INCREASING CONCENTRATION OF GLYCERINE AS THE NON-PARTICLE MEDIUM

Two diameters of beaker were used: 170mm (5ℓ), 90 and 70mm (250 mℓ). In both cases, the probe was positioned at the centre of the beaker so that its centre was 85mm, and 35mm respectively, away from the wall of the beaker.

Using glycerine, the value of V_0 changed from 21,89 in the 250 mℓ beaker to 22,73 in the 5ℓ beaker; using the expression on page 20, this represented a change in density of 0,145 (1,125 to 1,27)(density of glycerine is 1,26).

Using slurry, this effect was very greatly reduced - the apparent density change from small to large beaker being only 0,005 (1,225 to 1,230).

These results, shown in Table 6b, indicate that the volume of medium analysed depends upon the attenuating quality of the medium - the more absorbant, the smaller the volume needed and vice versa.

TABLE 6b : The comparison of the apparent changes in density in different sizes of vessel, using glycerine and slurry

DIAMETER OF BEAKER (mm)	DISTANCE OF CENTRE OF PZT FROM WALL (mm)	APPARENT CHANGE IN DENSITY	
		GLYCERINE	SLURRY
70	35	1,125	1,225
170	85	1,270	1,230
	APPARENT CHANGE	0,145	0,005

As the glycerine has a lower attenuating quality than the slurry, a greater distance, is necessary to absorb the energy radiated from the PZT. If the wall of the container happens to be closer to the PZT than the required distance for total absorption, then some of the energy will be reflected back towards it, changing its impedance and hence the value of V_0 (Blitz, 1971; Kinsler, 1982). This implies that the position of the probe, relative to the container wall, has a bearing on the operation of the instrument.

5.3 Re-calibration

Because of the different operating frequency used and the re-building of the instrument, a similar set of experiments to those mentioned in section 4.5, was performed; the results of these experiments are shown in Figures 25 and 26.

Compared with the first set of calibration curves, these show a more pronounced decrease in the value of V_0, as temperature increases. This could be due to the change in operating characteristics of the PZT, with the change in operating frequency. (Section 5.1.2).

Again, curve fitting was applied to the experimental data and as expected, the expression for the curve fitted is similar to the previous result. For clarity, both expressions are shown below.

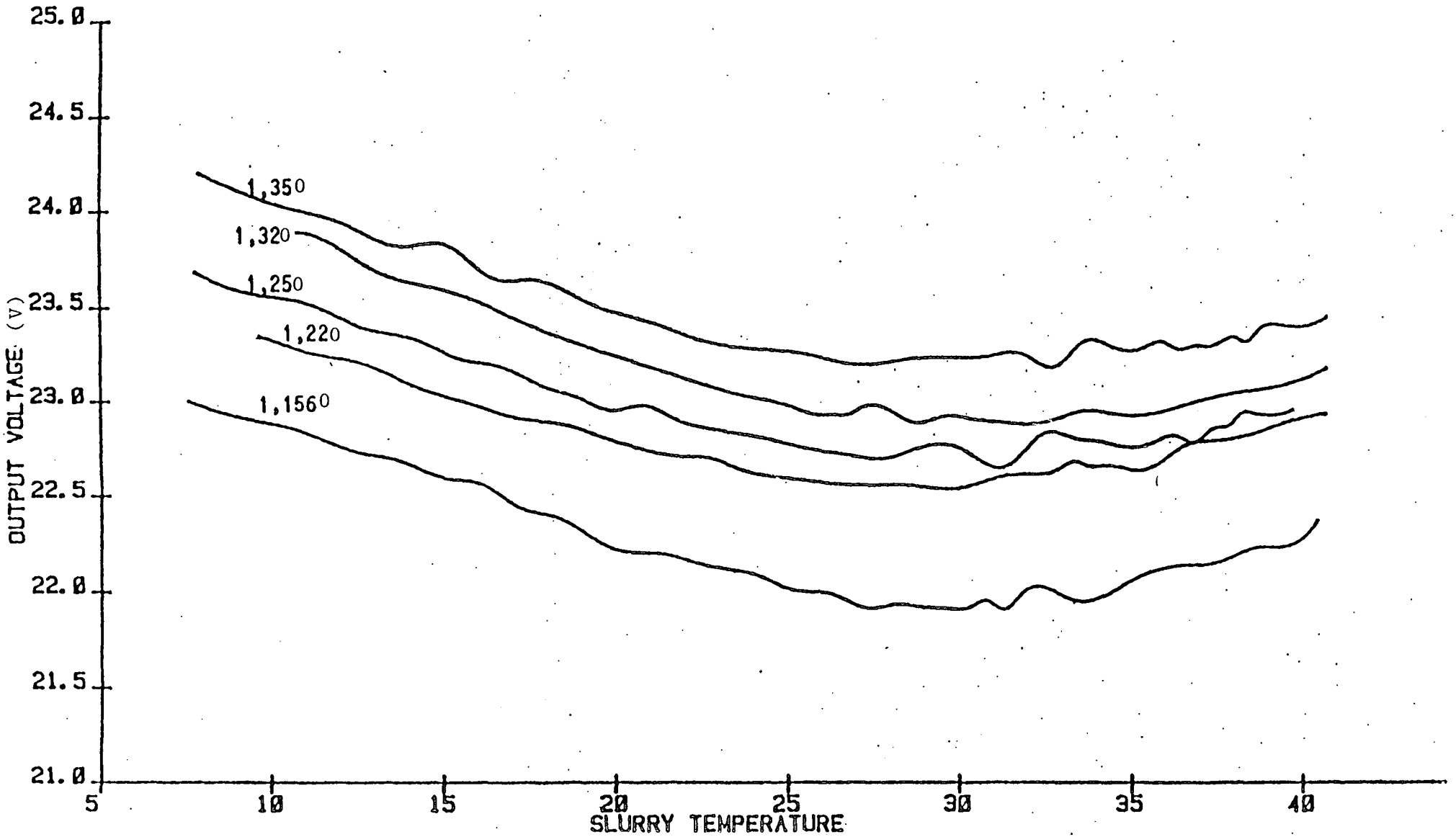

FIGURE 25 : OUTPUT VOLTAGE AS A FUNCTION OF TEMPERATURE AT DIFFERENT DENSITIES OF SLURRY FROM 1,156 to 1,350

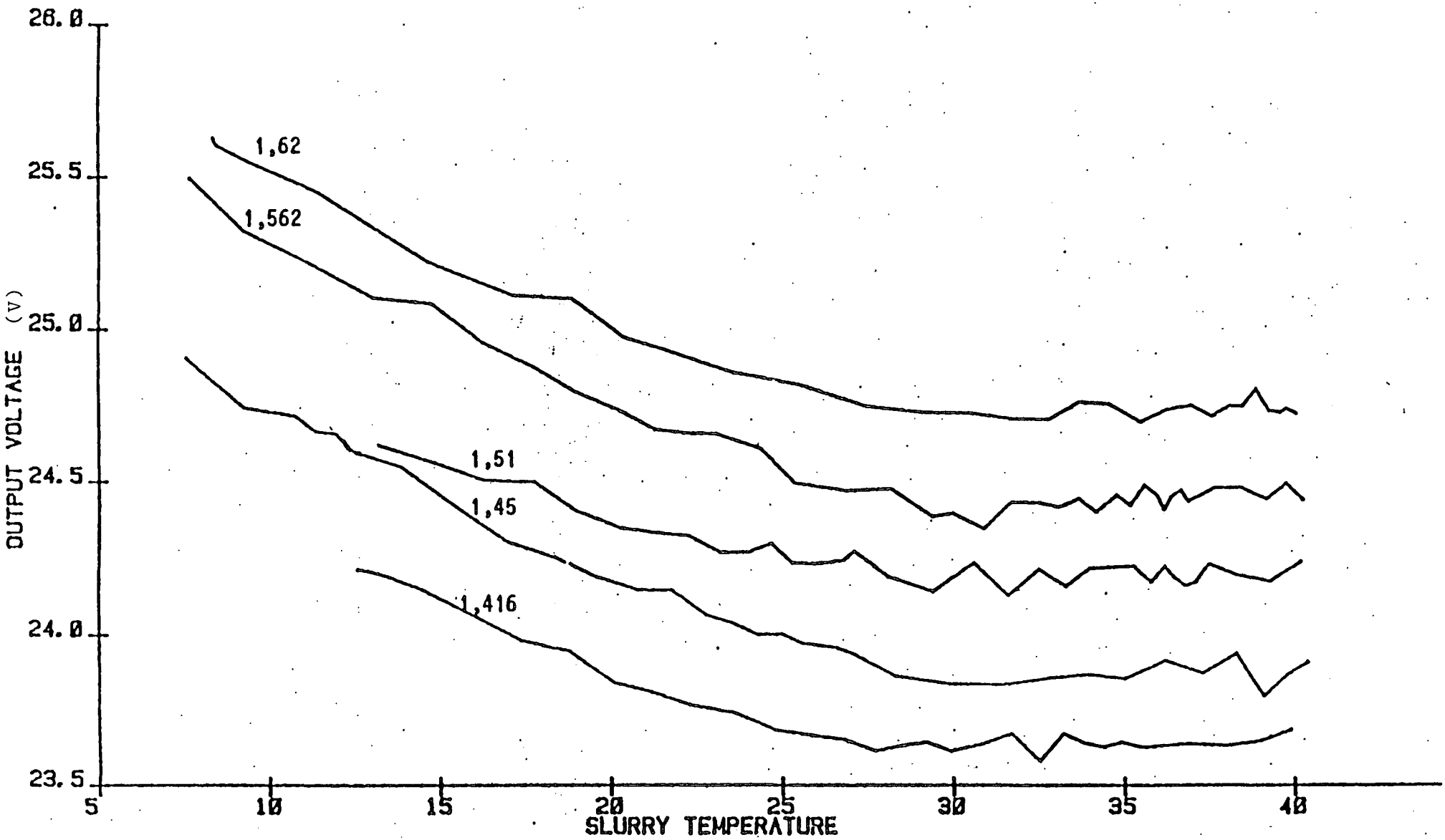

FIGURE 26 : OUTPUT VOLTAGE AS A FUNCTION OF TEMPERATURE AT DIFFERENT DENSITIES OF SLURRY FROM 1,416 to 1,620

First Calibration

$$D = -1,942 + 0,115\ V_0 - 8,228 \times 10^{-3} V_T + 5,38 \times 10^{-4}.V_0.V_T - 1,68 \times 10-4V_T^2$$

Second Calibration

$$D = -2,786 + 0,1649\ V_0 + 10,54 \times 10^{-3} V_T + 3,825 \times 10^{-4}.V_0.V_T - 3,101 \times 10^{-4} V_T^2$$

Figure 27 shows the plot of actual density vs. fitted density.

5.4 Plant Trials

5.4.1 Pilot Plant Experiments

Initial plant trials were conducted on the pilot resin-in-pulp plant at Mintek. Several methods of agitation were employed in the various adsorption vessels, but the one chosen for the experiment was the impeller and down-draught tube type, as this is the method adopted in various processes in the gold mining industry. The duration of the experiment was five weeks, and the method of data collection was as follows: the samples were collected at three pre-determined depths, namely: 0,75m, 1,25m and 2m.

Each observation, shown in Table 7a, is the average of three readings taken at the three depths in the vessel. Two methods of measurement were used. 'Probe Sample' results were collected using the instrument readings and 'Manual

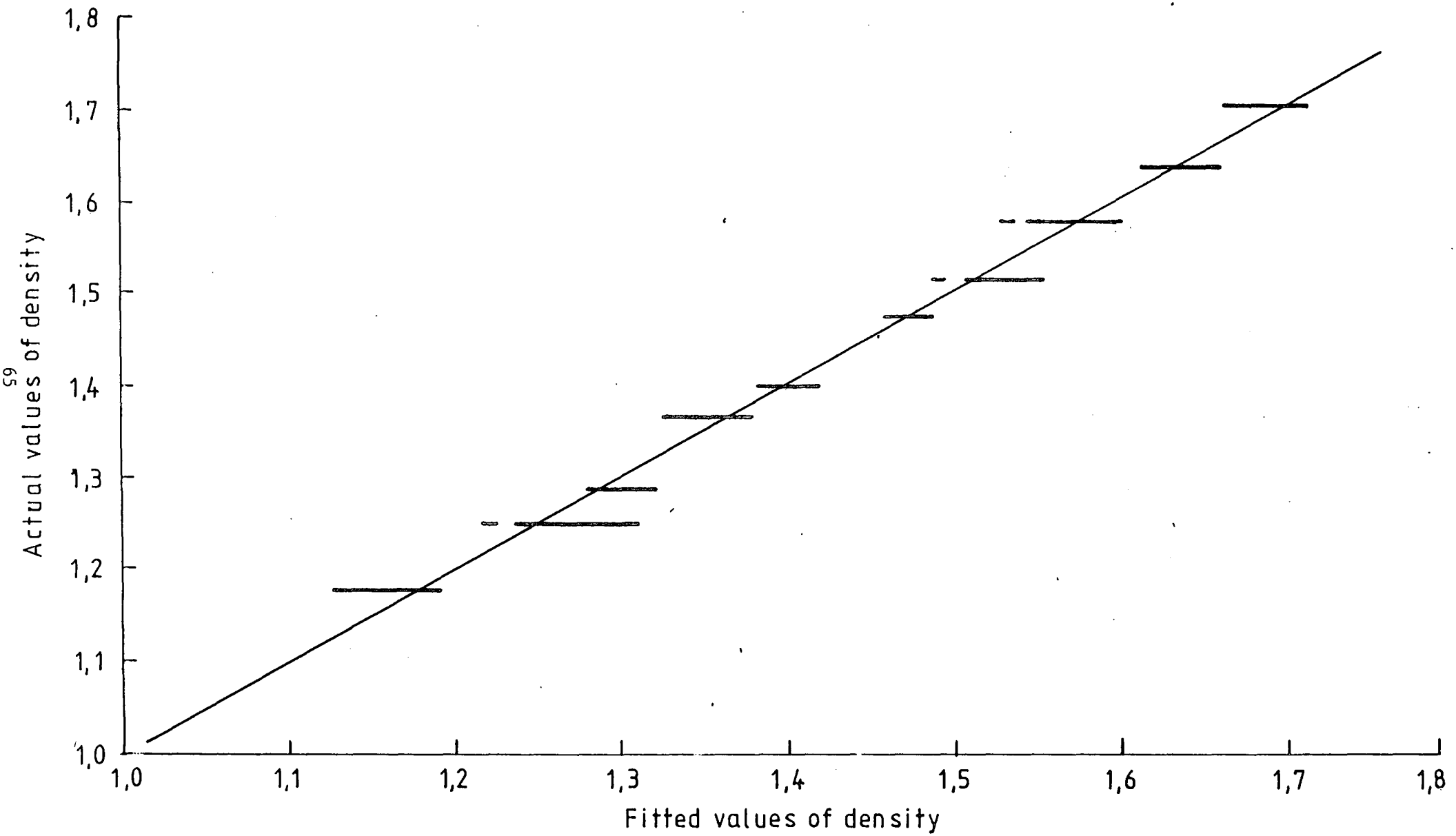

FIGURE 27 : ACTUAL DENSITY vs. FITTED DENSITY

Sample' results were collected using a specially constructed sampling device capable of removing a fixed volume of slurry at any particular depth. The latter results were obtained using a spring balance density meter. Care was taken to ensure that the depth of sampling for both methods was identical.

TABLE 7a : Comparison of manually taken samples and the corresponding instrument readings

OBSERVATION NUMBER	MANUAL SAMPLE	PROBE SAMPLE
1	1.63000	1.65000
2	1.72000	1.66000
3	1.54000	1.54600
4	1.55600	1.55500
5	1.56000	1.52000
6	1.56000	1.53000
7	1.56000	1.54700
8	1.58600	1.56400
9	1.59000	1.57700
10	1.59500	1.58200
11	1.54200	1.50600
12	1.55700	1.52400
13	1.56100	1.54200
14	1.57900	1.55700
15	1.58100	1.56200
16	1.62000	1.59800
17	1.65800	1.60500
18	1.66900	1.62300
19	1.65800	1.62900
20	1.63200	1.63200
21	1.67100	1.63900
22	1.67900	1.65700
23	1.66400	1.66800
2n	1.68800	1.67100
25	1.69900	1.68100
26	1.65000	1.66000
27	1.68000	1.68000
28	1.69000	1.68000
29	1.70000	1.71000
30	1.71500	1.73000
31	1.71000	1.72000
32	1.73000	1.72000
33	1.73200	1.72000

These results were definitely encouraging, as analysis of the figures returned a correlation co-efficient of 0,957. A plot of the linear regression appears in Figure 28. The data collected at the three depths is shown in Table 7b.

TABLE 7b : The comparison of manual and probe samples taken at the three depths of 0,75m, 1,25m and 2m on the pilot plant

0,75m		1,25m		2m	
PROBE	MANUAL	PROBE	MANUAL	PROBE	MANUAL
1,660	1,62	1,730	1,720	1,720	1,732
1,710	1,70	1,730	1,710	1,720	1,730
1,660	1,650	1,680	1,680	1,720	1,710
1,660	1,670	1,680	1,690	1,720	1,720
1,710	1,70	1,680	1,670	1,680	1,700
1,665	1,612	1,671	1,694	1,680	1,680
1,669	1,689	1,671	1,697	1,681	1,703
1,670	1,690	1,671	1,691	1,681	1,696
1,636	1,642	1,639	1,664	1,675	1,680
1.638	1.614	1.639	1,647	1,657	1,682
1,638	1,640	1,639	1,647	1,657	1,675
1,593	1,557	1,621	1,671	1,630	1,669
1,610	1,659	1,620	1,667	1,629	1,647
1,611	1,659	1,629	1,668	1,587	1,623
1,568	1,608	1,578	1,621	1,609	1,617
1,599	1,515	1,578	1,622	1,552	1,581
1,558	1,619	1,587	1,625	1,561	1,578
1,524	1,561	1,524	1,560	1,578	1,590
1,524	1,551	1,524	1,551	1,585	1,601
1,524	1,560	1,524	1,561	1,540	1,560
1,566	1,587	1,558	1,590	1,555	1,557
1,567	1,580	1,567	1,580	1,556	1,546
1,558	1,59	1,566	1,587	1,556	1,546
1,53	1,56	1,530	1,560	1,555	1,548

The results, calculated from table 7b, are as follows:

At 0,75m the correlation coefficient (r) is 0,795. The standard deviation for the 'PROBE'. Samples is 0,059 and the variance, 3,66%. For the 'MANUAL' samples, the standard deviation and variance are 0,0516 and 3,18% respectively.

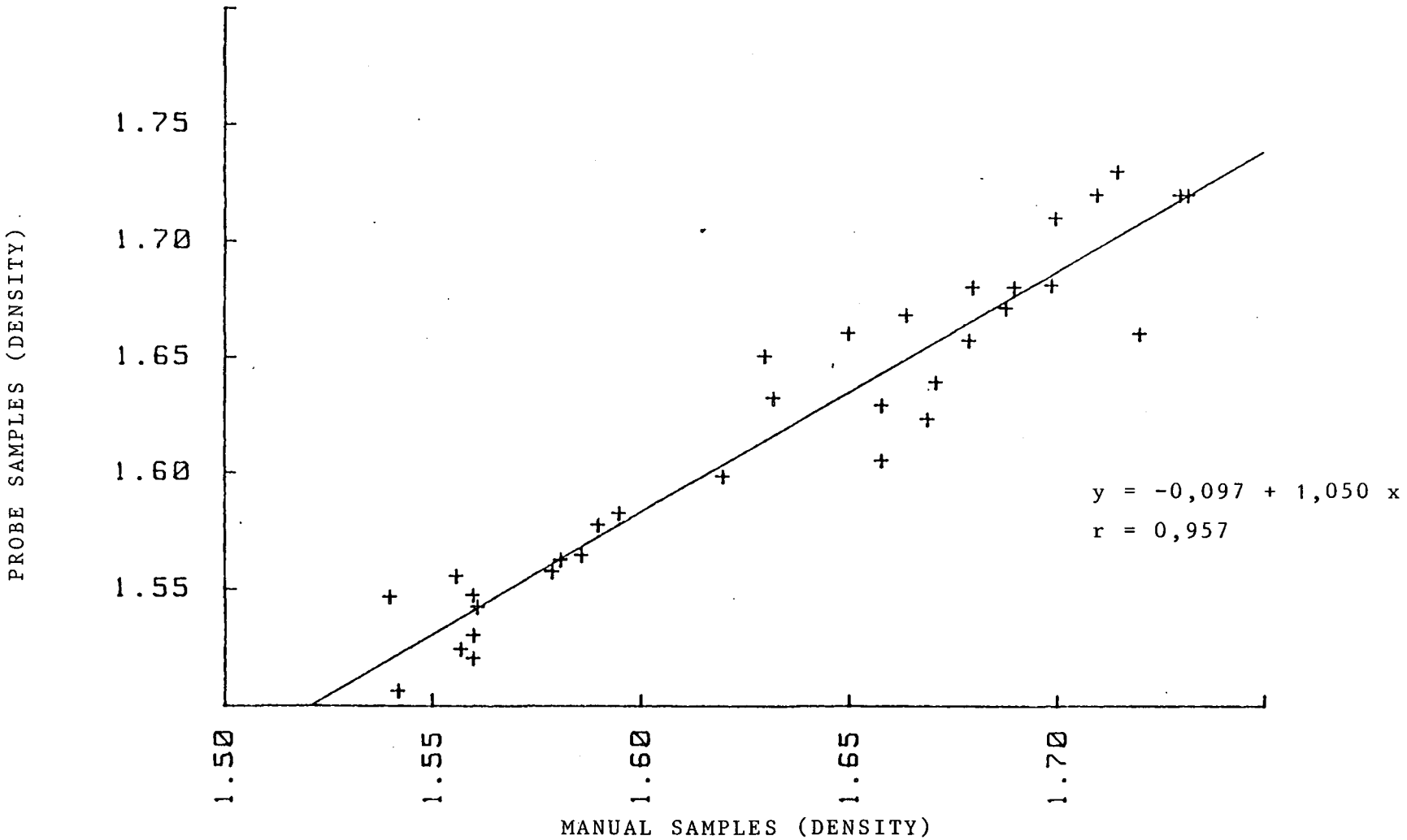

FIGURE 28 : RESULT OF A TEST TO DETERMINE THE CORRELATION BETWEEN ACTUAL VALUES OF DENSITY AND THOSE OBTAINED USING THE INSTRUMENT

At 1,25m, r is 0,963 - a considerable improvement. The standard deviation and variance for the 'PROBE' samples are 0,064 and 3,94% respectively. For the 'MANUAL' samples the standard deviation is 0,053 and the variance 3,23%

At 2m, r is 0,977. The standard deviation and variance for the 'PROBE' samples are 0,0635 and 3,87% respectively, and for the 'MANUAL' samples 0,065 and 3,96%.

From these results, it would seem that a better performance is obtained at the two deeper measuring points: this could be due to less turbulence and better mixing at these levels.

5.4.2 Production Plant Trials

The last phase of the instrument evaluation was testing on an actual production plant and the leaching process vessels of a gold mine were chosen for this test. The leach plant comprised of five operational vessels, and for purposes of the experiment, several density measurements were taken in each tank using the same technique as on the pilot plant, (Section 5.4.1) with the exception that sampling was done at the surface of the slurry. The result appears in Figure 29. The correlation coefficient is 0,953. As will be seen, less accurate results were obtained at densities below 1,2.

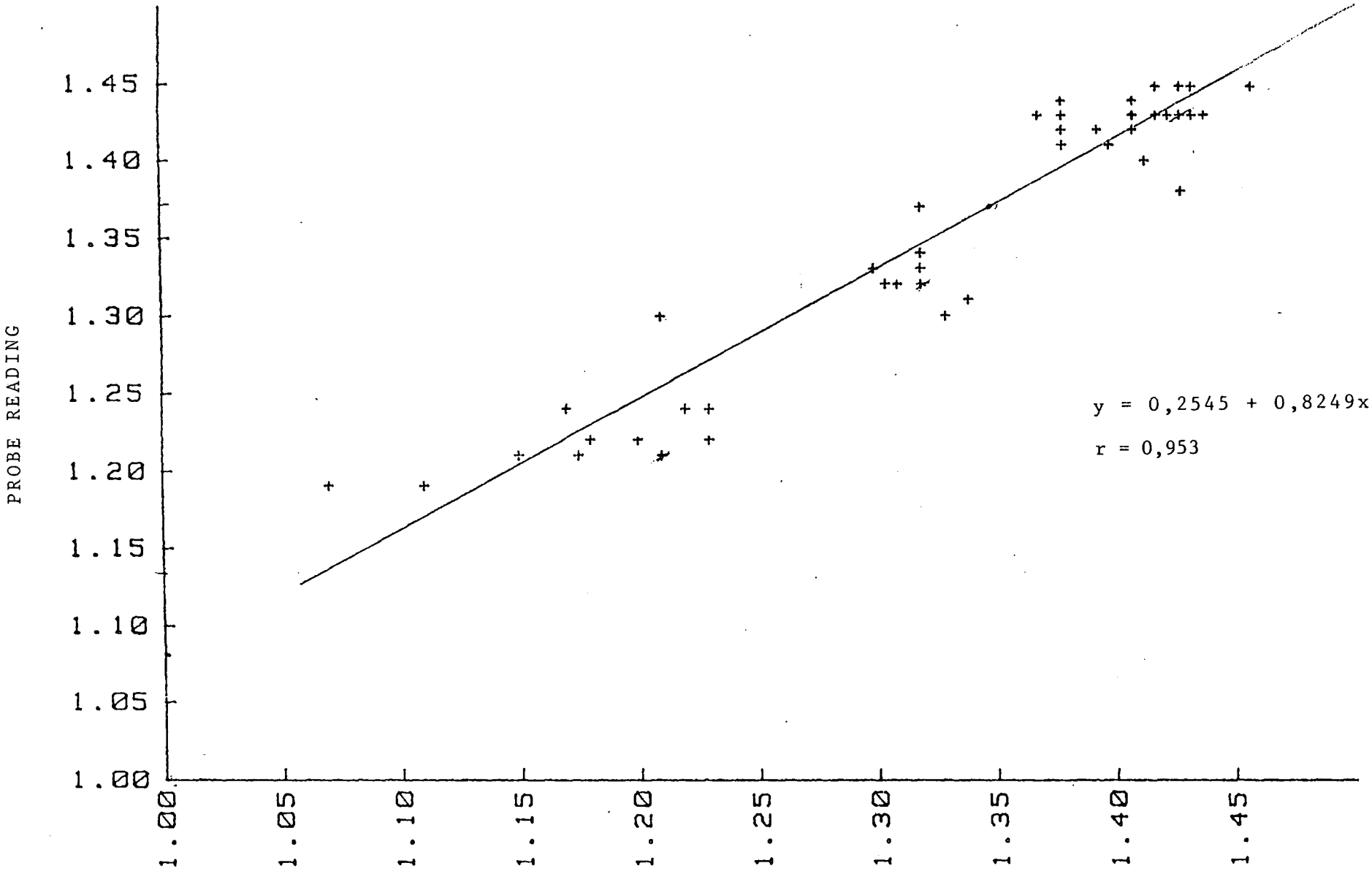

FIGURE 29 : PLANT TRIAL RESULTS

The sample data, for each individual tank, were then inspected and the relevant statistics are shown in Table 8.

As with previous results, the 'manual' and 'probe' samples were measured densities and instrument readings respectively. No obvious pattern emerges from the information in the table.

5.4.3 Calibration and linearity checks

As stated in 5.4.2, less accurate results were observed below a density of 1,2.

The linearity and calibration of the system were therefore re-checked in an attempt to determine the source of error. Carefully weighed slurries were used for the test and the results appear in Table 9. Once again, 'Manual' results are the actual density using a laboratory balance and 'Probe' the calculated density. V_0 is the output voltage proportional to density. The experiment was conducted at room temperature.

TABLE 8 : A Statistical comparison of five leach tanks

S T A R I A R I C	TANK 1		TANK 2		TANK 3		TANK 4		TANK 5	
	MANUAL	PROBE	MANUAL	PROBE	MANUAL	PROBE	MANUAL	PROBE	MANUAL	PROBE
CORRELATION COEFFICIENT	0,9529		0,8335		0,7755		0,8720		0,7233	
MEAN	1,4200	1,408	1,3900	1,4000	1,0326	1,322	1,1870	1,1960	1,4160	1,4160
STANDARD DEVIATION	0,0362	0,0486	0,2010	0,0183	0,0232	0,0371	0,0422	0,0178	0,0090	0,0180
VARIANCE %	2,5500	3,450	1,4460	1,3000	1,75	2,800	3,5550	1,4900	0,6400	1,2700

There is a good correlation between the two density readings -the co-efficient being 0,9965. The plot of linearity appears in Figure 30, As a final test, the system was re-evaluated at various densities and temperatures. Four densities were used: 1,663, 1,529, 1,434 and 1,327. In each case the slurry was heated from 8^0 to 40^0C and the output of the instrument logged at regular intervals.

TABLE 9 : Results of a test to check linearity

VARIABLE # 1 (MANUAL)	VARIABLE # 2 (PROBE)	VARIABLE # 3 (Vo)
1.62100	1.63000	24.95000
1.56600	1.58000	24.65000
1.51400	1.53000	24.39000
1.46400	1.48000	24.07000
1.42400	1.43000	23.82000
1.35600	1.36000	23.43000
1.29300	1.29000	23.02000
1.22900	1.24000	22.73000
1.18800	1.21000	22.57000
1.16000	1.19000	22.47000
1.12400	1.12000	22.05000

From these results, the density was calculated for each slurry at 10^0, 20^0, 30^0 and 40^0; the result appears in Figure 31. As with the result of the initial temperature experiments, it was found that inaccuracies occur at the lower densities: this is thought to be due to reflections of the sound waves from the wall of the vessel. (The less dense the slurry the less absorbant it is to sound waves).

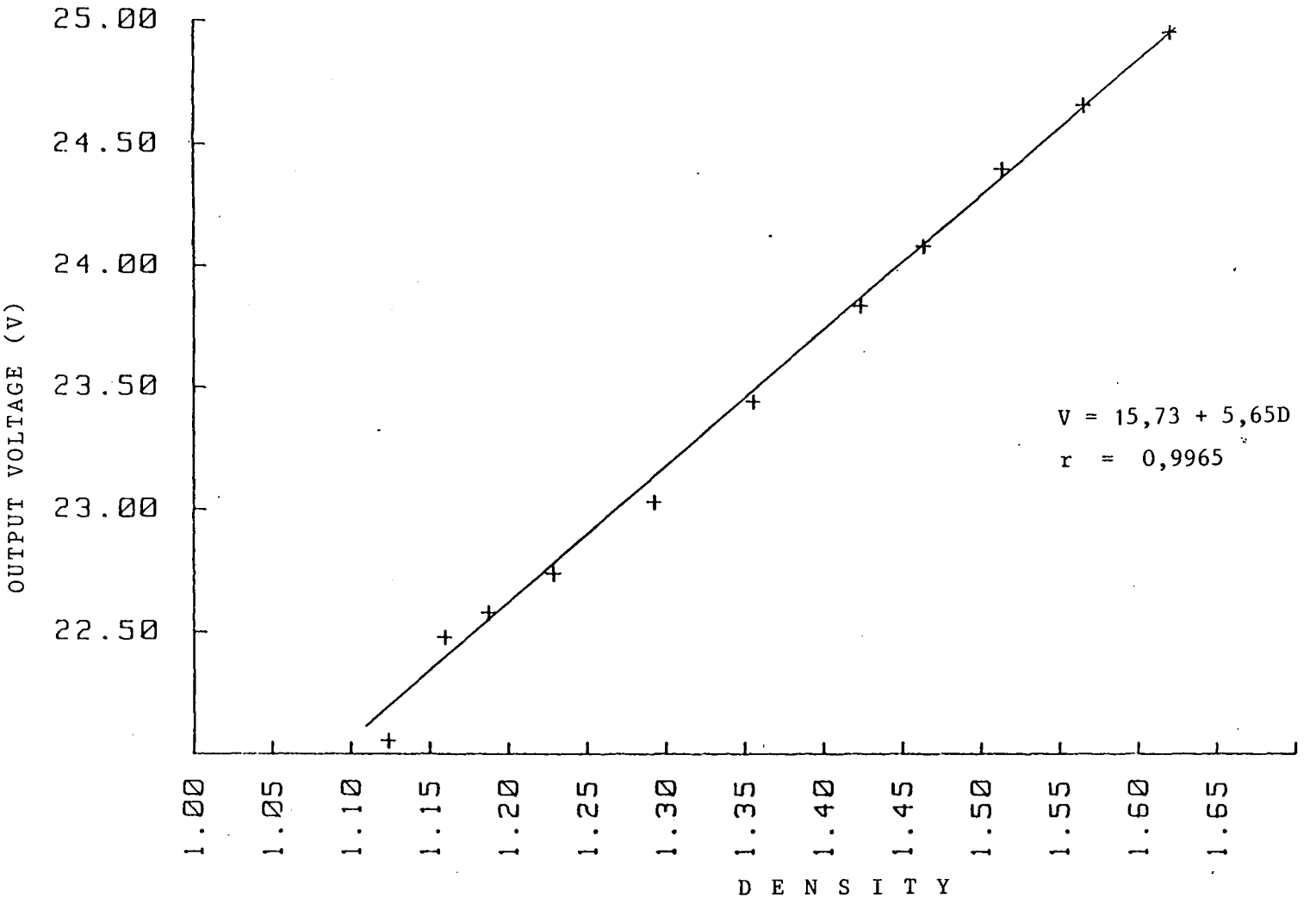

FIGURE 30 : LINEARITY RESULTS

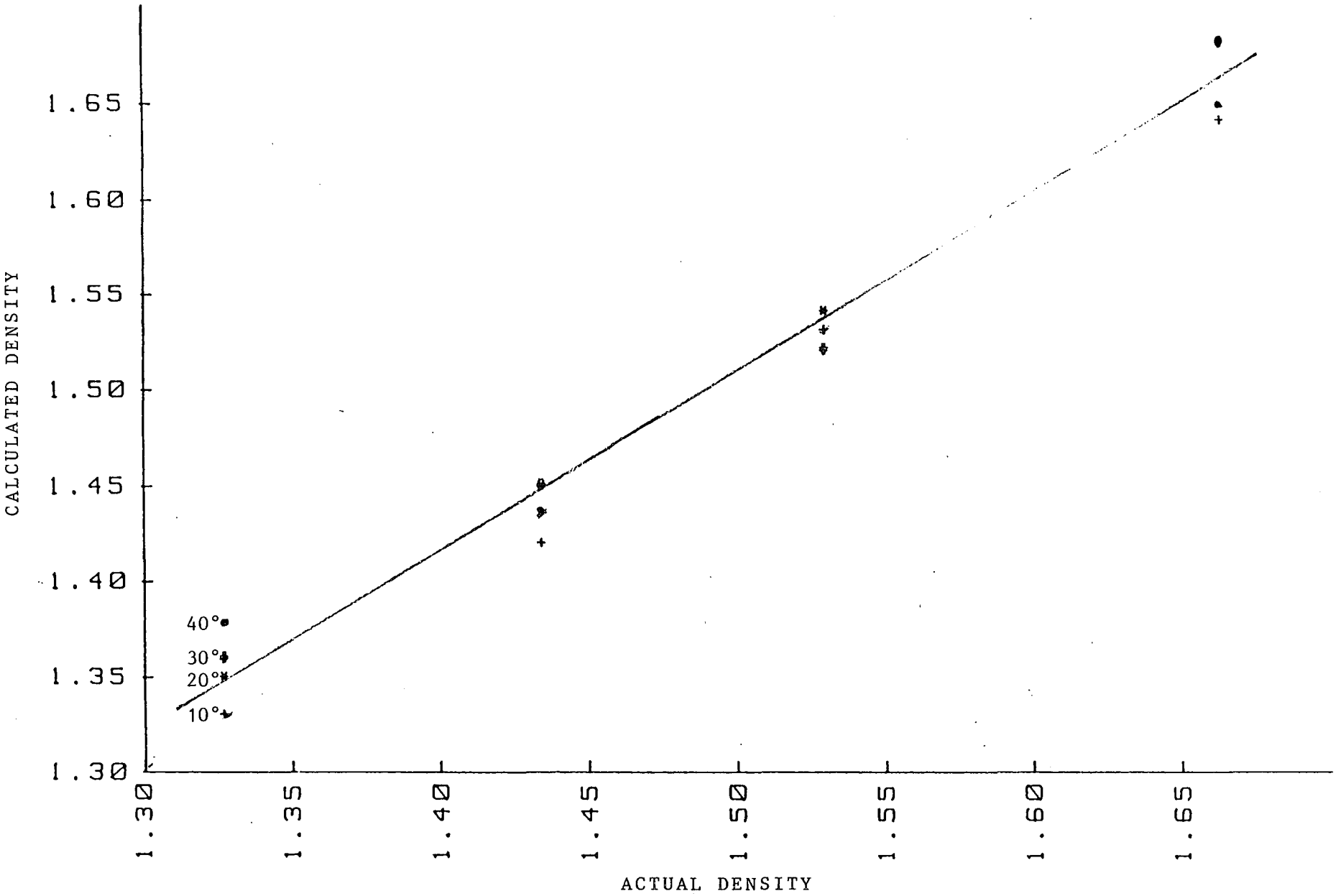

FIGURE 31 : RESULTS OF TEMPERATURE EXPERIMENTS SHOWING DIFFERENCE IN PERFORMANCE AT DIFFERENT TEMPERATURES

Regression analysis on the data from the above experiment resulted in the following expression:

$$\text{Density} = -2,697 + 0,1637V_0 - 0,00286V_T + 0,000695V_0V_T - 0,0002064V_T^2$$

For comparison, the expression from the first calibration (used in the plant trials) appears below.

$$\text{Density} = 2,786 + 0,1649V_0 + 0,01054V_T + 0,0003825V_0V_T - 0,000310V_T^2$$

Table 10 shows the calculated against actual density using the first and second calibrations with a number of slurries. Clearly the calibration has changed, but considering that the probe had been operating in a highly abrasive medium for some 1200 hours, the change is relatively small. This suggests minimal erosion of the epoxy encapsulation. As the objective of this study is to develop a portable instrument, the probe would not be subjected to lengthy periods in a slurry, therefore the effects of erosion on the performance would be of no consequence.

TABLE 10 : The comparison of the accuracy of the two calibrations

ACTUAL DENSITY	1ST CALIBRATION SEPTEMBER 1984	2ND CALIBRATION FEBRUARY 1985
1,621	1,63	1,62
1,566	1,58	1,56
1,514	1,53	1,51
1,464	1,48	1,46
1,356	1,36	1,34
1,293	1,29	1,26
1,229	1,24	1,21
1,188	1,21	1,18
1,160	1,190	1,16
1,124	1,12	1,09

5.4.4 Plant Calibration

Because the proximity of the vessel wall to the probe had been thought to be the cause of the deviation in linearity and error in calibration at lower densities, it seemed logical that better results would be obtained in a larger vessel.

A new density expression was therefore derived, using the data from the plant trials at the leach vessels. (Section 5.4.2). Using this new calibration, further readings were taken in the same vessels. Figure 32 shows how the performance has improved, particularly at the lower densities. The correlation coefficient is 0,956. This suggests that calibration should be conducted in large vessels for greatest accuracy.

The viability of the technique as a method for measuring slurry density had been established and a programme of probe optimization was initiated.

6. OPTIMIZATION OF THE PROBE ASSEMBLY

Several parameters need to be considered when the sensor assembly is being designed. These are: the frequency and size of the transducer, its backing, the coupling medium between the transducer and the facing, and the means by which the temperature of the medium will be sensed. Ideally, the same materials and construction should be used for all applications.

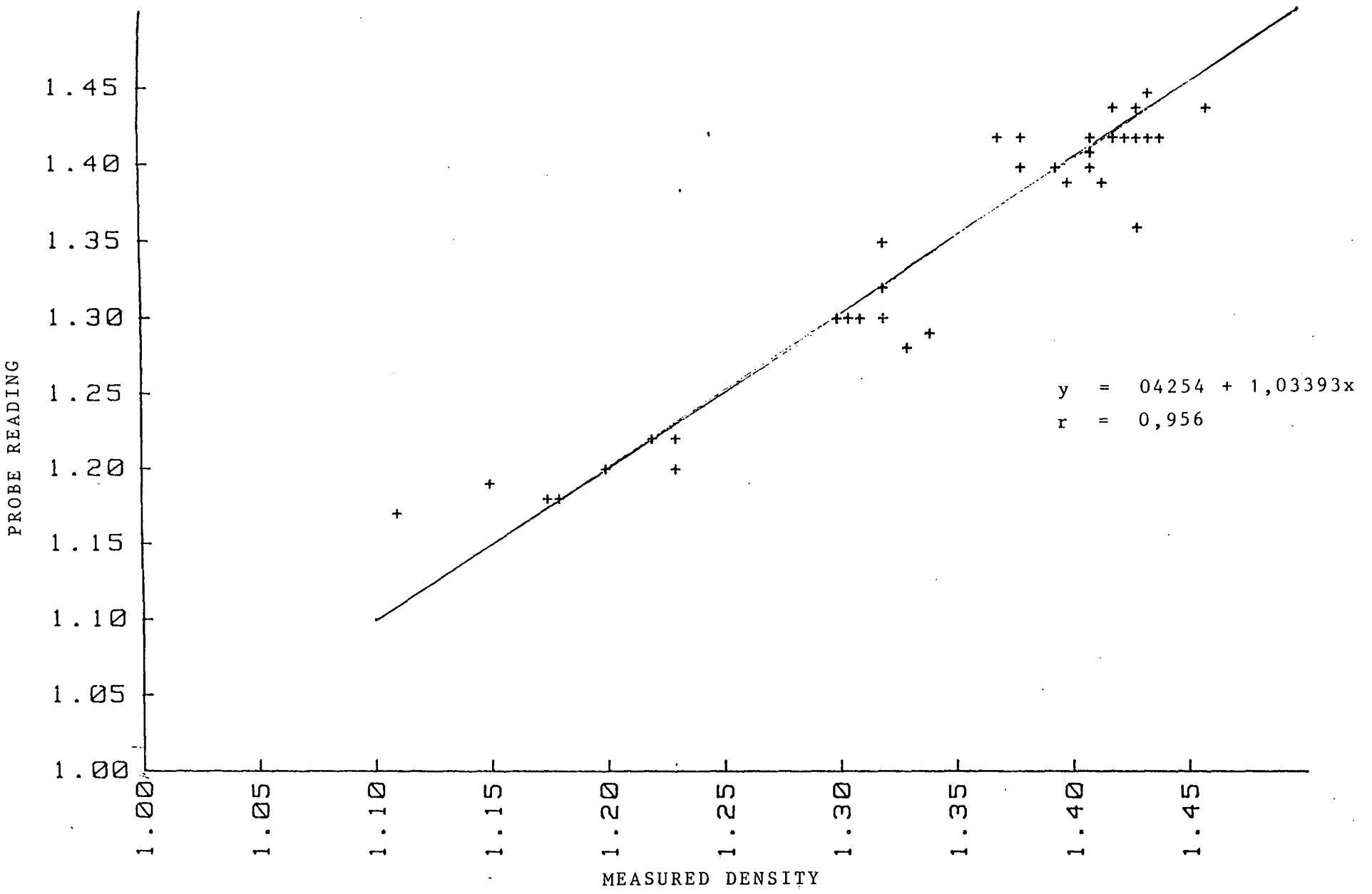

FIGURE 32 : LEACH TANK RESULTS

6.1 Determining the Optimum Operating Frequency

In an evaluation of the sensitivity of transducers of different frequencies, six PZT's, varying in frequency from 0,2 to 3 MHz were used. For these tests, the devices were not encapsulated. These devices were chosen as they covered a fairly wide range of frequencies on either side of the 500 kHz device.

Each device was first immersed in demineralized water, and a signal generator was adjusted until the voltage across the device was at a maximum (parallel resonance). The voltage was then noted. The device was then immersed in paraffin, and the new voltage was noted. The difference between the two voltages, Δv, was taken as the sensitivity of the device to the change of medium. The results are summarised in Table 11.

TABLE 11 : Comparison of PZT discs of various operating frequencies

Device No.	FREQUENCY MHz	IN WATER	IN PARAFFIN	Sensitivity Δv mV
1	0,20	230	320	90
2	0,25	136	200	64
3	0,50	98	118	20
4	1,50	17,4	21,5	3,1
5	2,00	13,6	15,6	2,0
6	3,00	5	5,7	0,7

As can be seen, in the 'sensitivity' column, devices 1, 2 and 3 are reasonably sensitive to the change in medium. At higher frequencies, the sensitivity drops off rapidly.

Although devices 1 and 2 (0,2 and 0,25 MHz respectively) exhibited the greatest change in voltage (and hence in impedance), they were found to lack sensitivity after being encapsulated in Araldite 'M' resin or polyester resin. There was little or no difference in impedance when these encapsulated devices were immersed in different clear liquids or in slurries of different densities. In contrast, the 0,5 MHz device (3) showed a good response to changes in slurry density. The reason for this seemingly anomalous behaviour is not known at this stage.

The fact that the initial transducer chosen happened to be one with the optimum operating frequency of 500 kHz was purely coincidental.

6.2 DETERMINING THE OPTIMUM DIAMETER

An ideal ultrasonic transducer would be a thin disc with faces vibrating in a piston-like manner. At the fundamental resonance, where the thickness is half a wavelength, its performance would be represented by the widely used equivalent circuit shown earlier in Figure 1. In practice, this is difficult to realize since the thickness mode combines with a multitude of flexural and in-plane modes to give close multiple responses. In the present application, pure resonance is vital since the better the transducer couples to the medium, the greater will be its sensitivity and resolution as a density-measuring instrument. Figure 33 shows the response of a variety of transducers of different frequencies. Ideally, the transducer should have a high

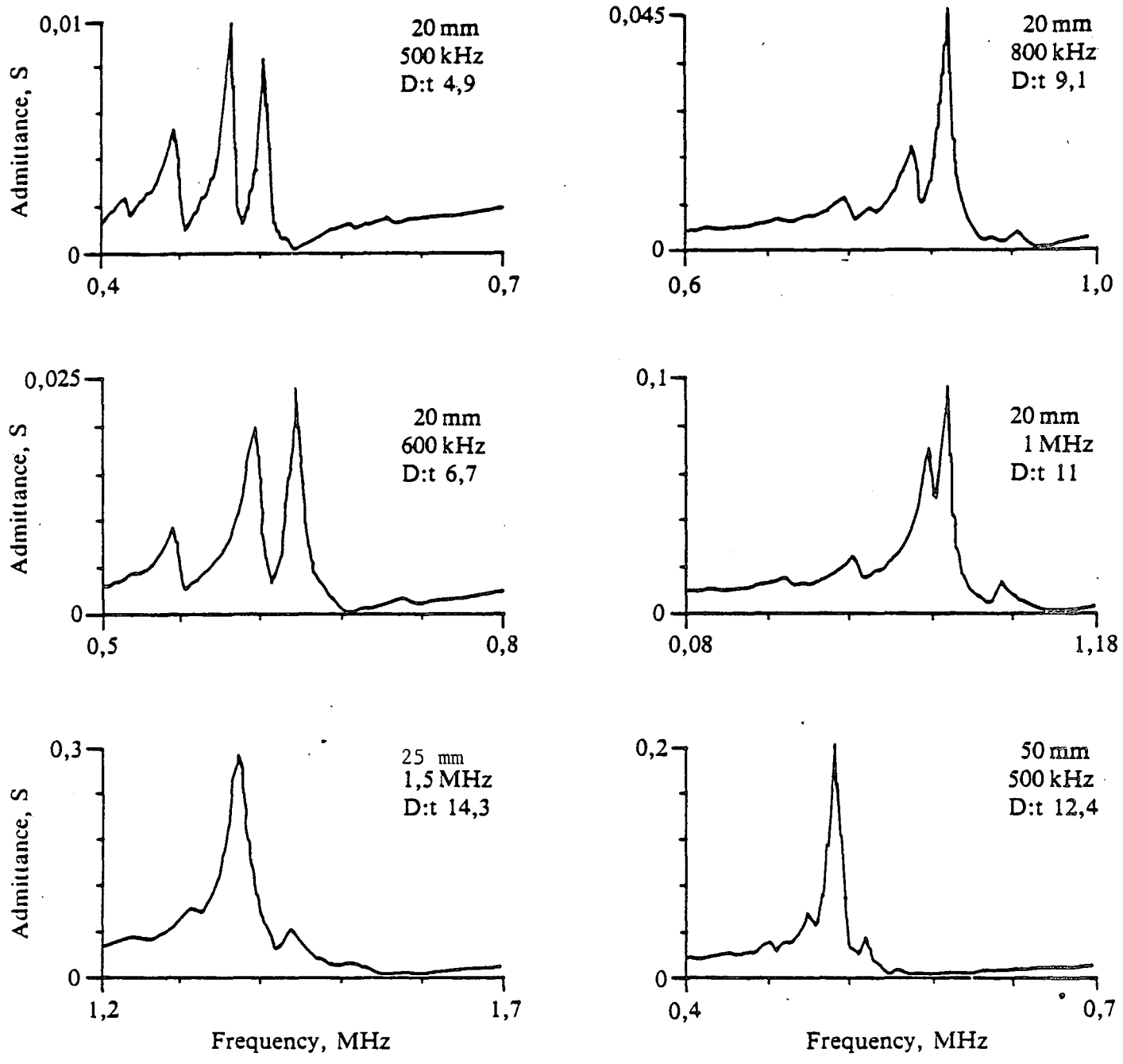

FIGURE 33 : Comparison of responses of transducers with different ratios of diameter (D) to thickness (t)

If one compares the spectrum of 20mm 500 kHz device with that of the 25mm 1,5 MHz device, it will be seen that the amplitude of the satellite responses decreases as the D:t ratio increases.

series resonance peak with small satellite responses or preferably none at all. Examination of the response of the series of transducers shown in Figure 33 indicates that the diameter-to-thickness ratio is the determining factor.

This is confirmed by a comparison of the admittance - frequency response of the 1,5 and 0,5 MHz transducers with similar diameter-to-thickness ratios (about 13). The weak satellite responses follow the same pattern in both cases, and the peak admittances, which give the amplitudes, are very large.

Testing these unencapsulated devices in different media showed that the transducers with the single resonance exhibited a better coupling to, and sensitivity to changes in the surrounding medium. Figure 34a to 34c show how an increasing diameter-to-thickness ratio improves sensitivity. The liquids used were paraffin and carbon tectrachloride, chosen because of being insulators and because of their different characteristic impedances (ρc).

Maximum coupling of energy to the surrounding medium is achieved when Rm is a minimum and Rr is a maximum. Rm is calculated by taking the reciprocal of the admittance of the transducer- at series resonance, (fs) in air. The value of Rr for a particular medium is then calculated by taking the reciprocal of the admittance of the transducer in that medium, and subtracting Rm. An example of the calculation is shown below.

D/t RATIO = 4,9

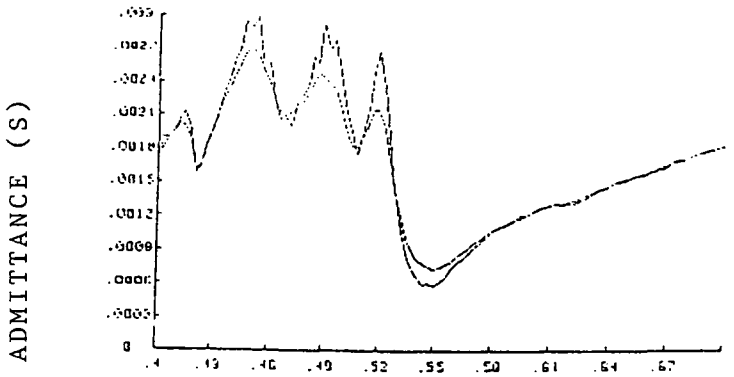

a

D/t RATIO =12.4

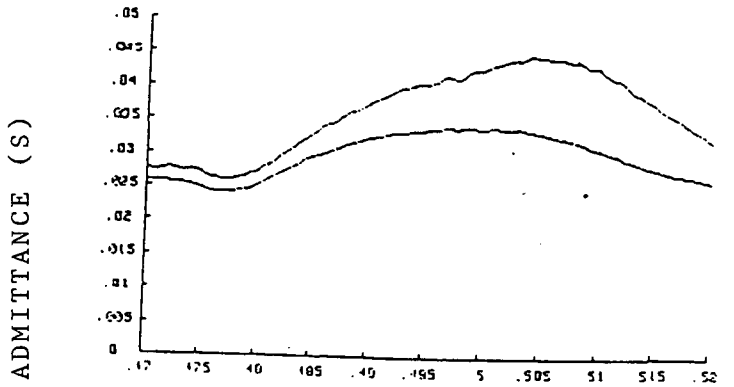

b

D/t RATIO =14.3

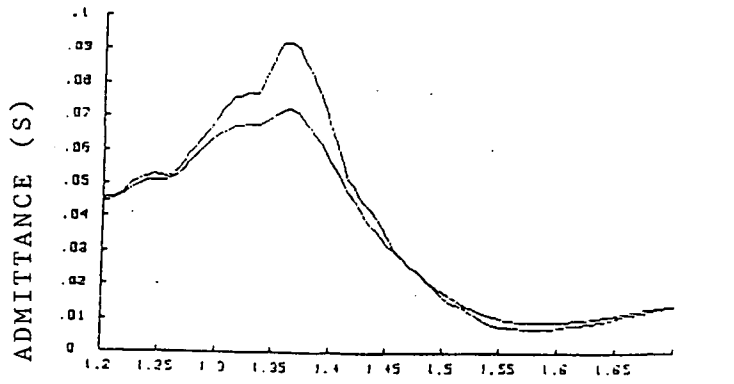

c

FIGURE 34 : IMPROVEMENT IN SENSITIVITY TO CHANGES IN DENSITY AS THE D:t RATIO INCREASES

A transducer has an admittance in air of .01S or $\frac{1}{.01}=100\Omega$

(Rm) and an admittance in CCL4 of .0037S or $\frac{1}{.0037}=270\Omega$ then R_r for the CCL4 is 270-100 or 170 ohms.

Three single resonance and one multiple-resonance transducers were evaluated in paraffin and carbon tetrachloride: the results appear in Table 12, and show the superiority of the device with a single resonance.

TABLE 12 : Comparison of single and multiple-resonance devices

DEVICE	f_s MHz	DIA. mm	THICKNESS mm	D/t	R_m Ω	R_{rp} Ω	R_{rCT} Ω	COUPLING COEFF. $\frac{R_{rCT}}{R_{rP}}$	
1,5MHz	1,37	20	1,4	14,3	3,3	7,6	10,6	1,39	Single resonance
2,0MHz	1,87	25	1,0	25	1,9	3,1	4,3	1,39	
0,5MHz	0,5	50	4,1	12,2	5,2	17	24	1,4	
0,5MHz	0,49	20	4,1	4,9	100	233	270	1,16	multiple resonance

On the strength of the above results, use of the 20 mm device was stopped, and a 50 mm PZT disc, operating at the same frequency, (500 kHz) was adopted as the transducer for further development.

6.3 The Facing Material

6.3.1 The optimum thickness

The PZT disc must be isolated electrically from the surrounding medium, and this is achieved by the use of an epoxy resin as a coating. As can be seen in Figure 14, both sides of the disc are covered with resin in the original prototype.

A coating of the optimum thickness will allow the maximum amount of energy to be coupled to the medium, thus ensuring that the probe will have maximum sensitivity. In the determination of the optimum thickness, in the present work, the transducer was encapsulated to an arbitrary thickness and the material on both sides of the disc milled away in stages, sensitivity being measured at each cut. Figure 35 shows how the sensitivity changes with changes in epoxy thickness. In this case, the epoxy is 'M' resin and the thickness is expressed in wavelengths.

The wavelength, λ, of sound in 'M' resin, at 560kHz,is given by:

$$\lambda = \frac{C}{f}$$

where C is the velocity of sound in 'M' resin ($2300 ms^{-1}$) and f the frequency (560 kHz):

$$\text{hence, } \lambda = \frac{2300 \text{ mm}}{560} = \underline{4,107 \text{ mm}}$$

Slurries of densities 1,1 and 1,6 were used to measure the sensitivity. As will be seen in Figure 35, there are several thicknesses at which there is little, or no, response to the change in density: for example at $0,7\lambda$ and $0,215\lambda$.

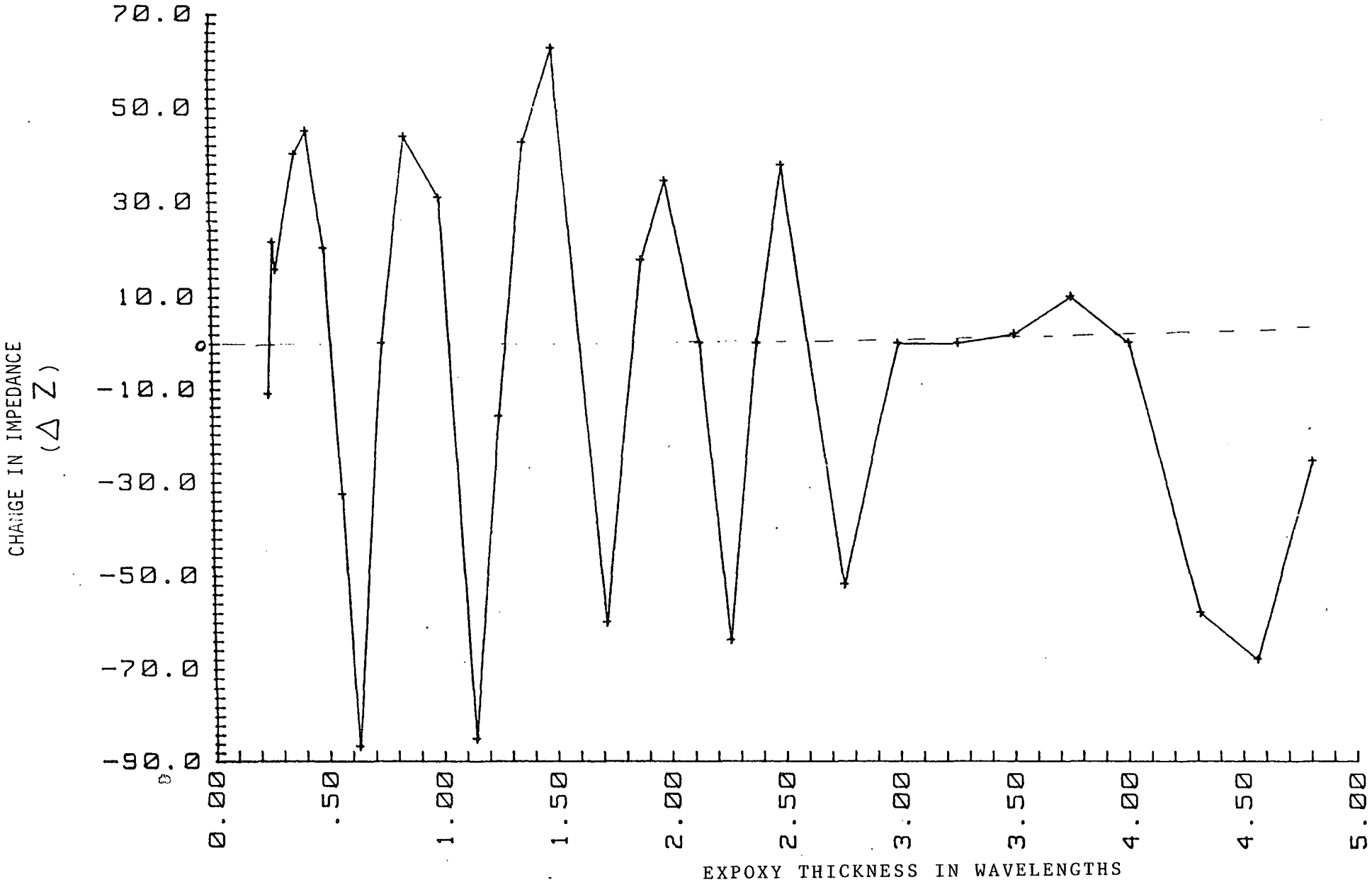

FIGURE 35 : SENSITIVITY AS A FUNCTION OF EPOXY THICKNESS

This difference in sensitivity is more obvious in Figure 36 and 37: the thicknesses of epoxy are 2,5 mm and 2,28 mm respectively. For this decrease of 0,22 mm there is a decrease in sensitivity of approximately 73 % (104Ω down to 28Ω) at 560 kHz. This serves to illustrate the importance of the epoxy thickness.

Obviously, the method of milling away the epoxy to obtain an acceptable sensitivity, would be impractical on a production scale and so the construction of the probe assembly had to be simplified. Figure 38 shows a diagram of the new probe: it is much simpler to construct, as all the parts can be manufactured separately and then assembled. In this assembly the facing material is a disc cut to a pre-determined thickness. To determine the correct thickness, PVC, machined to various thicknesses, was the facing material. The results are summarized in Table 13, which gives the percentage change in impedance, at series resonance for the probe exposed to air and then immersed in water. The percentage changes are large owing to the large difference between the acoustic properties of air and water. Improved performance tends to be obtained with thinner facing material, but an extremely thin face is not practical since it lacks mechanical rigidity and robustness. A compromise at about 0,3λ where λ is the wavelength at resonance, was used.

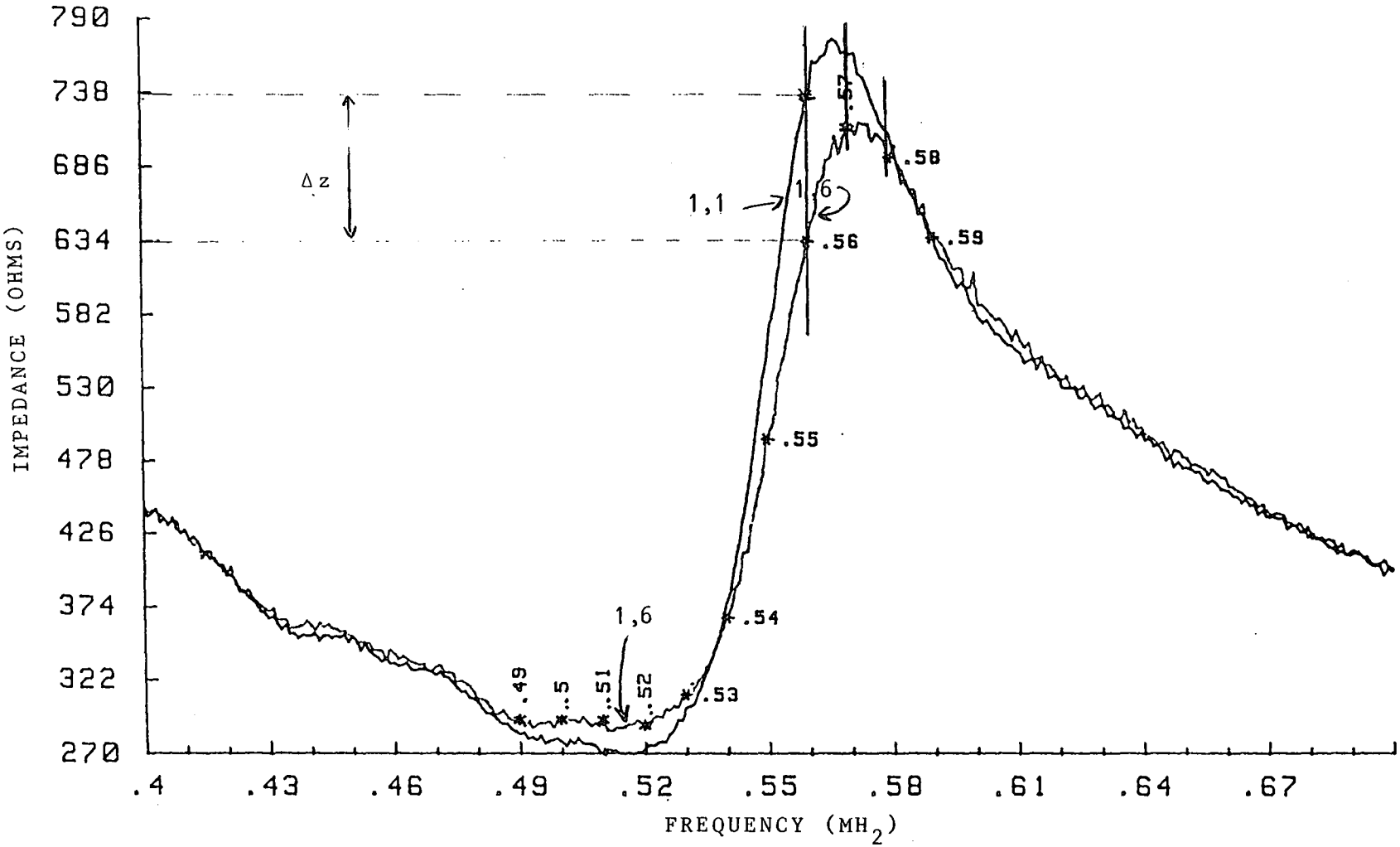

FIGURE 36 : RESPONSE CURVES FOR AN EPOXY THICKNESS OF 2,5 mm

Where Δz = 104 OHMS

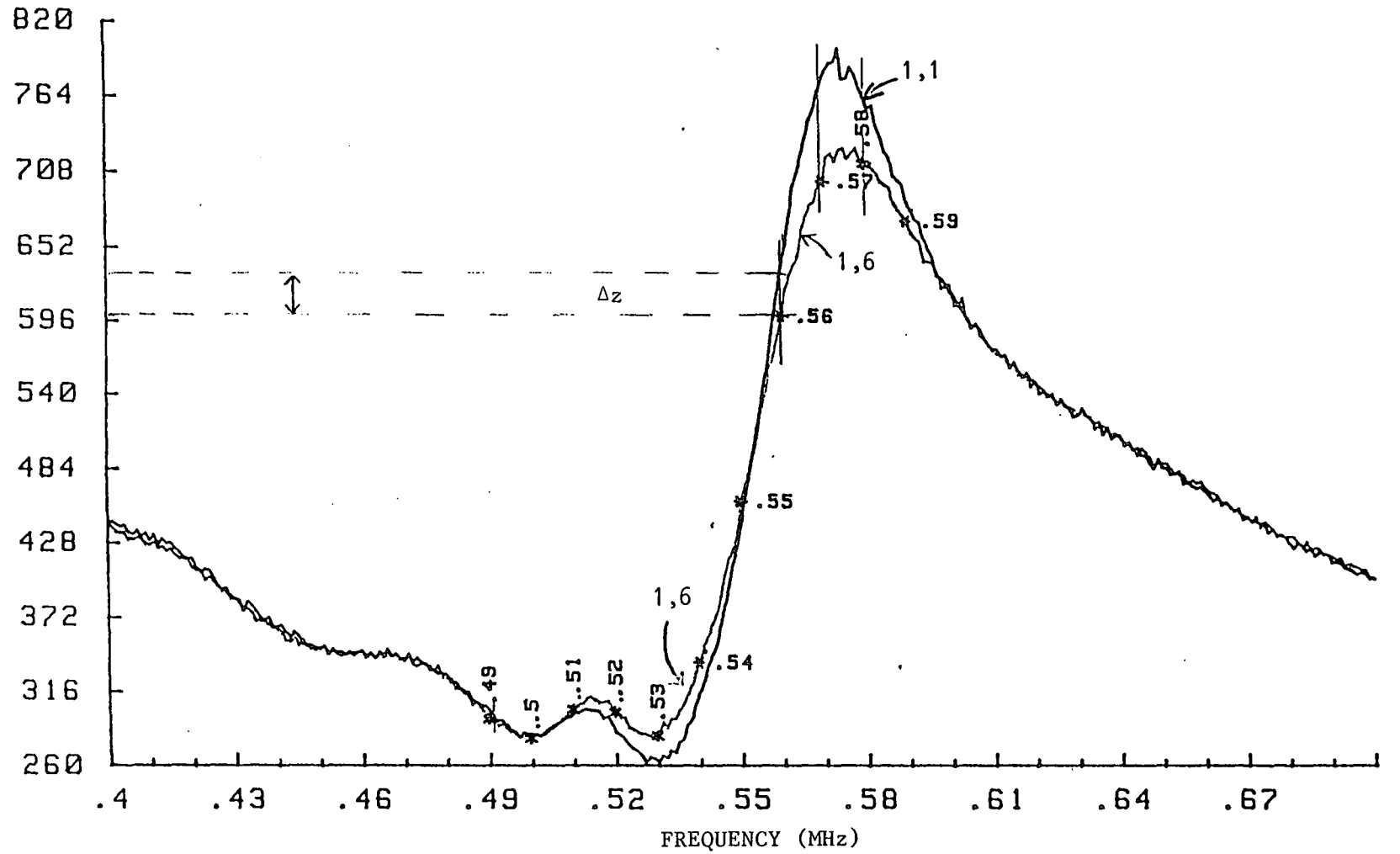

FIGURE 37 : RESPONSE CURVES FOR AN EPOXY THICKNESS OF 2,28 mm

Where Δz = 28 OHMS

FIGURE 13 : Effect of facing thickness on sensitivity of probe, for PVC, at series resonance

THICKNESS OF FACING mm	RELATIVE CHANGE IN ADMITTANCE %
2,4 (0,53λ)	7,5
1,75 (0,39λ)	43
1,3 (0,29λ)	69

6.3.2 Choice of Facing Material

In addition to the thickness of the facing, the material used is of great importance as this provides the interface between the disc and the fluid medium. With the design illustrated in Figure 38, it is relatively easy to test various materials. The actual probe is shown in Plate VII.

The materials tested were Polyvinylchloride (PVC) polyester and polypropylene - all of which are acid resistant and mechanically stable with temperature (Gackenbach, 1960). The coupling agent used was silicone grease, since this allowed the transducer to be removed and used again. The results of the tests are summarized in Table 14, which compares the percentage change in impedance at series and parallel resonance for the three materials. The first two columns compare the results obtained when the probe was dipped in water and subsequently in paraffin, and the last two columns refer to results obtained in water and in a slurry with a relative density of 1,7. The results for the

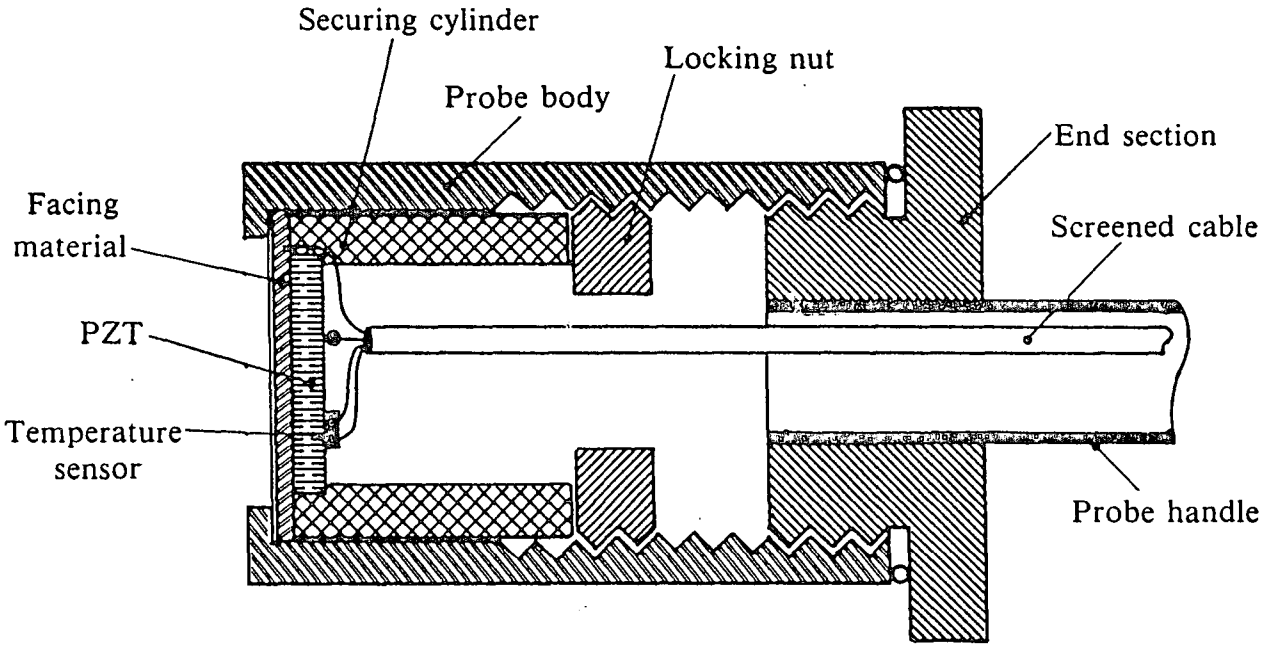

FIGURE 38 : THE FINAL PROBE ASSEMBLY

PVC as well as the polyester facings are acceptable, but those for the polypropylene facing show that its performance was poor. Polypropylene also has the disadvantage that it is fairly pliable and can distort easily. Of the three, polyester is the better material, and has the additional advantage that its peformance at elevated temperature (higher than 40^0C) is also acceptable.

TABLE 14 : Effect of various materials on the sensitivity of the probe

FACING MATERIAL	CHANGE IN IMPEDANCE OR ADMITTANCE, %			
	In water and then in paraffin		In water and then in slurry (r.d. 1.7)	
	Series resonance	Parallel resonance	Series resonance	Parallel resonance
PVC	15	11	25	20
Polyester	20	10	30	21
Polypropylene	-	-	8	4

6.3.3 Matching theory

After having decided on the material to use for the facing, and the thickness, a disc is made to the correct dimensions and the PZT disc is fixed to the facing by means of a suitable adhesive. Polyester resin was chosen as the adhesive, as the facing itself is polyester - therefore, no extra losses are introduced. The transducer is airbacked and this has the effect of diverting most of the ultrasonic energy into the medium.

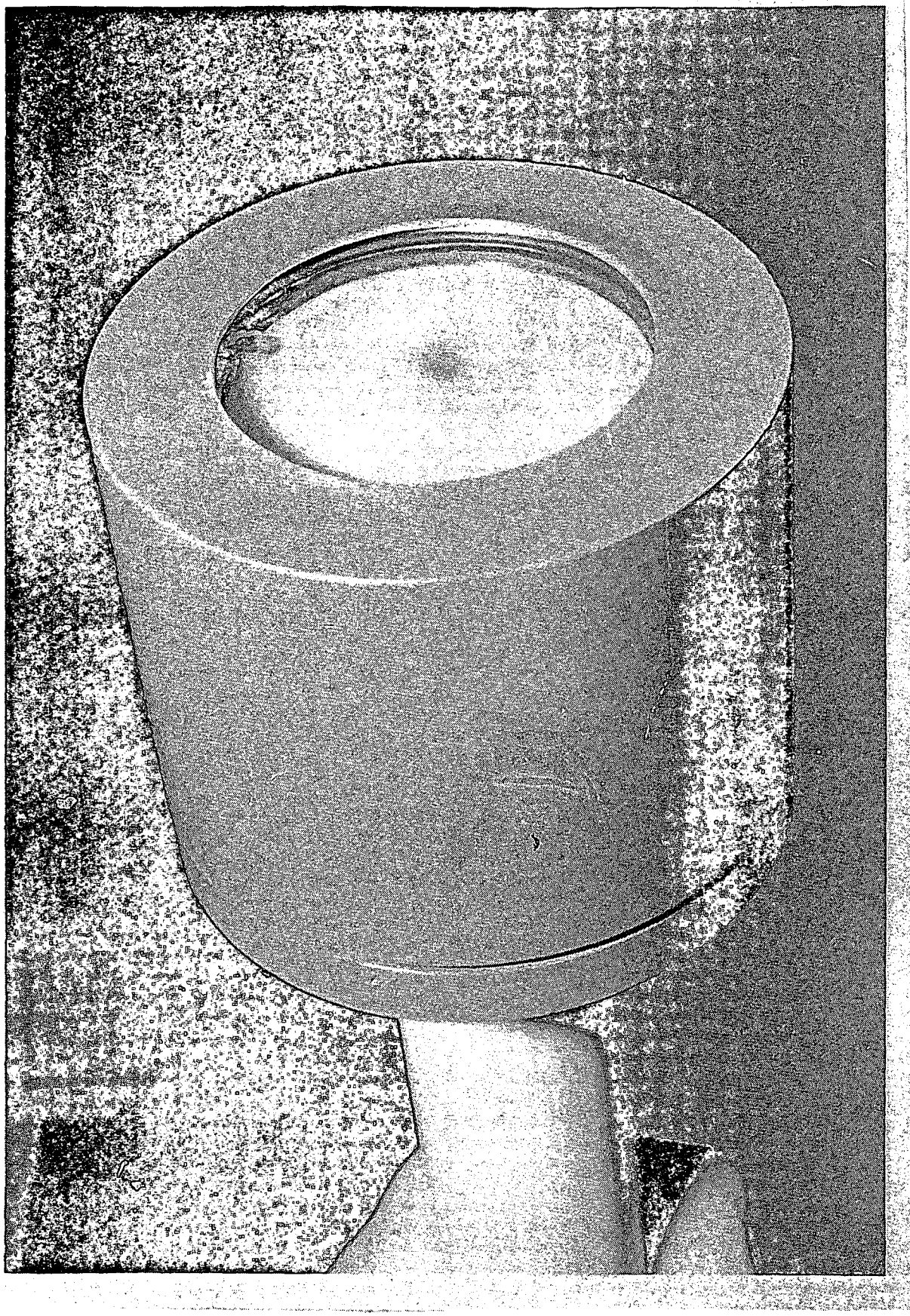

PLATE VII : The final probe design

It has been shown that the thickness of the facing material is of importance when the maximum amount of energy has to be coupled from the PZT to the medium: however the matching is a function not only of the thickness of the material, but also of its characteristic impedance (ρc).

Theory states that when a beam of plane waves strikes a plane boundary separating two materials, some of the energy is transmitted forwards and the remainder reflected backwards (Blitz, 1971). The relative amounts of transmitted and reflected energy can be expressed by the transmission and reflection coefficients defined below (Blitz, 1971).

$$\text{Transmission Coefficient} = \frac{\text{Intensity of transmitted waves at boundary}}{\text{Intensity of incident waves at boundary}} \quad ..(1)$$

$$\text{and reflection coefficient} = \frac{\text{Intensity of reflected waves at boundary}}{\text{Intensity of incident waves at boundary}} \quad ..(2)$$

It can be shown that

$$\text{Transmission coefficient} = \frac{4\ Z_1\ Z_2}{(Z_1+Z_2)^2} \quad ..(3)$$

$$\text{and that reflection coefficient} = \frac{(Z_1-Z_2)^2}{(Z_1+Z_2)^2} \quad ..(4)$$

where Z_1 and Z_2 are the characteristic impedances of the two materials i.e. ρc_1 and ρc_2.

The expressions show that the transmission coefficient approaches unity and the reflection coefficient tends to zero when Z_1 and Z_2 have similar values.

This means that the net acoustic load, 'seen' by the PZT transducer should have a similar characteristic impedance to its own. However, because of the degree of mismatch between the PZT impedance (33,7) and that of the slurry (1,63 to 2,37), impedance transformer sections would be needed between the PZT and the load (slurry), complicating the construction of the probe.

When only one transformer section is used, the acoustic load may be calculated from:

$$Z_T = \frac{Z_s^2}{Z_L} \qquad ..(5)$$

where Z_s is the ρc of the section and Z_L is the ρc of the load.

Substituting the ρc values of slurries for Z_L and the ρc value of polyester for Z_s:

$$Z_{T1} = \frac{2,86^2}{1,63}$$

$$= \underline{5,02} \text{ (for a density of 1,1)}$$

$$Z_{T2} = \frac{2,86^2}{2}$$

$$= \underline{4,09} \text{ (for a density of 1,35)}$$

and $$Z_{T3} = \frac{2,86^2}{2,37}$$

$$= \underline{3,45} \text{ (for a density of 1,6)}$$

Substituting these values of Z_T in equation (2), the transmission coefficient (t_c) for each slurry can be calculated.

$$t_{c1} = \frac{4\ Z_1\ Z_{T1}}{(Z_1 + Z_{T1})^2} = \frac{4 \times 33,7 \times 5,02}{(38,72)^2}$$

$$= \underline{0,451}$$

$$t_{c2} = \frac{4\ Z_1\ Z_{T2}}{(Z_1 + Z_{T2})^2} = \frac{4 \times 33,7 \times 4,09}{(37,79)^2}$$

$$= \underline{0,386}$$

$$t_{c3} = \frac{4\ Z_1\ Z_{T3}}{(Z_1 + Z_{T3})^2} = \frac{4 \times 33,7 \times 3,45}{(37,15)^2}$$

$$= \underline{0,337}$$

Therefore, over the density range of interest (1,1 to 1,6) there is a change of 11,4 % in transmission (33,7 % to 45,1 %) for a change in net acoustic load impedance of 1,57.

Using the facing of polyester as discussed, is only a compromise: optimum coupling would be achieved if the facing had a characteristic impedance of:

$$Z_s = \sqrt{Z_0 \times Z_L} \quad \text{(Goll, 1979)} \qquad \ldots\ldots(6)$$

where Z_0 is the PZT impedance and Z_L the load. For a slurry of density 1,1 (ρc of 1,63):

$$Z_s = \sqrt{33,7 \times 1,63}$$

$$= \underline{7,41}$$

However, construction of the probe would be complicated, as discussed previously.

7. IMPROVEMENTS TO THE ELECTRONICS

Additional sensitivity has been obtained by measuring the voltage across the PZT via a peak detector (A1) which replaces the diode bridge configuration. The peak detector is followed by a low-pass filter, A2, that removes the rapid voltage fluctuations due to slurry turbulence. The differential amplifier, A3, allows zeroing of the output in the densest slurry of the range. The gain of the final amplifier, A4, is set to give an output of 5v in the least dense slurry of the range. The output of the circuit is therefore 0 - 5v over the desired density range. Figure 39 shows the new circuitry.

8. LABORATORY TESTING OF THE FINAL DESIGN

8.1 System Linearity

The linearity of the system was tested over the density range 1,437 to 1,606. Starting with a density of 1,606, carefully measured volumes of water were added, and the output voltage noted. The result appears in Figure 40.

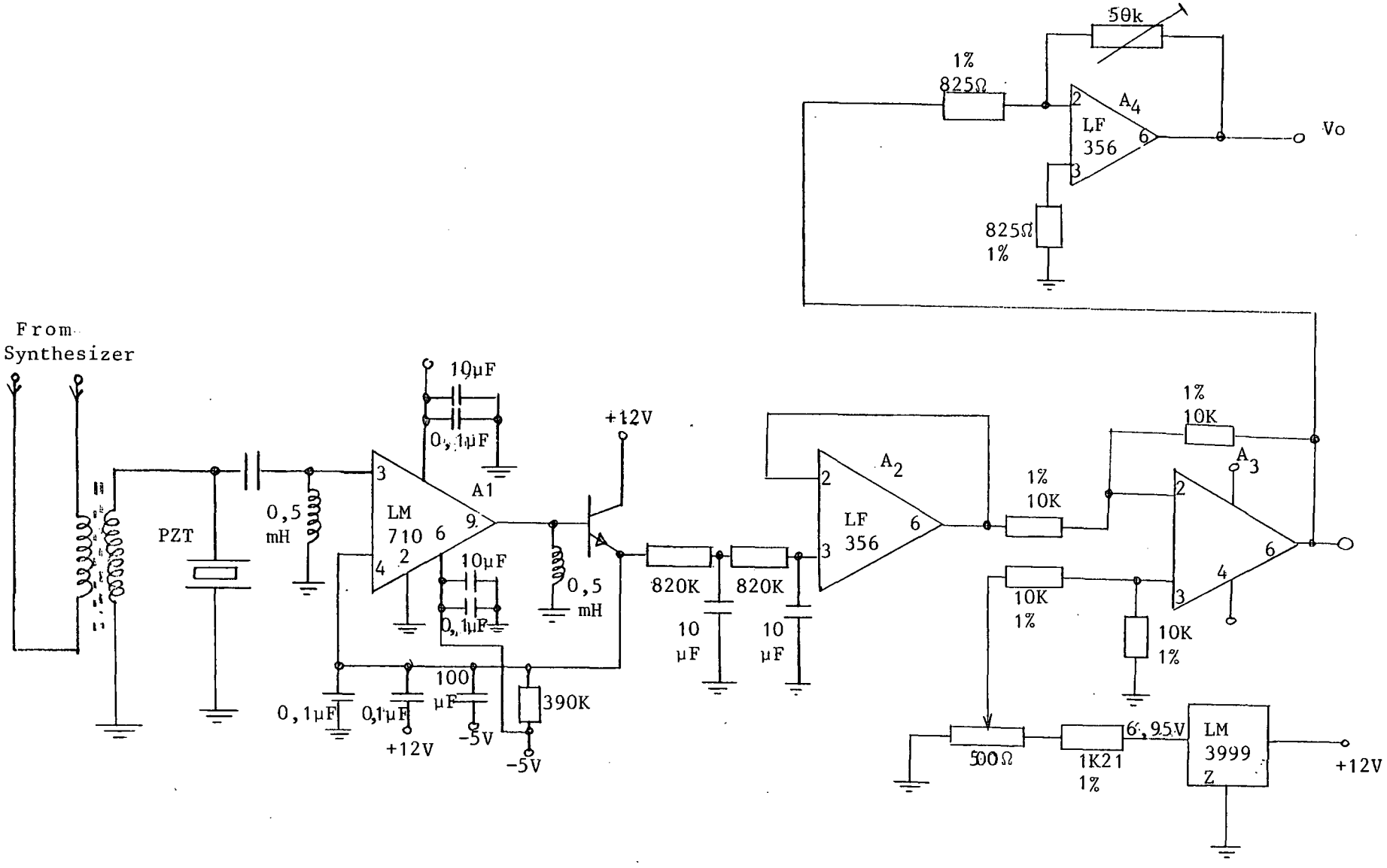

FIGURE 39 : THE MODIFIED CIRCUITRY

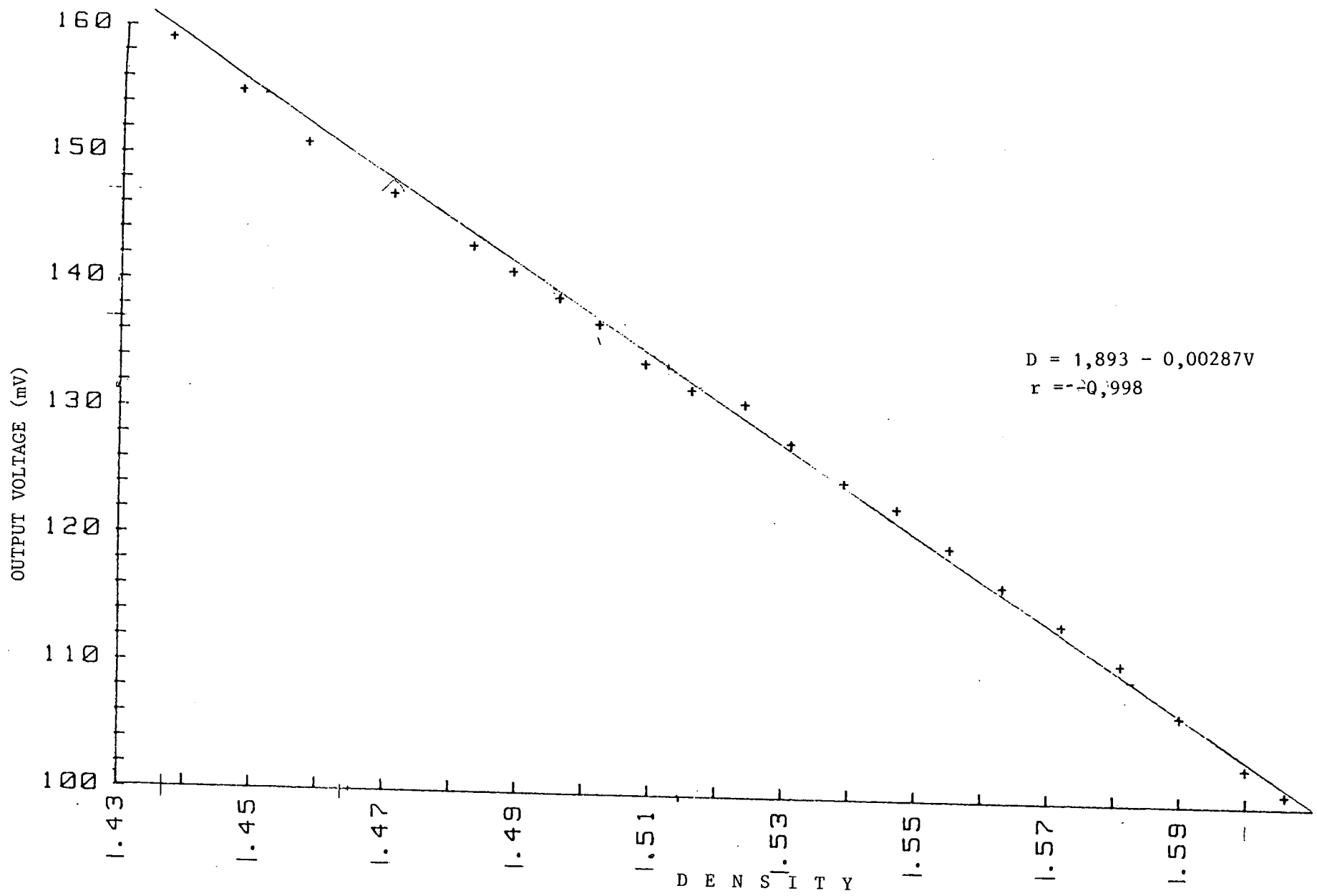

FIGURE 40 : LINEARITY OF NEW PROBE

8.2 Effect of Viscosity

It is known that the viscosity of a slurry increases with an increase in density (Marsden, 1962) and, for some time, it was thought that viscosity had some effect on the operation of the instrument and so an experiment was conducted to determine just how large the effect (if any) was.

Viscosity changes dramatically with the pH of the medium and so the investigation was approached in two ways.

8.2.1 Method 1

Starting with a slurry of density 1,4 several amounts of dry lime (CaO) and dry slurry were added. During the procedure, the output voltage and density were monitored. At the end of the experiment, the slurry was very viscous, but as will be seen, apart from the first addition of lime, the density increase is fairly linear, (Figure 41) indicating that, in this case, the change in viscosity had little effect.

After investigating the effect of pH on viscosity at greater length, it seems that after the initial addition of 100 gm of CaO in the previous experiment, the pH of the slurry would have reached a maximum of about 13,5, after which the viscosity would remain fairly stable; further additions, therefore would have been seen as changes in density.

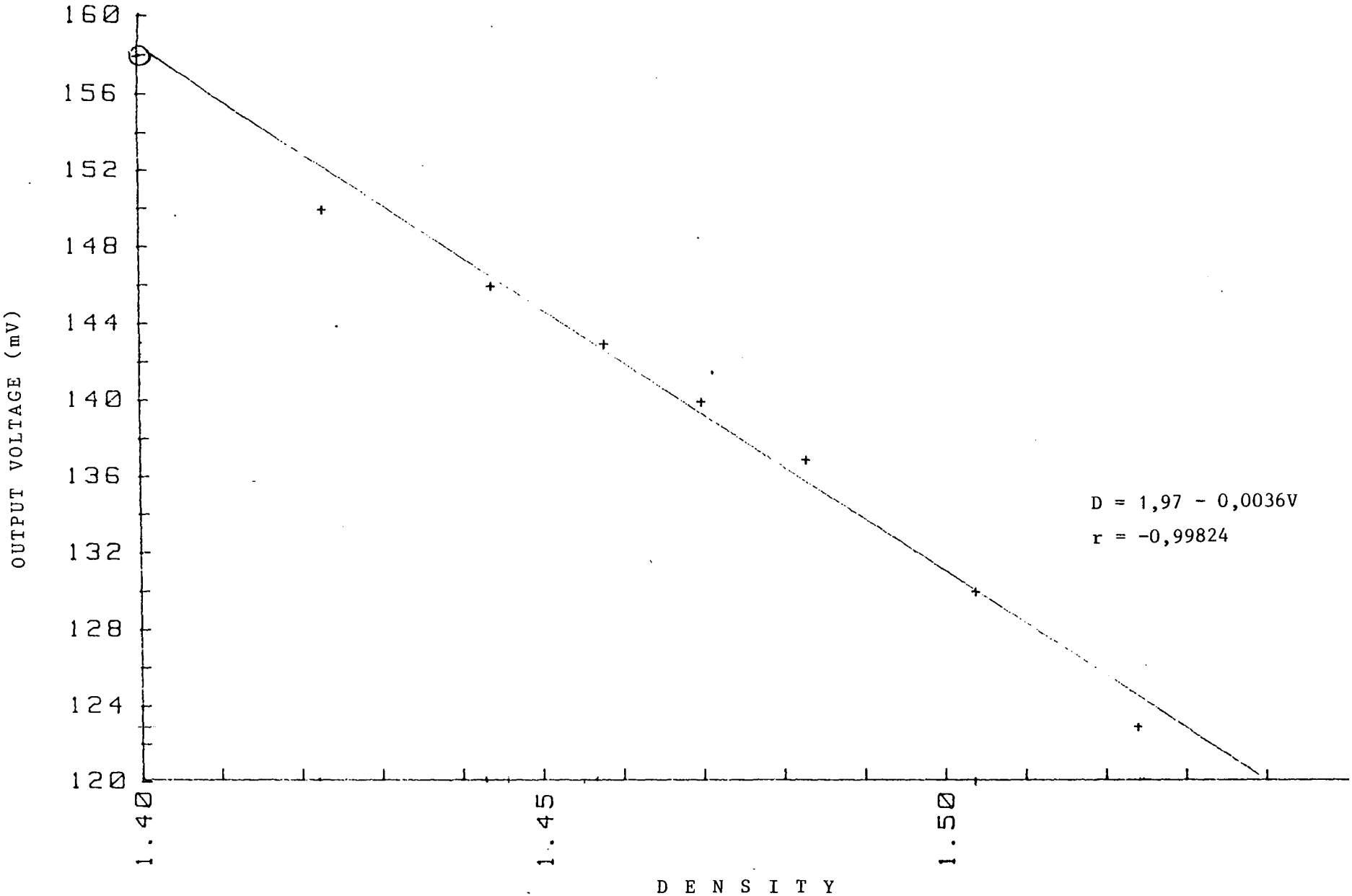

FIGURE 41 : VISCOSITY TEST WITH CaO

8.2.2 Method 2

Only a small addition of lime is needed to change the pH of a slurry, and hence the viscosity, by a large amount. Starting with a density of 1,6 small amounts of CaO were added: values of pH and output voltage were noted. Any change in output voltage would be due to a viscosity effect, as the addition of 4,5 gm in 4,8 kg (0,094 % by mass) would have a negligible effect on the density. The result of the experiment appears below in Table 15.

TABLE 15 : The effect of changes in viscosity

LIME (CaO) ADDITION (gm)	pH	OUTPUT VOLTAGE	Δv(mV)
	8,1	1,082	- 2
0,5	10,15	1,080	
0,5	10,85	1,080	
0,5	11,15	1,079	
0,5	11,45	1,079	
0,5	11,65	1,079	- 1
0,5	11,75	1,079	
0,5	11,85	1,079	
1,0	12,00	1,079	

According to the graph in Figure 40, the initial 2 mV change represents an apparent change in density of 0,007. From pH 10,15 to pH 12, the 1 mV change represented an apparent change of 0,0035. Over the range of the instrument, 1,2 to 1,6, there are errors of 1,75 % and 0,875 % respectively. As these errors occur over an enormous range of pH, the changes due to viscosity under normal plant operating conditions would be negligible.

9. SUMMARY AND DISCUSSION

9.1 Summary

A relatively simple and inexpensive measurement system has been developed for the measurement of the density of a slurry in a stirred tank. The system can also be applied to the measurement of the relative concentrations of two liquids provided that the accustic properties of the two liquids are sufficiently different. (Appendix III).

The measurement probe consists of a PZT disc which is separated from the medium being measured by a thin layer of polyester resin. The optimum resonant frequency of the PZT sensor is around 500 kHz for a disc of 50 mm diameter. The diameter of the disc is selected so that a single dominant admittance peak, with the minimum amount of satellite responses, will be obtained. (Section 6.2).

Compensation must be made for temperature, and it is necessary to locate a temperature sensor close to the PZT disc and to use the signal obtained from the sensor in an appropriate compensation arrangement. (Appendix II).

The electronic circuit required for the probe is relatively simple. An oscillator tuned to the resonant frequency of the PZT disc is used to drive the sensor, and the impedance of the probe is then measured, preferably in a bridge configuration.

The appropriate operating frequency of the probe is determined as follows. The probe is exposed to the media being measured, one of which should have a low and the other a high density (or mixture ratio). A range of frequencies around the resonance point is then applied. The frequency at which the maximum change in impedance occurs is selected as the operating frequency. (Section 3.1)

Each instrument has to be calibrated for its operating environment. This involves the following: the density (or mixture ratio) is varied in steps and the response is measured. The procedure has to be repeated at several temperatures over the range of interest. Finally, standard curve-fitting techniques are used to derive an expression relating the impedance and temperature signals to the density of the medium. (Section 4.5)

Because the characteristics of PZT's may differ, the instrument has to be re-calibrated for each new probe assembly.

The results obtained from the investigation suggest that an important parameter in the choice of a PZT is as high a diameter-to-thickness ratio as practical. Such a device will exhibit a single, dominant peak at series resonance, and hence couple the maximum amount of energy to the medium at that frequency. Used as a receiver, the device will be correspondingly more sensitive. (Section 6.2).

It has been found that changing the pH of the slurry, and hence its viscosity, has an effect on the instrument, but the effect was noticed over a very large range of pH (about pH 7 to pH 12). Over the normal plant range of about pH 10 to pH 12, the apparent change in density, due to the change in the viscosity was negligible. (Section 8.2)

Because of its fairly good abrasion resistant quality, the probe could be used as an on-line instrument as well as a portable unit. It has been successfully used as an on-line instrument for the measurement of solvent content at a solvent extraction plant. (Appendix III)

9.2 Discussion

It is possible that the instrument could be used in applications other than the mining industry, such as measuring the density of paper pulp or fertilizer slurries.

Another possibility is the measurement of density in fermentation vessels in the liquor industry, although the success of these applications depends upon the change in acoustic impedance of the medium being detectable over the range of interest.

The construction of the instrument is straightforward and all the materials and components are locally available.

The probe design shown in Plate VII is easy to manufacture and assemble. The body of the assembly is made of PVC, and the facing of the PZT is made of polyester. However, the design of the probe would have to be tailored to suit the application.

Although the object of the investigation was to develop a portable instrument, the technique is equally applicable to on-line measurement and possibly the control of a process.

It must be stressed that the instrument is a prototype and therefore no design or operating specifications have yet been formulated.

10. CONCLUSION

A single-transducer, portable density measuring instrument has been designed and constructed. The instrument has been extensively tested in the laboratory and on various mining processes where open slurry vessels are encountered and the results obtained correlated well with readings obtained with the commonly used spring balance.

The instrument has also been evaluated at a solvent extraction plant where an emulsion of aqueous and organic liquids was the medium of interest. In this application, the ratio of strip solvent to raffinate had to be determined thereby making it possible to calculate the percentage of solvent in the emulsion.

The result from the instrument correlated well with samples taken manually. (Appendix III, Section 5.)

Unlike other on-line instruments, such as the gamma density gauge, that operate in one place only, the ultrasonic density meter may be used both in portable or on-line applications.

The objectives of the investigation have been realised.

11. REFERENCES

ADAMSON, J. Gold Metallurgy in South Africa, Chamber of Mines of South Africa. *Cape and Transvaal Printers Limited.* 1972.

BLITZ, J. Ultrasonics, Methods and Applications. *Butterworths.* 1971.

CADY, W. Piezoelectricity - an Introduction to the Theory and Application of Electromechanical Phenomena in Crystals. *McGraw-Hill,* 1946.

CARLSON, D. Level and Density Measurement using Non-Contact Nuclear Gauges. *Measurement and Control* March 1977.

CONSIDINE, D.M. Process Instruments and Control Hand Book, 2nd Edition, *McGraw-Hill.* 1974.

FRIBANCE, A.E. Industrial Instrumentation Fundamentals. *McGraw-Hill.* 1962.

GACKENBACH, R.E. Materials Selection for Process Plant. *Reinhold Publishing Corporation.* 1960

GOLL, J.H. The Design of Broad Band Fluid-Loaded Ultrasonic Transducers. *I.E.E. Transactions on Sonics and Ultrasonics.* Vol. SU-26, No. 6, Nov., 1979.

HERBST, J.A. and ALBA, F. A New System for On-Line Measurement of Multi-Point Size Distributions on Solids Concentrations in Mineral Slurries. ISA 1985. Paper # 85-0280.

HICKS, R.W. and DICKEY, D.S. Applications for Turbine Agitators. *Chemical Engineering*. November 8, 1976.

HIDNERT, P. and PEFFER, E.L. Density of Solids and Liquids. *National Bureau of Standards Circular 487*. 15 March 1950.

HIND, A.L. and LLOYD, P.J.D. Real-Time Particle-Size Analysis in Wet, Closed Circuit Milling. *Powder Technology*, 12. 1975.

HODGINS, M.G. and BEAMS, J.W. A Magnetic Densimeter-Viscometer. *Department of Physics, University of Virginia*. 1971.

HOWARTH, W.J., WENK, G.J. and WILKINSON, L.R. Radio-Isotope On-Stream Analysis. Australian Mineral Development Laboratories. *Canadian Mining and Metallurgical Bulletin*. Sept. 1973.

KINSLER, E., FREY, A., COPPENS, A. and SANDERS, J. Fundamentals of Acoustics, 3rd Ed. *Wiley*. 1982.

MARSDEN, D.D. The Effect of pH Value, Temperature and Density on the Kinematic Viscosity of some South African Gold Mine Slurries. *Journal of the South African Isntitute of Mining and Metallurgy*. Jan. 1962.

MILLER, J.T. Industrial Instrument Technology. *United Trade Press*. 1964.

SHERWOOD, T.K., PIGFORD, R.L. and WILKE, C.R. Mass Transfer. International Student Edition. *McGraw-Hill*. 1975.

ROWE, S. and COOK, H.L. Nuclear Gauges for Density and Level Control. *Chemical Engineering*. Jan. 27, 1969.

STEMME, E. EKELÖF, J. and NORDIN, L. Measuring Liquid Density with a Tuning Fork Transducer. *IEEE Transactions on Instrumentation and Measurement*. Vol. 1M-32, No. 3. Sept. 1983.

INTERNAL REFERENCES

* DANN, M.S. An Ultrasonic Measuring System for Mineral *Pulp Suspensions. Measurement and Control Division. Council for Mineral Technology*. August 1987.

RUBIN, M. Hydrometallurgy Division. *Council for Mineral Technology*. August 1987.

* SMITH, K.L. An Ultrasonic Transducer Analysis Sytem Developed on the H.P. 9816 Computer. Measurement and Control Division, *Council for Mineral Technology*. July 1985.

VETTER, D. Measurement and Control Division, *Council for Mineral Technology*. March 1988.

---

* These publications may be released for inspection with the permission of the Director, Measurement and Control Division, *Council for Mineral Technology*.

TABLE 16 : THE ELECTROMECHANICAL REPRESENTATION OF AN ULTRASONIC TRANSDUCER

The circuit of the fundamental thickness resonance	MECHANICAL Velocity, v (vibration) 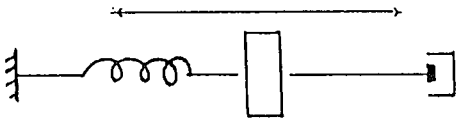 Stiffness, k. Mass M losses	ELECTRICAL i (a.c.) 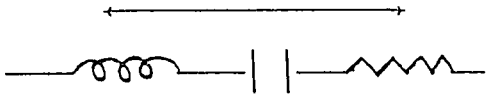 Inductance L Cap. C All losses	COMMENTS For a lumped system
Definitions of v and i	$v = v_o \sin\omega t$	$i = i_o \sin\omega t$	These apply to the transducer surface
The energy stored	$\frac{1}{2} M v_0^2$	$\frac{1}{2} L i_0^2$	The mass, M and inductance, L correspond
Frequency expression	$\omega^2 = \frac{k}{M}$	$\omega^2 = \frac{1}{LC}$	Knowing f and one other component allows second to be calculated. f is independent of R
Expression for piezoelectric coupling	$i = kv$ (or $q = ky$	$v = \frac{dy}{dt}$ and $i = \frac{dq}{dt}$	y is displacement and q is charge hence

TABLE 16 (continued)

	MECHANICAL	ELECTRICAL	COMMENTS
Energy radiated	$\frac{1}{2}(\rho c)AV_0^2$	$\frac{1}{2} R_L \quad i_0^2$	Enables ρc to be determined from R_L. This is the parameter which gives the density
Relationship of equivalent circuit	$R_L = \frac{\rho c A}{k^2}$		The instrument measures R_L and hence ρ is a linear function of R_L
Q factor	$2\Pi f \frac{\text{Energy Stored}}{\text{Power radiated}} = \frac{2\pi f \frac{1}{2} L i_0^2}{\frac{1}{2} i_0^2 R_L}$ $= \frac{\omega L}{R_L}$		This a a classical definition of Q in a series electrical circuit

2. THE MEASUREMENT OF k

At high frequency (above resonance), ωL is high and the energy (current) in the mechanical circuit is negligible, therefore Co can be measured. At low frequency (below resonance) ωL is small and Co + C is measured. k is a property of the PZT and it can be shown to be proportional to C/Co+C.

i.e. $$k \propto \frac{C}{Co + C}$$

13. APPENDIX II

THE THERMOMETER CIRCUIT

1. METHOD

The temperature sensor in the probe assembly is a device having a positive temperature coefficient (TSP102). A constant current is passed through this device, from which a voltage, proportional to temperature, is derived.

2. CIRCUIT ARRANGEMENT

The circuit arrangement is shown in Figure 42.

The temperature sensor (R5) is connected in parallel with resistors R2 and R3, in the feedback circuit of amplifier A1, thus the total resistance, Rt, in the feedback circuit is 2350R5 (2350 + R5). The graph in Figure 43 shows, the linearity of this arrangement over the range -25 ^{0}C to +125 ^{0}C. Capacitor C1 is simply a noise filter. Resistor R1 and potentiometer VR1 are connected in series between the positive supply rail and the inverting input of A1. Vr1 is adjusted so that a current of 1mA flows through Rt. The voltage at the output of A1 will have a value of -(Rt x 1) mV and since Rt is proportional to temperature, this voltage is directly proportional to temperature.

The negative output of A1 is connected to the input of a second amplifier, A2, together with a positive voltage from potential divider R4, VR2, that is used to back off a portion of the voltage from A1.

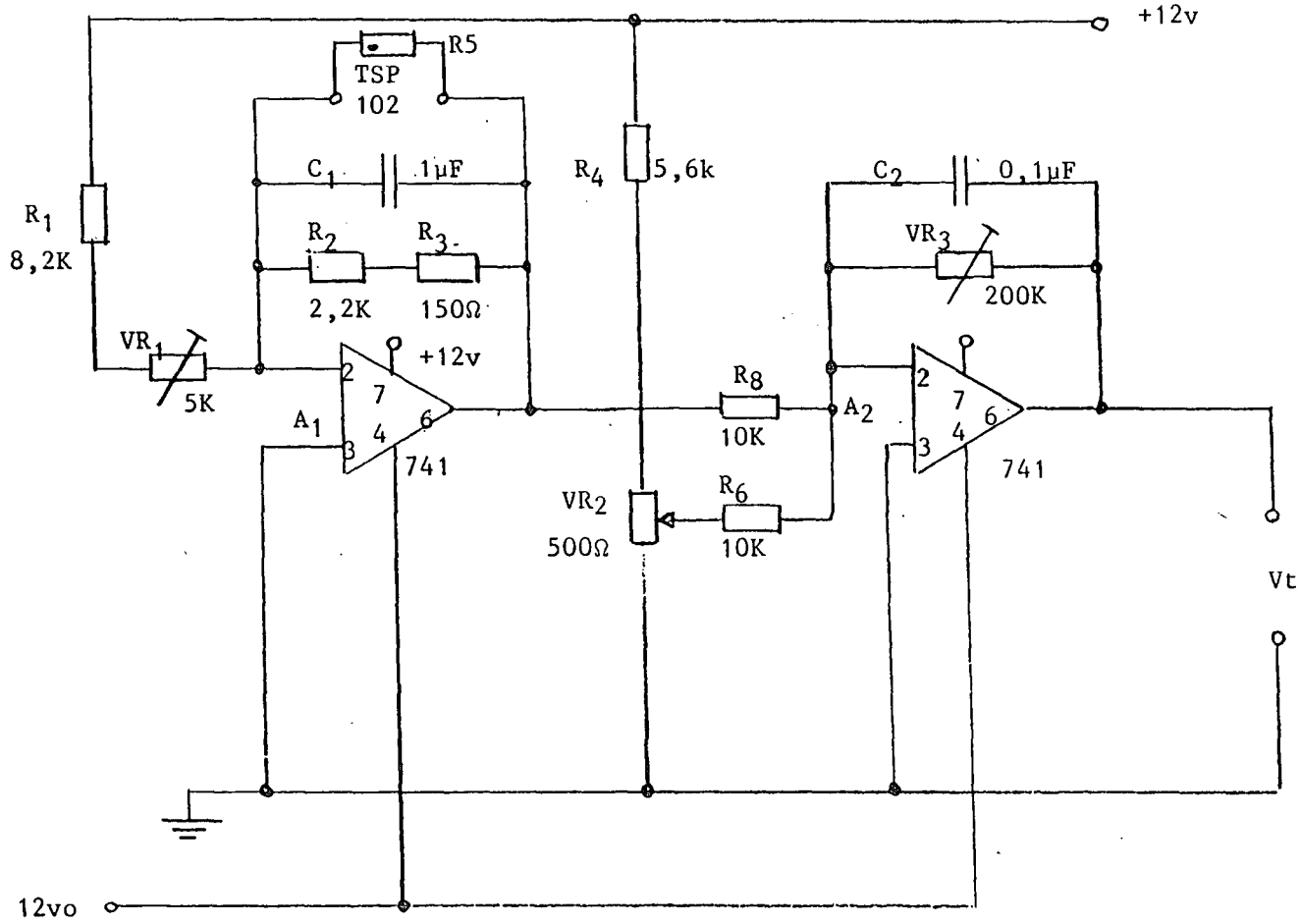

Figure 42: THE TEMPERATURE MEASURING CIRCUIT

3. CALIBRATION

As the values of the sensor resistance and Rt can be obtained from the graph, Figure 43, for various temperatures, a resistance decade box can be used in place of the sensor for calibration purposes.

The resistance box is set to 826Ω(0^0) and VR1 is adjusted to give a voltage of -613mV at the output of A1. Vr2 is then adjusted so that the output of A2 is Ov.

To simulate a temperature of 25^0C, the resistance box is set to 1kΩ; Rt is then 703Ω and the output of A1 rises to -703mV. Assuming unity gain for A1, the output would rise to 90mV (613mV was subtracted at the input to A2).

Vr3 is adjusted to provide an output voltage of a convenient value: in this particular application, the calibration is 10mV/^{0}C, so Vr3 is adjusted until the output voltage (Vt) is 250mV - a gain of 2,78.

After the calibration has been checked with several values of resistance, the decade box is removed and the sensor reconnected.

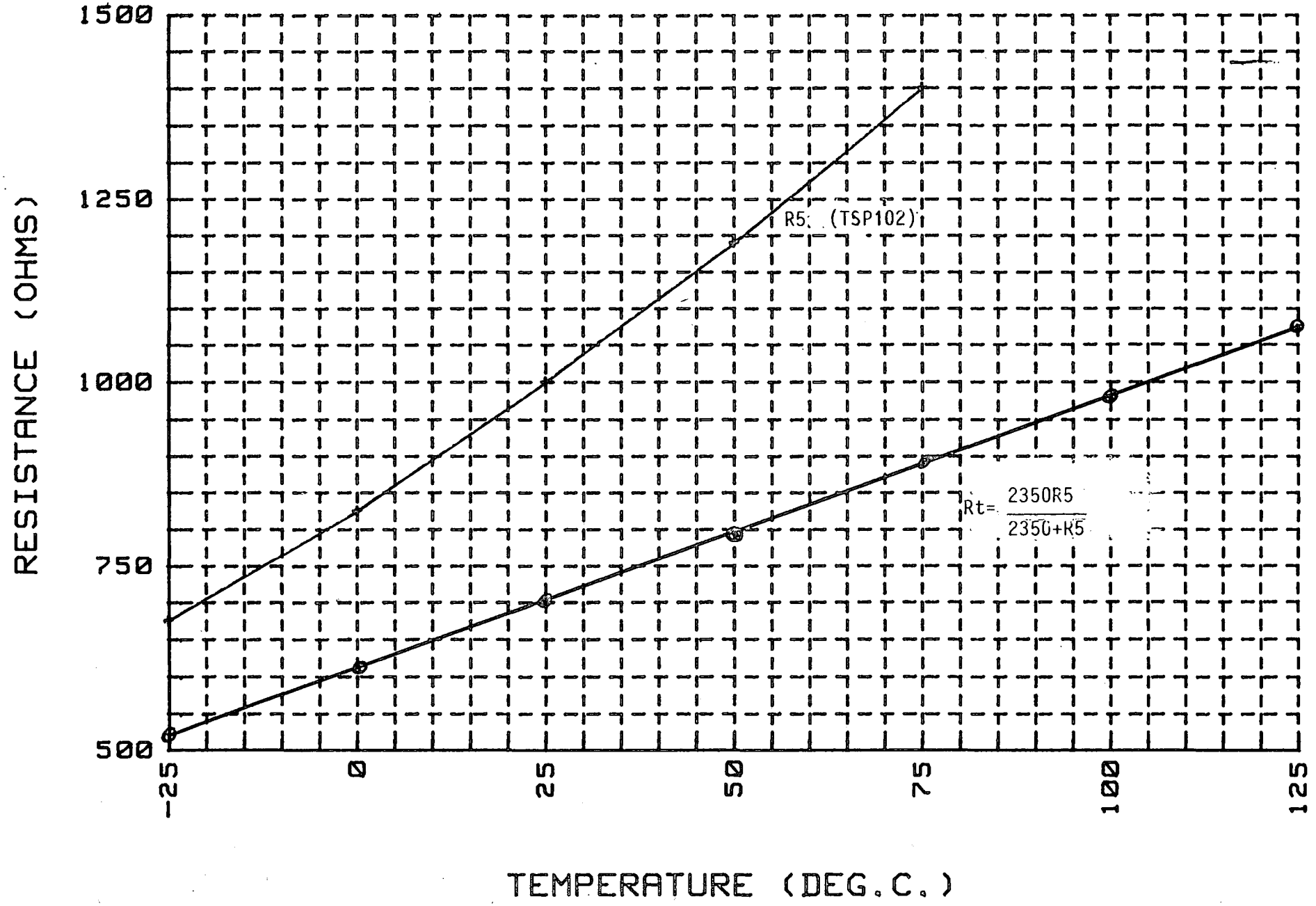

FIGURE 43: SENSOR RESPONSE CURVES

14. APPENDIX III

THE INSTRUMENT USED AS A RATIOMETER

In this application, the instrument was adapted to measure the ratio of strip solvent to raffinate (organic to aqueous) in a solvent extraction plant. It was decided to use polyester resin as the encapsulation for the sensor assembly as the emulsion being monitored has a pH of 1 and a temperature of about 45 ^{0}C - chemically a very hostile medium.

1. DESCRIPTION OF THE INSTRUMENT

As with the instrument for slurry density measurement, the transducer used is a 20 mm, 500 kHz PZT. This is encapsulated together with a Pt 100 temperature sensor, in acid-proof epoxy resin. The sensor assembly support consists of a 30 mm O.D. polypropylene tube, lined with a mild steel tube to provide rigidity. The electronics enclosure is mounted on top of the support to keep the interconnecting cable as short as possible, hence minimizing electrical losses.

Plate 1 shows the interior of the enclosure, with the position of the major components indicated.

The instrument is shown in Plate 2.

2. OPERATION OF THE INSTRUMENT

The procedure for determining the operating frequency is similar to that in Section 3.1 except that different concentrations of solvent and raffinate are used. Figure 44 shows the impedance/frequency curves for the probe in solvent, raffinate and a 1:1 emulsion of the two, with a range of operating frequencies from 550 kHz to 560 kHz.

In Figure 45 it will be seen that the PZT forms one leg of an active bridge, A1, the supply to the bridge being a signal of constant frequency and amplitude. The source of this signal is the crystal-controlled frequency synthesizer shown in Figure 46. This is a similar circuit to that mentioned in section 5.1.1.

The output of bridge A1 is rectified and filtered by A2 and A3: the output of A3 is therefore a d.c. voltage representing the state of balance of the bridge.

The 5 K potentiometer is adjusted to give the greatest voltage change, at the output of A1, when the sensor is immersed in raffinate and then solvent: the bridge is then correctly set up.

Provided that the temperature of the emulsion being measured remains constant, the output of the circuit is a 4 - 20 mA signal for a variation in solvent concentration of 40 % to 60 %. However, the PZT is temperature dependant and as the

instrument has to operate over the temperature range 30 - 50 ^{0}C, emulsion temperature has to be taken into account and compensated for.

Because of this temperature dependence the lower and upper limits of the output current are set as follows: with the probe immersed in an emulsion of 40 % solvent and 60 % raffinate at a temperature of 50 ^{0}C, VR1 and Vr2 are adjusted to give 4 mA at the output (1V if a 250 load is used). With the probe immersed in an emulsion of 60 % solvent and 40 % raffinate at a temperature of 30 ^{0}C, VR5 is adjusted to give 20 mA at the output (5V). This output signal of 4 - 20mA represents a voltage change of 0 - 10V at the output of A5. The current source A6, A7 and A8 is preset for this voltage input range by means of the 'zero' and 'span' potentiometers.

3. TEMPERATURE MEASUREMENT

The temperature sensor, embedded in the sensor assembly, is a Pt100 resistance element: this is connected to a commercial temperature transmitter that provides 4 - 20 mA over the range 20 ^{0}C to 60 ^{0}C.

4. CALIBRATION

Temperature compensation is embodied in the method of calibration: values of voltage, for both the ratio and temperature outputs, were logged for various temperatures

and ratios, and non-linear regression applied to the resulting data: an expression was thus derived relating solvent content to the two output voltages, Vo and Vt.

The expression takes the form:

$$F = a_1 + a_2 x_1 + a_3 x_2 + a_4 x_1 x_2 + a_5 x_2^2 + a_6 x_1^2 + a_6 x_1^2 + a_7 x_1^2 x_2^2$$

where F = % solvent

a_n = fitted coefficients

X1 = Vo (ratio) (1 - 5 V)

X2 = Vt (temperature) (1 - 5 V)

The values of the coefficients are as follows:

a_1 = 294,41

a_2 = -97,48

a_3 = -99,99

a_4 = 22,17

a_5 = 9,01

a_6 = 8,17

a_7 = -0,25

5. PLANT TRIALS

The instrument was installed at the mixer box of one of the extractors at the plant and the two 4-20mA outputs, one for temperature and the other for solvent content, were connected through to the central process computer, that has, as part of its software, the calibration expression relating these two outputs to the percentage solvent. The results appear below in Table 17, showing good correlation between the actual solvent content and that measured by the instrument.

T A B L E 17

PLANT RESULTS

ACTUAL % SOLVENT	Vo	Vt	CALCULATED % SOLVENT
44	4,59	2,3	43
46	4,50	2,53	45,9
47	4,66	2,35	45,2
50	4,70	2,53	49,7
57	5,20	2,30	55,5
65	5,20	2,53	61,5
70	5,40	2,53	67,2

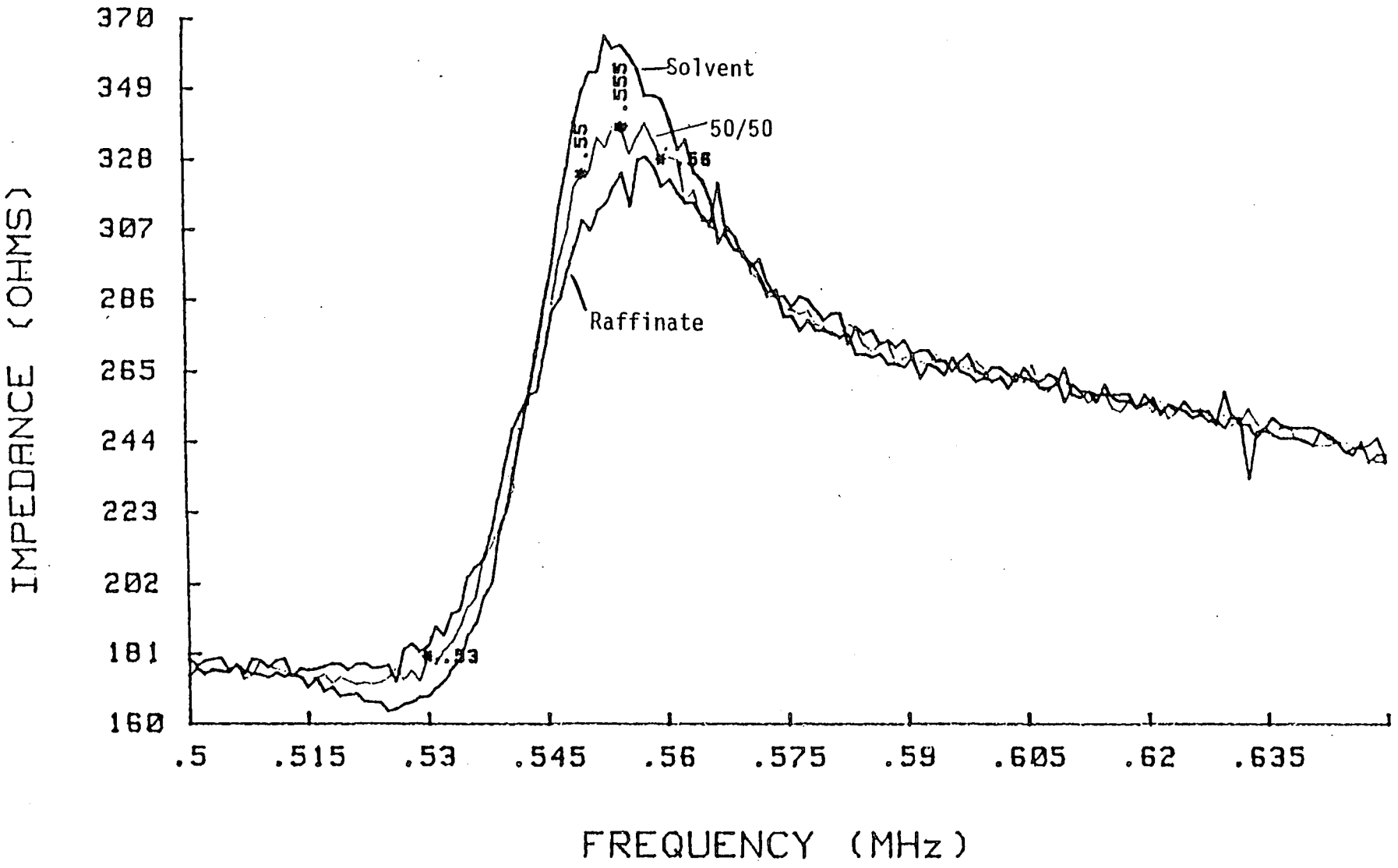

FIGURE 44: DETERMINATION OF OPERATING FREQUENCY

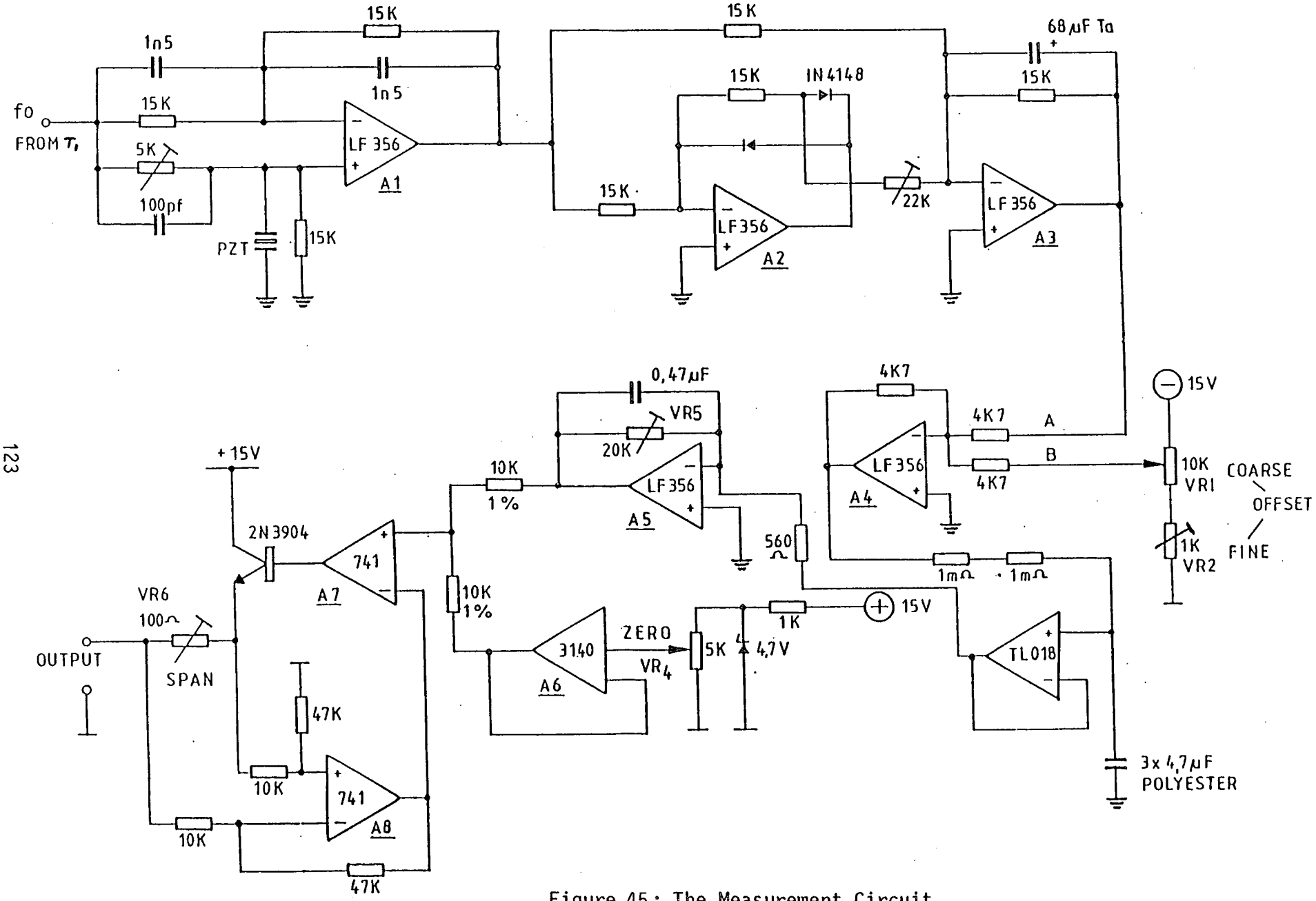

Figure 45: The Measurement Circuit

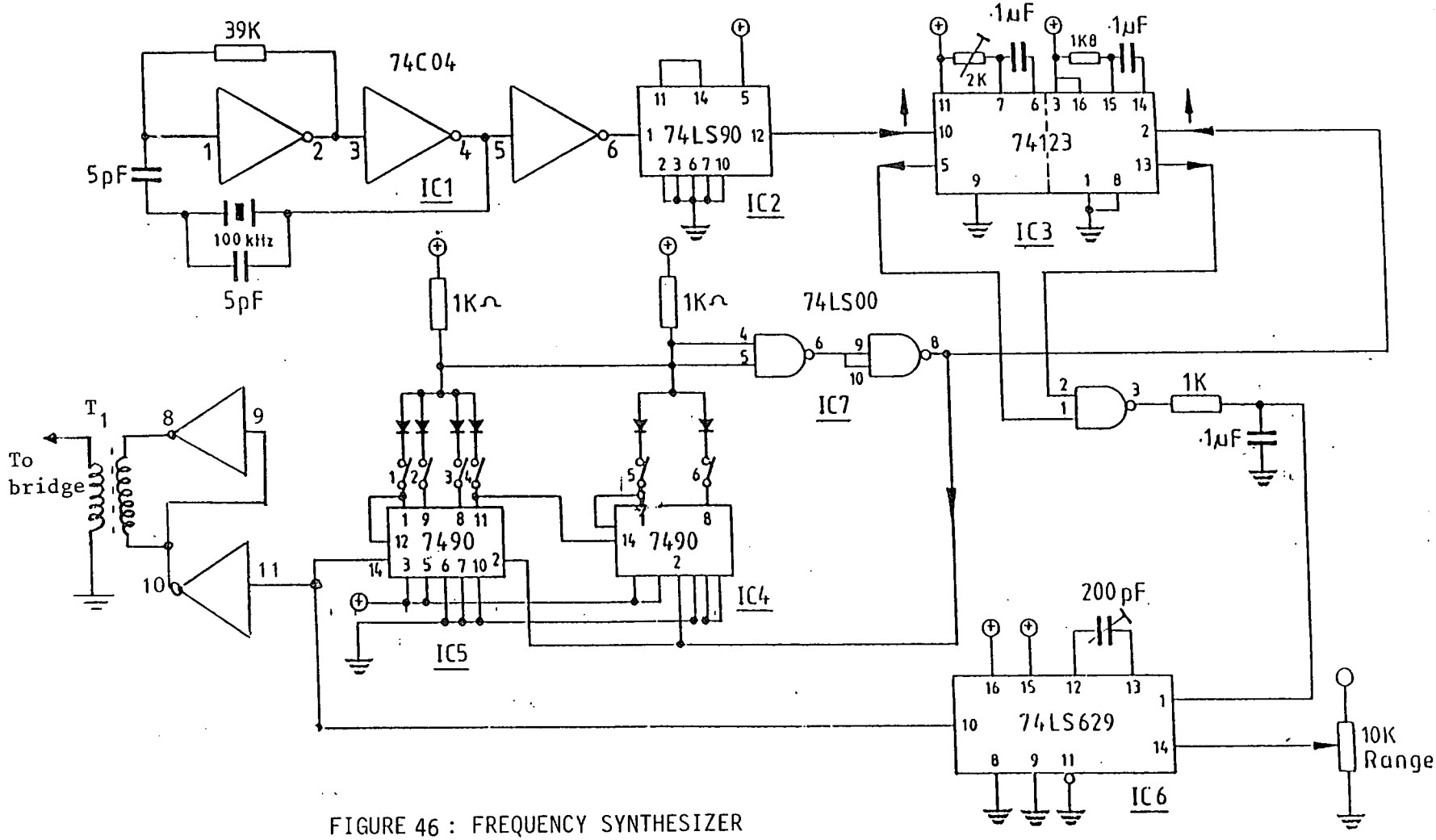

FIGURE 46 : FREQUENCY SYNTHESIZER

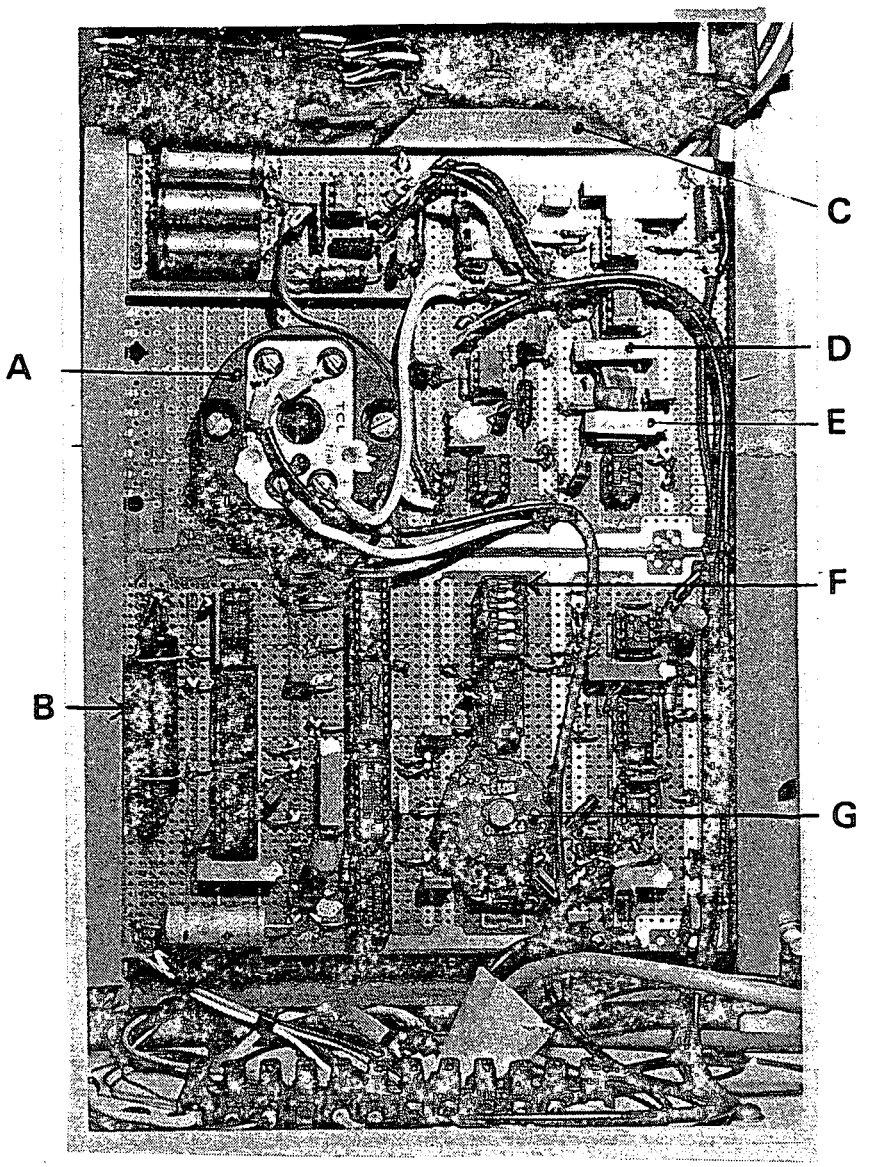

PLATE 1 : The Component Layout

Where A = Temperature transmitter
B = 100 kHz crystal
C = Power supply
D = Span control VR5
E = Zero control VR4
F = Frequency selection switches
G = Driver transformer

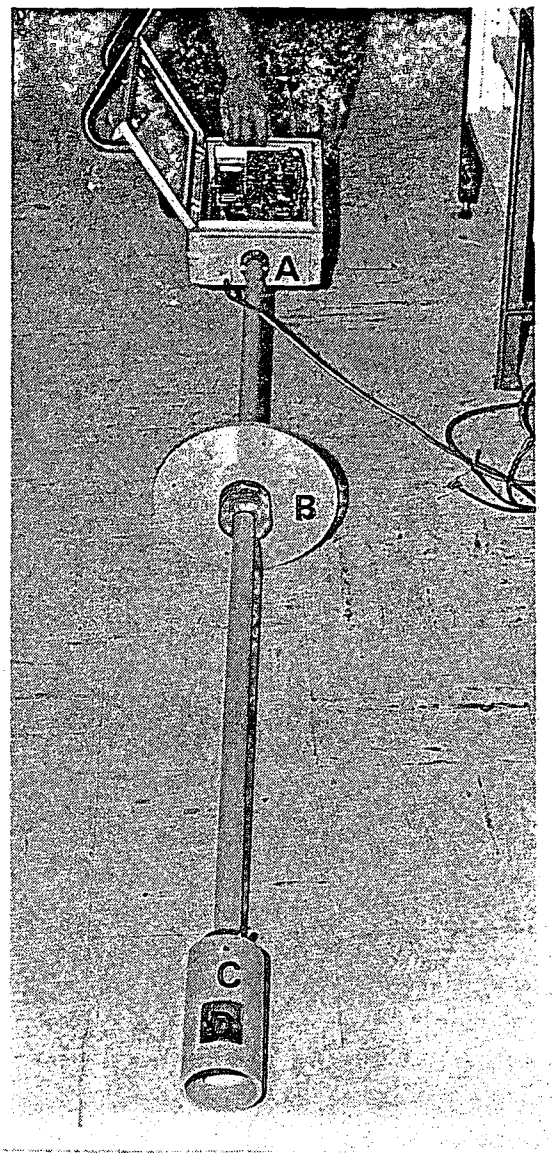

PLATE 2 : The Instrument

Where A = Electronics enclosure

B = Mounting flange

C = Protective cover

D = Sensor assembly